INTEGRATING GEOPHYSICS AND GEOCHEMISTRY TO EVALUATE COALBED NATURAL GAS PRODUCED WATER DISPOSAL, POWDER RIVER BASIN, WYOMING

by

Brian Andrew Lipinski

B.S. in Environmental Science, Slippery Rock University, 1999

M.S. in Environmental Geoscience, Michigan State University, 2002

Submitted to the Graduate Faculty of

Arts and Sciences in partial fulfillment

of the requirements for the degree of

Doctor of Philosophy in Geology

University of Pittsburgh

2007

UNIVERSITY OF PITTSBURGH

FACULTY OF ARTS AND SCIENCES

This dissertation was presented

by

Brian Andrew Lipinski

It was defended on

March 16, 2007

and approved by

Dr. Thomas Anderson

Dr. Rosemary Capo

Dr. Michael Rosenmeier

Dr. Bruce Smith

Dr. William Harbert
Dissertation Director

INTEGRATING GEOPHYSICS AND GEOCHEMISTRY TO EVALUATE COALBED NATURAL GAS PRODUCED WATER DISPOSAL, POWDER RIVER BASIN, WYOMING

Brian Andrew Lipinski, PhD

University of Pittsburgh, 2007

Production of methane from thick, extensive coalbeds in the Powder River Basin of Wyoming has created water management issues. More than 4.1 billion barrels of water have been produced with coalbed natural gas (CBNG) since 1997. Infiltration impoundments, which are the principal method used to dispose CBNG water, contribute to the recharge of underlying aquifers. Airborne electromagnetic surveys of an alluvial aquifer that has been receiving CBNG water effluent through infiltration impoundments since 2001 reveal produced water plumes within these aquifers and also provide insight into geomorphologic controls on resultant salinity levels. Geochemical data from the same aquifer reveal that CBNG water enriched in sodium and bicarbonate infiltrates and mixes with sodium-calcium-sulfate type alluvial groundwater, which subsequently may have migrated into the Powder River. The highly sodic produced water undergoes cation exchange reactions with native alluvial sediments as it infiltrates, exchanging sodium from solution for calcium and magnesium on montmorillonite clays. The reaction may ultimately reduce sediment permeability by clay dispersion. Strontium isotope data from CBNG wells discharging water into these impoundments indicate that the Anderson coalbed of the Fort Union Formation is dewatered due to production. Geophysical methods provide a broad-scale tool to monitor CBNG water disposal especially in areas where field based investigations are logistically prohibitive, but geochemical data are needed to reveal subsurface processes undetectable by geophysical techniques.

The results of this research show that: (1) CBNG impoundments should not be located near streams because they can alter the surrounding hydraulic potential field forcing saline alluvial groundwater and eventually CBNG water into the stream, (2) point bars are poor impoundment locations because they are essentially in direct hydraulic communication with the associated stream and because plants readily transpire shallow groundwater within them creating vadose zone salt accumulations that will be dissolved by infiltrating CBNG water, and (3) cation exchange reactions in vadose zone sediments may reduce soil permeability beneath infiltration impoundments through clay dispersion lowering their designed disposal capacity.

TABLE OF CONTENTS

LIST OF TABLES

LIST OF FIGURES

1. INTRODUCTION

1.1. COALBED NATURAL GAS BACKGROUND

The Powder River Basin (PRB) of Wyoming and Montana contains some of the thickest, most extensive, and economically attractive coal deposits in the United States (Flores and Bader, 1999). In this region, coalbeds as thick as 75 m are contained within Late Cretaceous to Early Tertiary strata at shallow depths (Flores et al., 1999). The coal is sub-bituminous to lignite in rank and has a low sulfur and ash content making it desirable for compliance with the Clean Air Act. As a result, approximately 34% of the nation's coal production comes from the Powder River Basin (Flores and Bader, 1999). In addition, these coalbeds contain unconventional natural gas, an important additional energy resource.

Coalbed natural gas (CBNG) was first observed the 1930's from the northern Appalachian basin and in the 1950's from the San Juan Basin, New Mexico (Ayers, 2002). Methane was observed in PRB coalbed artesian wells as early as 1957 (Flores et al., 2004). There was no commercial production of CBNG in the United States until the late 1970's when the United States Bureau of Mines, the Department of Energy, and the Gas Research Institute demonstrated economical CBNG extraction in the Black Warrior Basin, Alabama. Their goal was to remove methane from coalbeds to reduce mining hazards. However, the project was so successful that it is cited as the first commercial CBNG field in the United States (Pashin and Hinkle, 1997).

Extensive CBNG exploration and production in the United States began in the 1980's. Initial development occurred in the San Juan Basin of New Mexico, which accounted for approximately 73% of cumulative CBNG production by 2002 (Limerick, 2004). The most rapid growth has occurred in the Powder River Basin which contains over 22,000 CBNG wells (WOGCC, 2006), up from 360 wells in 1997 (De Bruin et al., 2004). Estimates of recoverable

gas volumes vary, but have been determined to be in the range of 14.3 trillion cubic feet (TCF) to 39 TCF (ARI, 2002; De Bruin et al., 2004; Flores et al., 2004), which is approximately 16% of US CBNG reserves (Limerick, 2004). On a national level, CBNG accounts for approximately 7% of natural gas production (ARI, 2002; USGS, 2003).

1.2. PRODUCTION ISSUES

CBNG is considered a continuous gas accumulation because there is no readily definable hydrocarbon-water boundary (Flores et al., 2004). Methane is primarily adsorbed to coal cleats, but it can also occur as free gas within pores or as dissolved gas in porewater (Ayers, 2002; De Bruin et al., 2004; Flores et al., 2004). To develop this resource, the hydrostatic pressure must be reduced by removing groundwater from the coalbed. This causes methane to desorb, flow to the extraction well, and then rise to the surface for compression and distribution. The extracted coalbed aquifer water is termed produced water or CBNG water.

Dewatering coalbeds is expected to have a negative impact on freshwater resources within the basin. PRB wells have some of the highest water/gas production ratios of current CBNG fields. For example, each PRB well produces 1.9 barrels (bbls) per 1000 cubic feet gas (MCF), while San Juan Basin CBNG wells produce approximately 0.031 bbls water per MCF gas (DOE, 2003). However, water production is variable with respect to well location and generally decreases throughout the 7 to 10 year well lifespan (ARI, 2002; BLM, 2003a). Since 1997, water production from CBNG wells has increased from 45 million barrels (Mbbls) to over 557 Mbbls in the Wyoming portion of the PRB using ~22,000 wells (WOGCC, 2006). Assuming 80 acre well spacing, approximately 40,000 additional wells are needed in Wyoming and 25,000 wells are needed in Montana to extract recoverable methane from PRB coalbeds (BLM, 2003a, b). This extensive dewatering operation is expected to lower hydraulic head in surrounding aquifers by approximately 60 to 120 m over the entire basin (BLM, 2003a) .

Groundwater is used extensively for domestic and agricultural purposes; therefore, water management is an important issue. Current disposal methods include, but are not limited to, direct surface discharge, infiltration impoundments, containment impoundments, land

application disposal, and reinjection (BLM, 2003a). Direct discharge systems use a series of pipes to direct produced water to ephemeral drainages. Infiltration impoundments are unlined ponds designed to promote near surface aquifer recharge. Containment impoundments are lined with an impermeable geofabric forcing water to evaporate leaving behind salt deposits that are trucked off-site for disposal. Land application disposal is used for beneficial purposes such as center-pivot and wheel line irrigation systems. Reinjection systems are constructed by piping produced water to a centralized injection well completed within an aquifer having similar water quality as CBNG water. In any of the aforementioned water management strategies, the water may have to be treated prior to disposal (ARI, 2002). Treatment can be passive, such as rip-rap aeration to oxidize iron, or active, such as reverse osmosis to lower total dissolved solids concentrations (BLM, 2003a). Presently, there are no federal guidelines regarding produced water and state agencies such as the Wyoming Department of Environmental Quality (WYDEQ) are responsible for regulating disposal.

Produced water may degrade surface water and groundwater quality. Coalbed aquifer water is moderately saline (TDS < 5,000 mg/L) and characteristically sodic (Bartos and Ogle, 2002; Rice et al., 2005; Rice et al., 2000). Direct discharge of production waters into existing stream channels will modify average streamflow characteristics, create artificial perennial streams, and may degrade water quality by elevating TDS and sodium levels within soils and groundwater (BLM, 2003a; Ganjegunte et al., 2005; Stearns et al., 2005). More than 98% of surface water withdrawals in the PRB are for irrigation purposes and increasing salinity and sodicity could render surface water unusable (BLM, 2003a). Additionally, individuals and municipalities rely heavily on deeper aquifers for potable water supplies. Infiltration of CBNG water may contaminate these freshwater reservoirs.

CBNG water negatively affects agricultural and grazing lands. Irrigating fields with CBNG water will increase soil salinity thereby limiting nutrient uptake in plants (Ganjegunte et al., 2005; USDA, 1954). PRB soils are characterized by high percentages of smectite clays, which have large cation exchange capacities (BLM, 2003a; Ganjegunte et al., 2005). CBNG water is typified by a high sodium adsorption ratio (SAR) that may damage soil structure through clay dispersion (Ganjegunte et al., 2005; USDA, 1954). An additional outcome of reducing soil permeability is that native plants will be stressed and potentially replaced by exotic invasive species (Stearns et al., 2005).

The profitability of CBNG production is highly dependent on the water management strategy used (ARI, 2002; BLM, 2003a). Direct disposal is preferred by industry because it does not appreciably reduce revenue (ARI, 2002; BLM, 2003a). Active treatment, such as reverse osmosis, prior to discharge would reduce revenue by approximately 4 to 5 billion dollars making CBNG unprofitable at current gas prices (ARI, 2002). Shallow reinjection would conserve water resources most effectively, but it would lower CBNG revenues by approximately 1.3 billion dollars (ARI, 2002). Infiltration impoundments would allow some produced water to recharge aquifers while only reducing CBNG revenues by approximately 850 million dollars (ARI, 2002).

Infiltration impoundments were recommended by the BLM as the preferred disposal method in Wyoming as a compromise between CBNG economics and environmental considerations (BLM, 2003a). Projected totals were that approximately 3,000 infiltration impoundments were needed to dispose produced water throughout the project life (BLM, 2003a). WYDEQ responded by implementing regulations that required gas companies to monitor groundwater and surface water quality near permitted impoundments. However, the rapid expansion of CBNG coupled with manpower shortages in the WDEQ have not allowed proper data evaluation with most resources directed towards permitting new impoundments. Reflecting this situation was a recent finding by the Wyoming State Engineer's office (WYSEO) that approximately 133 out of 200 impoundments within a small watershed were not permitted and they did not have pending permits (Malone, 2005).

1.3. RESEARCH NEEDS

There have been no studies published in refereed journals that evaluate groundwater impacts from produced water infiltration ponds within the PRB. Considering the current state of affairs in the Wyoming portion of the PRB, the anticipated development 5n the Montana portion of the PRB, and the predicted CBNG development in similar basins throughout the United States, research is needed to determine potential environmental impact from this disposal strategy. These needs include: (1) a more effective means of monitoring produced water disposal on a

regional scale and (2) understanding fundamental geochemical changes occurring in areas impacted by produced water disposal.

1.4. STUDY OBJECTIVES

The objectives of this dissertation are to integrate geophysics with hydrogeology and geochemistry to enhance understanding of produced water disposal using infiltration impoundments. The research involved:

1. Applying airborne electromagnetic geophysical techniques to map water quality in a near surface aquifer receiving produced water effluent from infiltration impoundments.
2. Measuring strontium isotopes and major ion concentrations to understand subsurface processes occurring in a near surface aquifer receiving produced water effluent from infiltration impoundments.
3. Integrating electromagnetic geophysical methods and geochemical methods to more fully understand subsurface processes associated with produced water disposal.

1.5. DISSERTATION OUTLINE

This dissertation is divided into seven chapters. The first four chapters are designed to provide background information about the study site and the geophysical/geochemical methods used in this dissertation. The final three chapters contain individual papers prepared for submittal to separate journals. A summary of each chapter is provided below:

- Chapter 1: Introduction – An introduction to the dissertation research is presented.
- Chapter 2: Study Area Description – A detailed description of the site geology and hydrogeology is presented.

- Chapter 3: Geophysical Methods –A detailed description of geophysical technique applied in this dissertation is summarized.
- Chapter 4: Geochemical Methods – A summary of sampling, laboratory, and analytical protocols used to process geochemical samples is presented.
- Chapter 5: Geophysical Investigation – Airborne geophysical surveys are used to monitor produced water disposal in an unconfined alluvial aquifer.
- Chapter 6: Geochemical Investigation – Strontium isotopes and major ions are evaluated as produced water tracers and indicators of subsurface processes.
- Chapter 7: Integrating Geophysics and Geochemistry – Results from chapters 5 and 6 are integrated to enhance conceptualization of the system.

Results of this research are expected to provide a better understanding of hydrologic process at produced water disposal sites within the Powder River Basin. Additionally, the final chapter should aid future investigations in the PRB. This research should also be applicable to anticipated CBNG production in other basins throughout the United States.

2. STUDY AREA DESCRIPTION

2.1. INTRODUCTION

The study site is located along the Powder River approximately 5 km south of Arvada, Wyoming (Figure 2.1). The Powder River flows northward through the study area. There are approximately 21 impoundments situated on terraces flanking the stream. Impoundments were installed by Pennaco Energy Inc. (PEI), a wholly owned subsidiary of Marathon Oil, and are permitted under the Wyoming Pollution Discharge Elimination System (WYDES) to receive coalbed natural gas (CBNG) produced water effluent. CBNG production within the study area began in 2001 and is limited to the Anderson Coalbed of the Fort Union Formation.

2.2. PHYSIOGRAPHY

Regionally, the study site is located within the Powder River Basin (PRB) (Figure 2.2). This structural basin is situated within the Great Plains physiographic province and includes approximately 57,000 km^2 in Montana and Wyoming. It is flanked on the east by the Black Hills, to the south by the Laramie Mountains, and to the west by the Bighorn Mountains. Major streams draining the basin are the Belle Fourche River, the Tongue River, the Powder River, and the Cheyenne River. The Tongue River and Powder River are part of the larger Yellowstone River Watershed (YRW) while the Belle Fourche is a tributary of the Cheyenne River; all streams drain to the Missouri River. These rivers have eroded deeply into underlying bedrock and typically have flat streambeds within broad floodplains (Bartos and Ogle, 2002). Upland areas have been dissected into badlands by numerous ephemeral streams (Choate et al., 1984).

2.3. CLIMATE

The climate of the PRB is semiarid. Temperature and precipitation levels are not constant and generally increase along an eastward traverse across the basin from the Bighorn Mountains. The mean annual temperature in Clearmont, Wyoming (approximately 20 km west of Arvada) is 8.2 ºC with annual precipitation of approximately 34.5 cm (WRCC, 2006). Evaporation from free-surface bodies is approximately 129 cm/yr (Curtis and Grimes, 2004). Low precipitation rates coupled with high evapotranspiration rates leave water resources in short supply, a typical situation for a semiarid environment. Subsequently, surface water and groundwater resources are allotted under the prior appropriation doctrine common in western water law (Jacobs et al., 2003).

2.4. GEOLOGIC SETTING

The PRB is an intermontane structural basin that formed as a result of the Laramide orogeny during Late Cretaceous to Early Tertiary time (Choate et al., 1984). The basin is asymmetric and the axis is located along the western margin. Strata dip approximately 12º east along the western margin and approximately 2° west along the eastern margin (Flores et al., 1999). Geologically, the basin is composed of basement Precambrian granite overlain by marine Paleozoic and Mesozoic rocks capped by a thick veneer of Late Cretaceous to Early Tertiary continental strata that are exposed at the surface (Figure 2.3). CBNG exploration and development is contained entirely within the Tertiary Fort Union and Wasatch Formations.

2.4.1. Tertiary Rocks

The oldest exposed unit in the study area is the Paleocene Fort Union Formation (Figure 2.3) that unconformably overlies Cretaceous strata including the Lance Formation, Fox Hills Sandstone, and Lewis Shale (Figure 2.4) (Montgomery, 1999). The unconformity records regional uplift

associated with the Laramide deformation (Curry, 1971). The Fort Union is subdivided into the Tullock Member, the Lebo Shale, and the Tongue River Member (Figure 2.4). The Tullock member is comprised of lenticular fine to medium grained sandstone beds interbedded with siltstone, mudstone, carbonaceous shale, and coal (Flores, 1986). The Lebo Shale is comprised of soft, clay-rich shale with interbedded siltstone, sandstone, and thin coalbeds (Ayers, 1986). The Tongue River Member is comprised of lenticular fine to medium grained sandstone interbedded with siltstone, mudstone, limestone, and many thick coalbeds (Flores, 1986). Fort Union strata are interpreted to be continental in origin and were deposited by a northeastward flowing fluvial system in the basin center fed by alluvial fans along the basin margin from ancestral uplifts (Flores, 1986).

Horizons within the Fort Union Formation are the most highly developed CBNG reservoirs in the basin. Coalbeds within the Tongue River Member are the major CBNG bearing units; coalbeds in the Tullock Member and Lebo Shale are too thin and discontinuous for economic production (Flores, 1986). The coalbeds are stratigraphically complex and commonly merge, split, and re-merge to form thick, locally extensive units (Ayers, 1986; Flores, 1986). The most widespread coalbed is referred to as the Wyodak-Anderson coal zone. It contains eleven named coalbeds with up to six located at any given position. Individual coalbeds merge near Gillette to form a single coalbed 45 m thick extending approximately 64 km northwest along strike (Ellis et al., 1998). The Anderson coalbed, which is part of the Wyodak-Anderson coal zone, is the production target within the study area.

The Eocene Wasatch Formation overlies the Fort Union Formation and crops out within the study area (Figure 2.3). Wasatch strata are lithologically similar to underlying Fort Union rocks being composed of lenticular sandstone with interbedded siltstone, mudstone, and coal (Choate et al., 1984). These rocks appear yellow to light gray in weathered outcrops and are from 300 to 600 meters thick in the PRB (Choate et al., 1984). Wasatch strata accumulated under conditions similar to those recorded by Fort Union strata.

Major coalbeds within the Wasatch Formation are the Arvada, Felix, and Lake De Smet seams (Figure 2.4). The Lake De Smet coalbed is reported to be the thickest in the United States averaging over 67 m thick in the Lake De Smet area (Choate et al., 1984). These coal deposits are generally sub-bituminous to lignite in rank (Flores et al., 2004). Few CBNG wells produce from the Wasatch as development is focused in the Fort Union (Flores et al., 2004).

The contact between the Wasatch and Fort Union Formations is mapped to occur within the study area (Figure 2.3). These formations are lithologically similar and were deposited in northeasterly flowing fluvial systems making them difficult to differentiate in the field (Flores, 1986; Flores and Bader, 1999). The boundary, although not well defined throughout the basin, is commonly placed above the Roland Coal (Flores, 1986; Flores and Bader, 1999). The contact can be identified where the Coquinoid Limestone is present, but it was not observed in the study area. Results suggest these formations can be differentiated by palynostratigraphic and mineralogical compositions (Flores, 1986; Flores and Bader, 1999), which was not warranted.

2.4.2. Quaternary Deposits

The Powder River is an alluvial alley that developed in the Quaternary (Figure 2.5). Three terraces record climatic variations that affected runoff and erosional patterns (Leopold and Miller, 1954). The Kaycee terrace is the uppermost and oldest terrace, which stands approximately 6 to 15 meters above the present stream level (Leopold and Miller, 1954). The Moorcroft terrace is developed into the youngest alluvium of the Kaycee terrace and stands approximately 2.5 to 3.5 m above the present stream level (Leopold and Miller, 1954). The lowest terrace is the Lightning terrace that stands approximately 1 to 2 m above the present stream level (Leopold and Miller, 1954).

Quaternary alluvium of the Powder River alluvial valley can be summarized into four units (Figure 2.5). The oldest unit is the Arvada Formation characterized by highly weathered gravelly sand stained red with many cobbles stained yellow-brown (Leopold and Miller, 1954). The Ucross Formation disconformably overlies the Arvada Formation and is composed of rounded gravels derived from igneous and metamorphic rocks of the Bighorn Mountains. The upper one meter is impregnated with calcium carbonate and gypsum interpreted to be a paleosol (Leopold and Miller, 1954). The Kaycee Formation overlies the Ucross formation and is generally classified as mixed colluvium/alluvium with a highly developed soil layer underlain by well sorted silt-sized quartz grains. The most recent alluvial fill is termed the Lightning Formation consisting of tan fine to medium sand with some fine gravel devoid of bedding planes (Leopold and Miller, 1954). The alluvium overlies thick, blue-gray clay overlying bedrock.

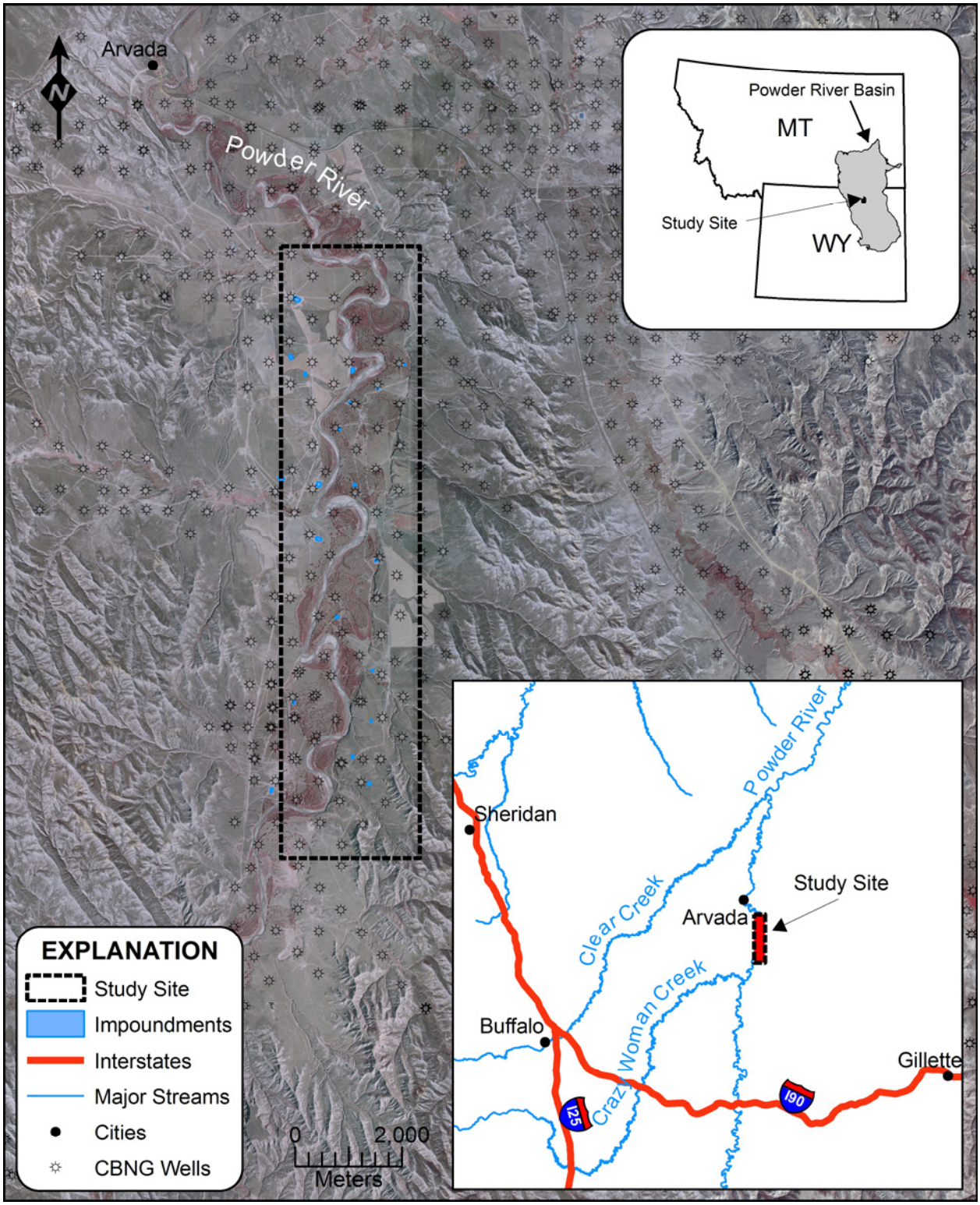

Figure 2.1. Location map of the study area along the Powder River. CBNG produced water impoundments (blue) have been receiving produced water effluent since late 2001 from the Anderson Coalbed.

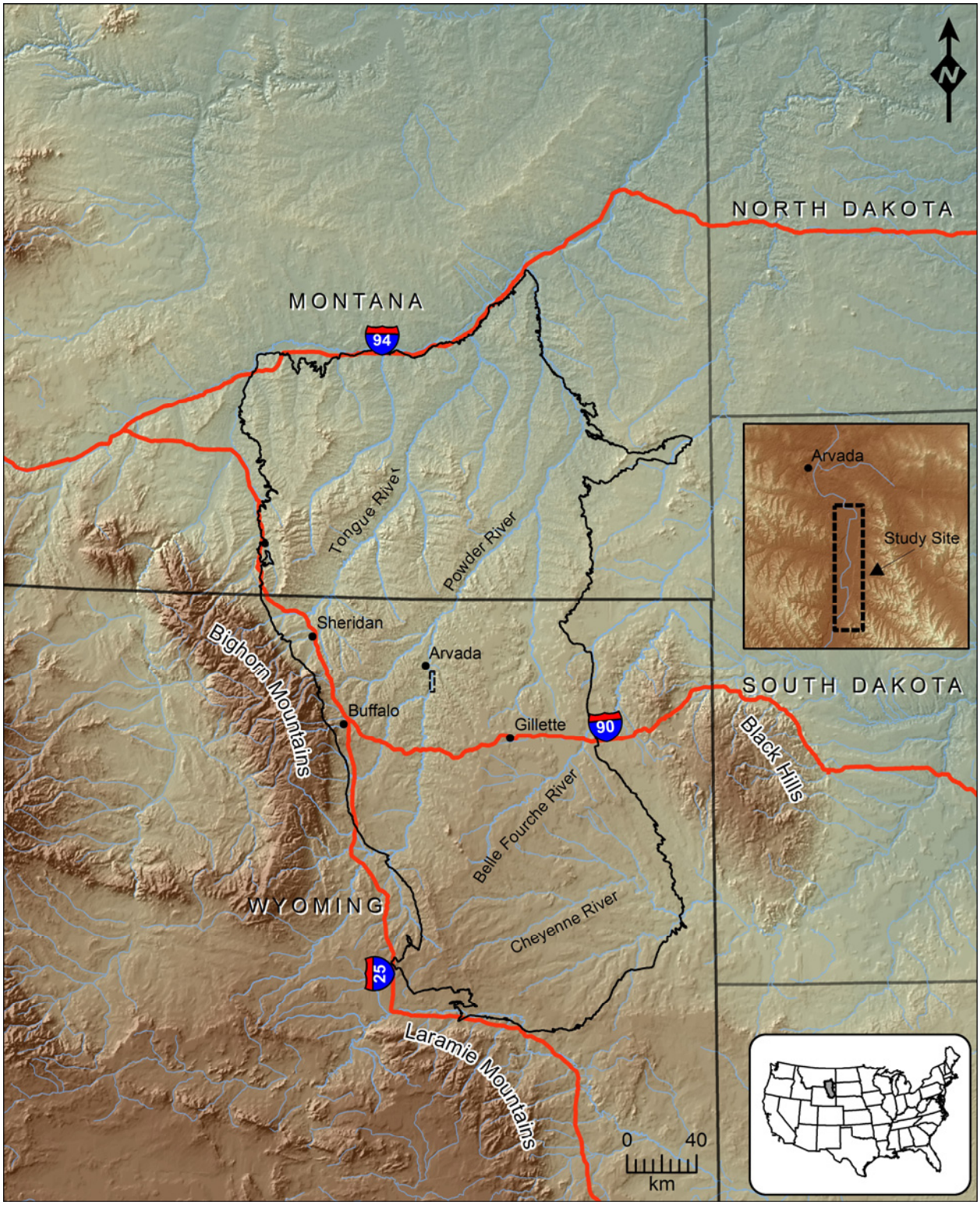

Figure 2.2. Physiography of the study site within the Powder River Basin depicting major topographic and drainage features. Small rectangle approximately 5 km south of Arvada, Wyoming outlines the study area.

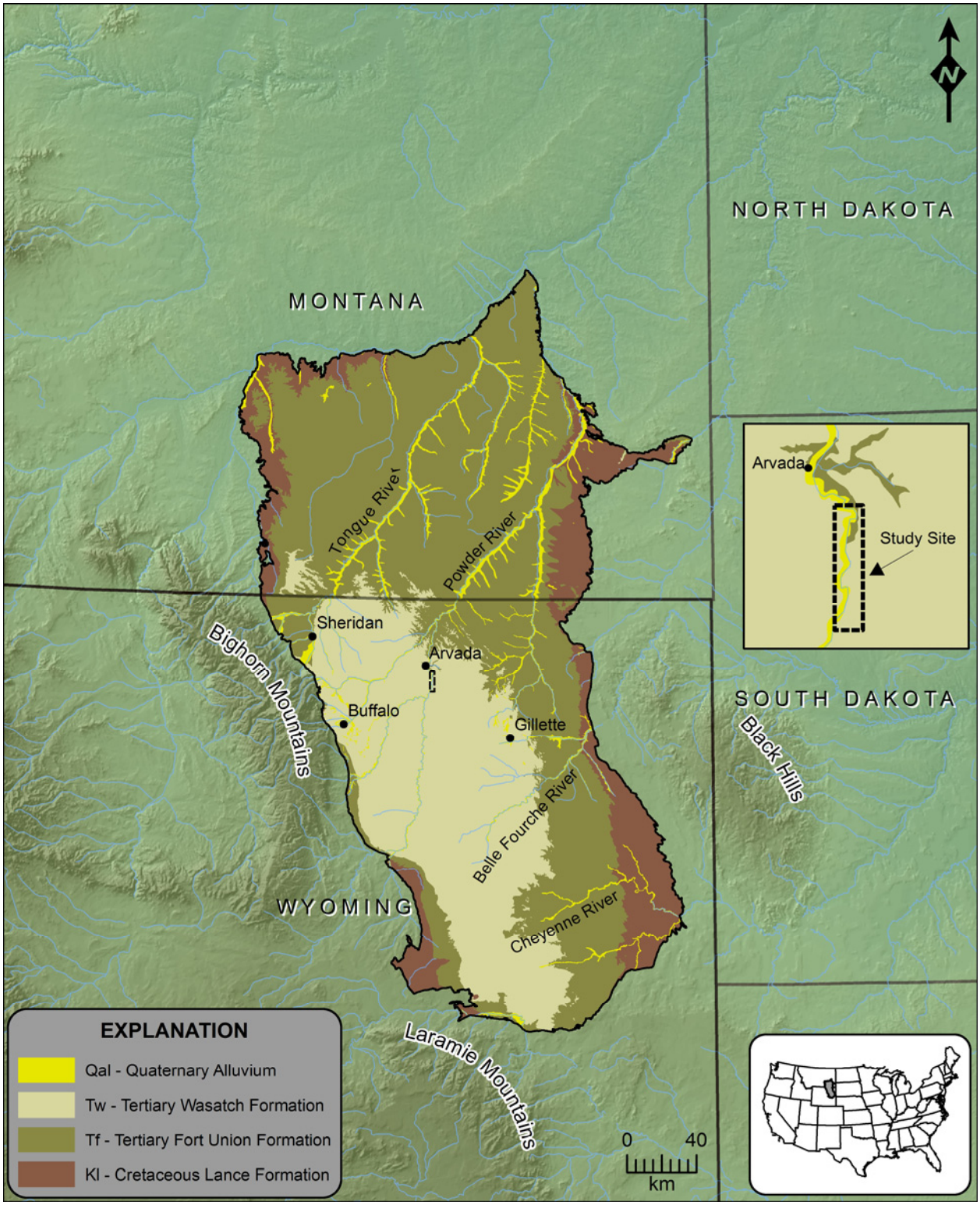

Figure 2.3. Generalized bedrock geology map of the Powder River Basin. Inset map shows exposed geologic units within the study area.

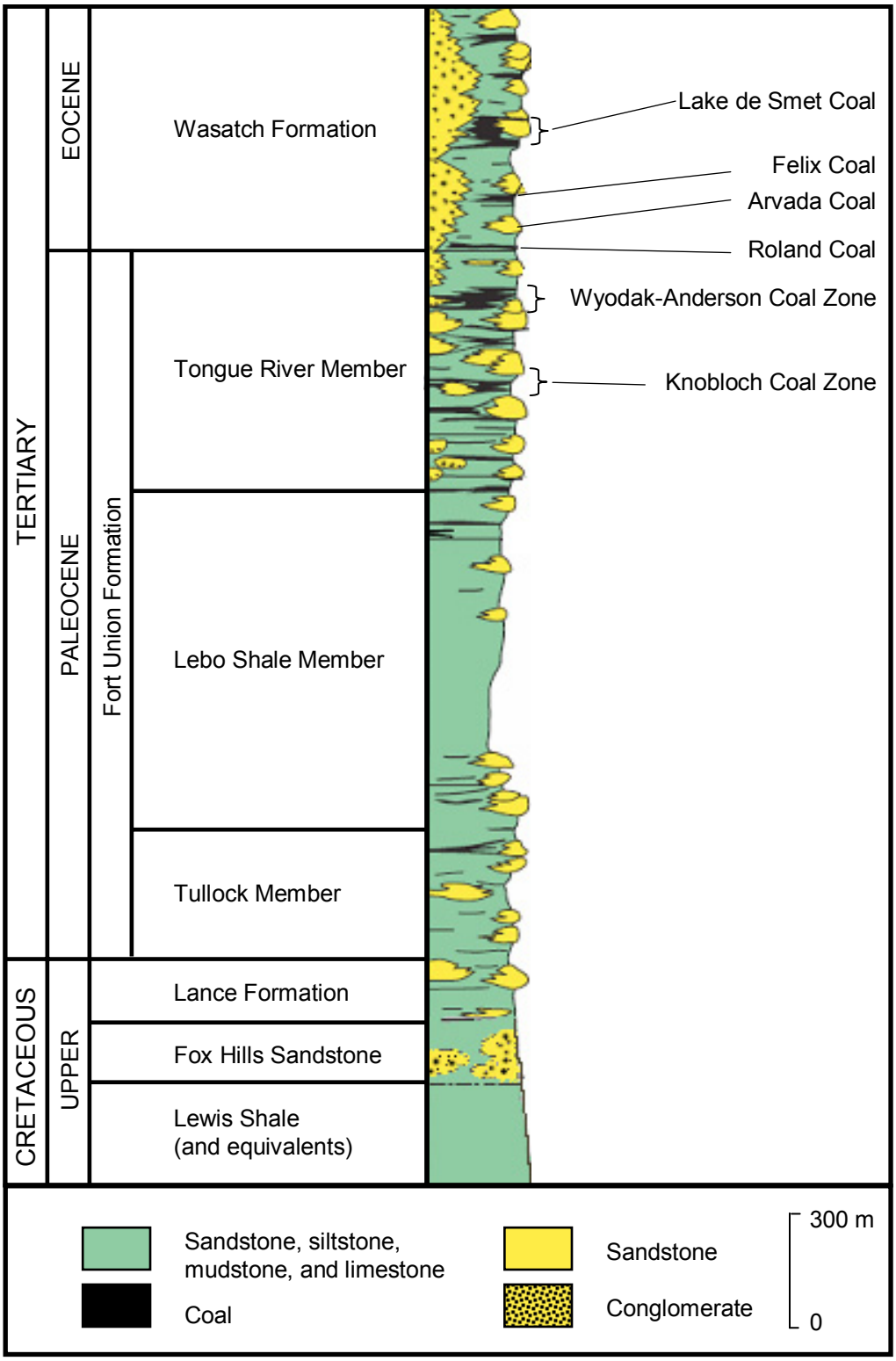

Figure 2.4. Stratigraphic section of Upper Cretaceous and Tertiary rocks in the Powder River Basin (modified from Flores et al., 2004).

2.5. HYDROGEOLOGIC SETTING

Regionally, the PRB is part of the Northern Great Plains Aquifer System. This system underlies most of North Dakota, South Dakota, one-half of Montana, one-third of Wyoming, and extends into Canada (Whitehead, 1996). Aquifer systems are recognized in Lower Tertiary, Upper Cretaceous, Lower Cretaceous, Upper Paleozoic, and Lower Paleozoic strata with the Precambrian granite basement serving as a regional basal confining unit. Paleozoic and Lower Cretaceous aquifers predominantly occur in marine carbonate beds separated from the overlying Upper Cretaceous and Tertiary aquifers by an aquitard composed of the Mowry Shale, Frontier Formation, Cody Shale, Steele Shale, Mesaverde Formation, and Lewis Shale (Whitehead, 1996). Research in the study area was limited to Lower Tertiary and Quaternary aquifers.

2.5.1. Tertiary Aquifers

Aquifers within Lower Tertiary and Upper Cretaceous strata can be subdivided into six distinct hydrostratigraphic units based upon borehole geophysical characteristics (Hotchkiss and Levings, 1986). Previous research suggests that units with more than 50% sand serve as regional aquifers and those that don't are aquitards (Hotchkiss and Levings, 1986). The six units determined using these criteria are the Tongue River-Wasatch (TRW) aquifer, the Lebo confining unit, the Tullock aquifer, the Upper Hell Creek confining unit, the Fox Hills-Lower Hell Creek aquifer, and the Lewis Shale basal confining unit (Figure 2.6). CBNG development is limited to strata within the TRW aquifer.

The TRW aquifer is the shallowest hydrostratigraphic unit in the basin (Bartos and Ogle, 2002; BLM, 2003a, b). Major aquifers are limited to permeable sandstones, coalbeds, and conglomerates. Interbedded mudstone and shale units serve as aquitards. The Wyodak-Anderson coal zone occurs within this hydrostratigraphic unit and is considered the most continuous hydrogeologic unit in the PRB (BLM, 2003a). This aquifer is mainly confined except near recharge and discharge areas where localized water table conditions exist. Recharge occurs in topographically high areas and discharge is mainly to large stream systems (Hinaman, 2005). Groundwater in the TRW generally flows to the northwest (Daddow, 1986).

2.5.2. Quaternary Aquifers

Quaternary alluvium along the Powder River contains a thin, unconfined aquifer. Alluvium ranges in thickness from about 3 to 15 m, but averages 6 m. The aquifer occurs approximately 2 to 3 m below the ground surface, is limited vertically by clay overlying bedrock (Ringen and Daddow, 1990), and extends laterally to the bedrock erosional surface along the Kaycee terrace (Figure 2.7). As such, groundwater within the aquifer generally flows northward at the site mimicking the bedrock topography.

Alluvial aquifer recharge is provided by the Powder River. It is generally considered a losing stream throughout the study area formed by the confluence of the North Fork Powder River, the Middle Fork Powder River, the South Fork Powder River, and Salt Creek south of the study area. The North Fork and Middle Fork of the Powder River contribute approximately 50% of the flow at the study site (Ringen and Daddow, 1990). These streams originate in the Bighorn Mountains as snowmelt runoff, are generally perennial, and have annual hydrographs characterized by a large spring snowmelt peak with little variability in daily discharge throughout the rest of the year (Zelt et al., 1999). The South Fork Powder River contributes approximately 25% of the flow as plains runoff (Ringen and Daddow, 1990). The remaining discharge comes from Salt Creek as plains runoff and brine effluent from the Salt Creek oilfield (Ringen and Daddow, 1990). Streams with plains headwaters are moderately saline and predominantly ephemeral with annual hydrographs characterized by a moderate spring snowmelt peak followed by several short duration storm peaks throughout the remainder of the year (Zelt et al., 1999). At Arvada, the Powder River display characteristics both aforementioned stream types; it is generally perennial but can dry out during the late summer months with poor water quality (Zelt et al., 1999).

Additional recharge to the alluvial aquifer is provided by 21 off-channel infiltration impoundments that have been receiving produced water discharge under Wyoming Pollution Discharge Elimination System Permits (WYPDES) permits since late 2001 and early 2002 (Figure 2.7). Production water is from the Anderson Coal seam of the Fort Union Formation approximately 230 m below grade. Discharge rates into each pond have steadily decreased from approximately 150-200 m^3/s in April 2002 to 1-5 m^3/sec in June 2006.

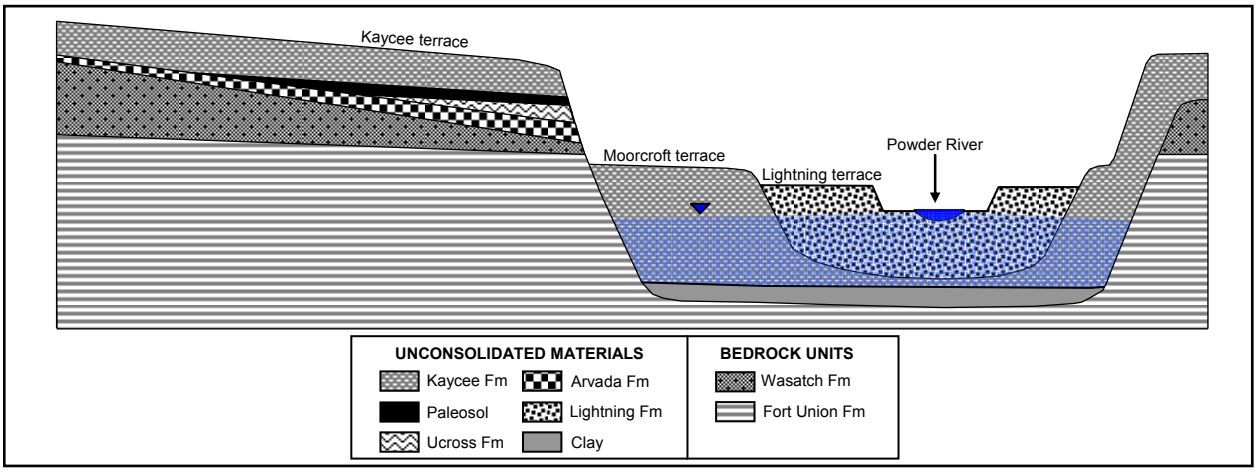

Figure 2.5. Schematic cross-section of the Powder River alluvial valley. The section depicts prototypical deposits characteristic of the Powder River system and the unconfined aquifer domain.

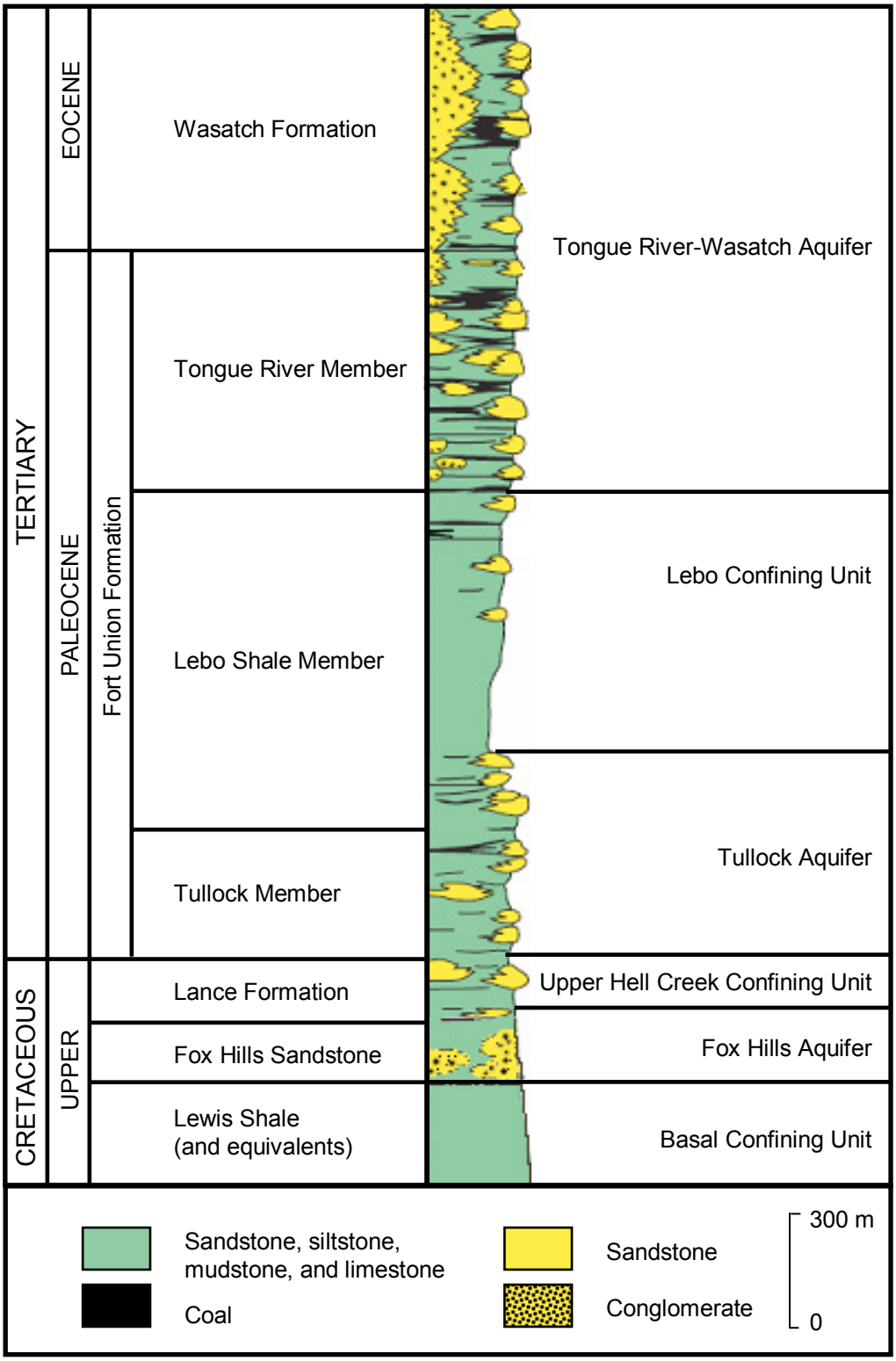

Figure 2.6. The relationship of geologic units to hydrostratigraphic units for Upper Cretaceous and Early Tertiary rocks in the Powder River Basin (modified from Flores et al., 2005 and Hinaman, 2005).

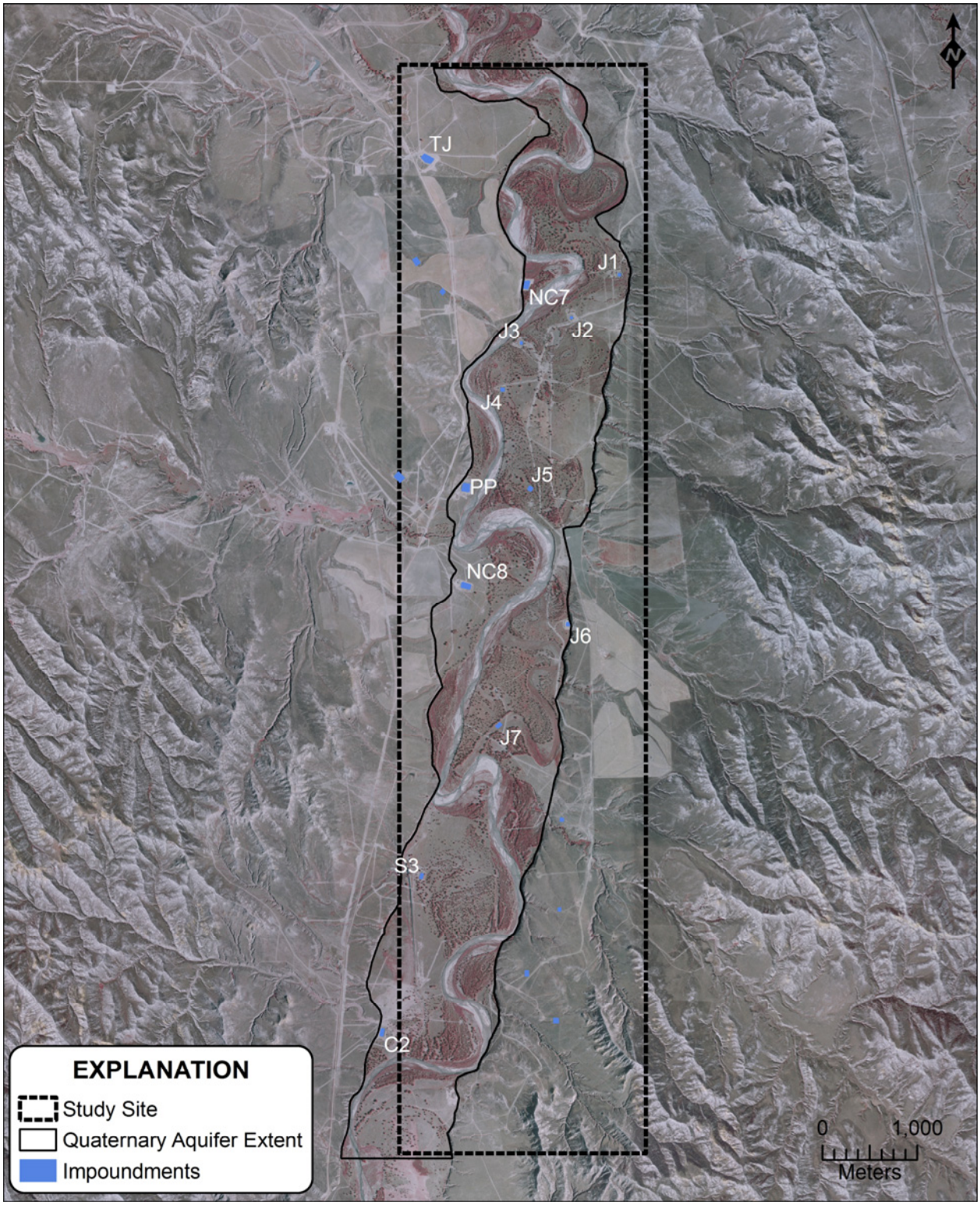

Figure 2.7. Map of the study area depicting CBNG impoundments and the approximate lateral extent of the Quaternary aquifer.

3. GEOPHYSICAL METHODS

3.1. INTRODUCTION

The first objective of this dissertation is to map alluvial aquifer water quality on a sub-regional scale. Traditional approaches to water quality mapping at this scale would be costly and time consuming, therefore an alternative was needed. Geophysical methods have become increasingly important in hydrogeologic investigations to more fully characterize, monitor, and delineate subsurface processes (Rubin and Hubbard, 2005). Hydrogeophysics integrates traditional geophysical methods used in the mining and petroleum industries to solve hydrologic problems. The choice of geophysical method depends on study scale and study objective. After considering the dissertation objective and available techniques (Figure 3.1 and Table 3.1), it was determined that the airborne electromagnetic (AEM) geophysical method best supports this research.

3.2. ELECTROMAGNETIC INDUCTION PRINCIPLES

3.2.1. Theory of Operation

Electromagnetic (EM) induction methods involve measuring the ground response to propagating electromagnetic fields. EM fields are composed of alternating electrical intensity and magnetizing forces. The primary EM field (in-phase) is typically generated by passing an alternating current through a small wire coil composed of many turns, which is termed the transmitter. The primary EM field propagates from the transmitter to the receiver through the air and subsurface. If the ground is geoelectrically homogeneous, then no difference in the primary

field is observed at the receiver other than a small decrease in signal amplitude. If an electrically conductive subsurface body is present, the magnetic component of the EM field induces eddy currents in closed loops within the conductive body normal to the primary EM field. Eddy currents subsequently generate their own secondary EM field, also known as the quadrature field (Figure 3.2). As a result, the total EM field at any point in space is the sum of the primary EM field generated by the transmitter and a secondary EM field generated by eddy currents. The receiver response of the secondary field differs in both phase and amplitude from the primary field. These differences ultimately reveal the subsurface electrical properties.

The induced current flow is purely caused by the EM field and neither the transmitter nor receiver need to be in physical contact with the ground surface (Reynolds, 1997). This feature is one of the main advantages to using EM methods over classical electrical methods. EM instruments can be deployed in portable handheld units, mounted on aircraft, or hung as a sling load from helicopters. It is for these reasons that AEM methods were initially developed to locate large ore bodies in remote regions such as Alaska and Canada (Fountain, 1998).

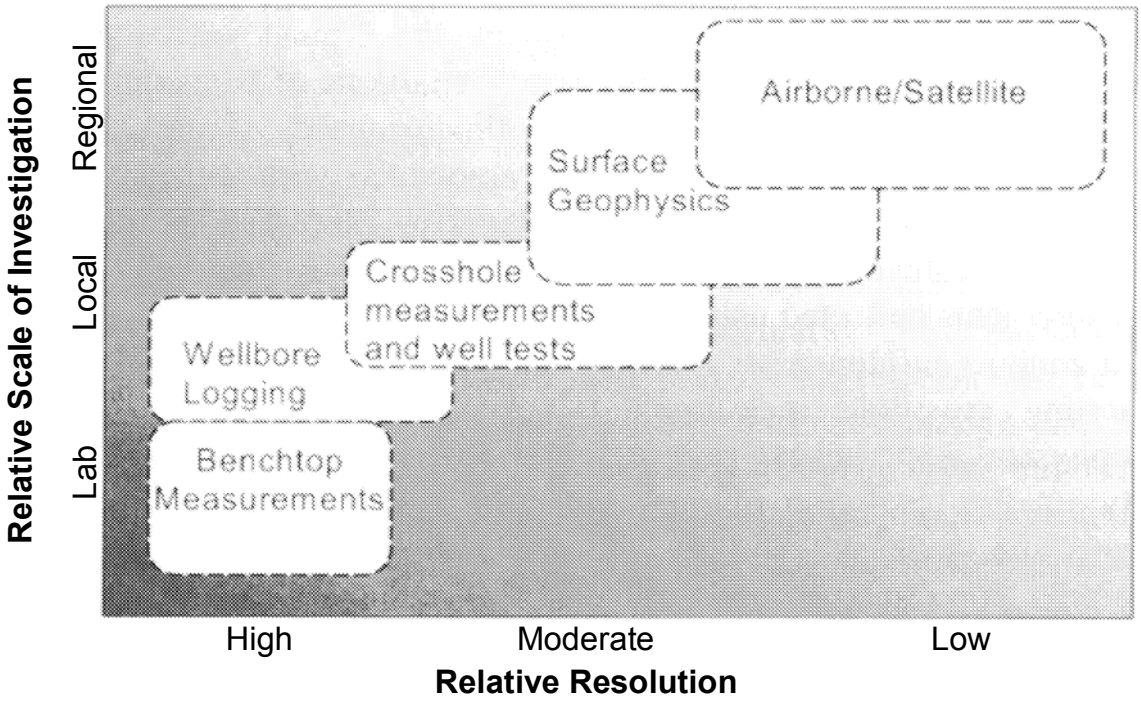

Figure 3.1. The relationship between study scale and resolution for various geophysical methods (modified from Rubin and Hubbard, 2005).

Table 3.1. Geophysical methods commonly used in hydrogeologic applications (modified from Rubin and Hubbard, 2005).

Method	Mapping Objective	Hydrologic Parameter	Field Implementation
Electrical Resistivity	Subsurface Geometry Water Table	Water Content Water Quality	Ground
Electromagnetic	Subsurface Geometry Water Table Bedrock Surface Plume Boundaries	Water Content Water Quality	Ground Airborne
Ground Penetrating Radar	Subsurface Geometry Water Table Plume Boundaries	Water Content Water Quality Spatial Correlation	Ground
Seismic Reflection	Subsurface Geometry Water Table	Permeability Spatial Correlation	Ground
Magnetics	Bedrock Surface Faults/Fracture Zones	None	Ground Airborne
Gamma-Ray Spectroscopy	Subsurface Geometry Bedrock Surface	None	Ground Airborne

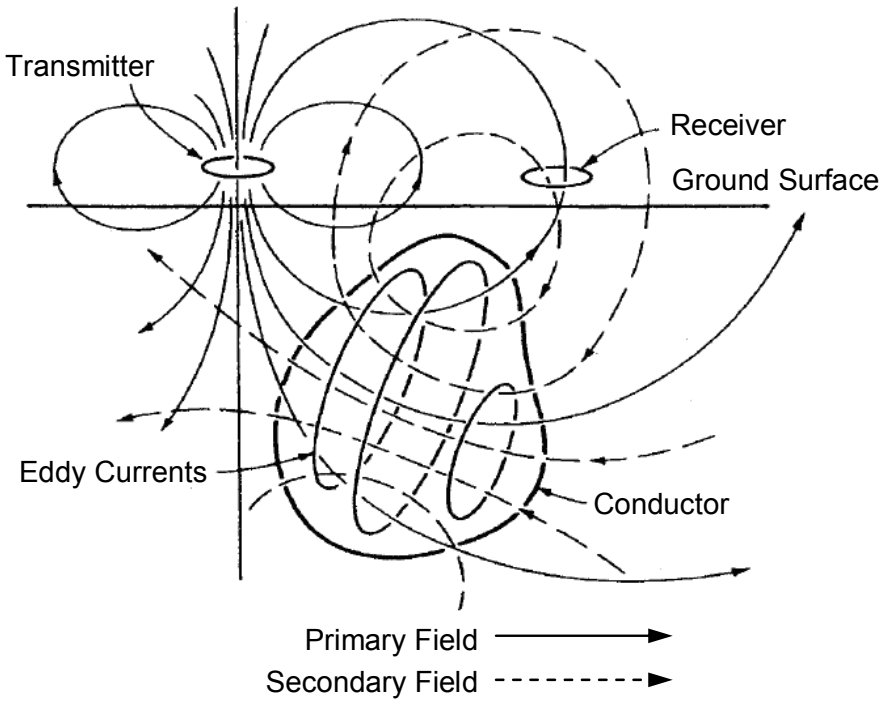

Figure 3.2. Conceptualization of the electromagnetic induction method (modified from Reynolds, 1997).

3.2.2. Electrical Properties of Earth Materials

The behavior of electromagnetic fields in earth materials is controlled by resistivity, dielectric permittivity, and magnetic permeability (Keller and Frischknecht, 1966). Resistivity is the resistance of the material to current flow. Environmental investigations often use conductivity (the inverse of resistivity) as a material property to infer subsurface characteristics. The dielectric permittivity of a material is the relative degree of polarizability. Magnetic permeability is the ratio of the magnetic induction to the inducing magnetic field. In areas characterized by moderate to high ground conductivities, the dielectric permittivity and magnetic susceptibility are negligible (Farquharson et al., 2003; Huang and Fraser, 2001).

Electrical properties of rock forming minerals are variable. Minerals conduct electricity through electronic and/or ionic processes. Accordingly, solid materials are classified as metals, semiconductors, or solid electrolytes. Metals conduct electricity through the movement of valence electrons from adjacent atoms, which requires minimal energy making metallic deposits highly conductive. Semiconductors transmit electricity in a similar manner as metals, but there are fewer mobile valence electrons making these materials less conductive. Most rock-forming minerals are solid electrolytes. In these materials, electricity moves through the transfer of valence electrons in ionic substances. Most movement occurs in crystal lattice defects. The conductivity of these materials is proportional to the number of charge carriers available.

Electrical properties of rocks are not solely controlled by the minerals comprising them. Near surface rocks are porous and partially filled with water. Fluids containing dissolved salts generally exhibit a far greater capacity to move electrical currents relative to dry bulk media. As a result, the bulk conductivity of rocks is not only a function of mineralogy, but also porosity, moisture content, and porewater salinity. Archie (1942) developed an empirical formula (Archie's Law) that mathematically described the effective resistivity of a bulk medium as:

$$\rho = a\rho_w\phi^{-m}$$

where:

ρ = bulk resistivity
a = saturation coefficient
ρ_w = porewater resistivity
ϕ = porosity
m = cementation factor

Archie's Law was developed by the petroleum industry to relate pore water resistivity measurements to rock resistivity values (Keller and Frischknecht, 1966). The most commonly encountered deviation from this law occurs where there is a significant quantity of clay present in the rock/sediments. It has been observed that the most important parameter in Archie's law is the porewater resistivity. The values of *a* and *m* have very little control on the results (Keller and Frischknecht, 1966).

3.2.3. Depth of Investigation

The maximum depth achieved by a propagating EM field dictates the depth of investigation. EM fields are attenuated exponentially in the subsurface as they propagate from a source. The depth of penetration occurs when the amplitude of the input field is decreased by a factor of 1/e. Mathematically, this is referred to as the skin depth (Spies, 1989), which is defined as:

$$d = \frac{503.8}{\sqrt{\sigma f}}$$

where:

d = the depth of EM field penetration (m)
σ = the ground conductivity (S/m)
f = the frequency of the EM field (Hz)

Although the skin depth is a theoretical concept, evaluation of the above equation reveals that penetration depth increases with decreasing frequency and ground conductivity. A more useful approximation of EM field penetration is defined as the effective depth of penetration (z_e). It is the maximum depth at which a conductor can produce a detectable EM anomaly, and is:

$$z_e \approx \frac{100}{\sqrt{\sigma f}}$$

where:

z_e = effective depth of EM field penetration (m)
σ = the ground conductivity (S/m)
f = the frequency of the EM field (Hz)

3.3. AIRBORNE ELECTROMAGNETIC SURVEY

3.3.1. Data Collection

Airborne electromagnetic data were collected within the study area on July 25, 2003 and July 31, 2004 by Fugro Airborne Surveys using the RESOLVE system (Table 3.2 and Figure 3.3) (Cain, 2003, 2004). The system consists of five coplanar transmitter/receiver (Tx/Rx) coil pairs separated by 7.9 m and one coaxial Tx/Rx coil pair separated by 9 m housed within a Kevlar gondola. The frequencies are logarithmically spaced and range from approximately 400 Hz to 132 KHz (Table 3.2). The gondola was attached to an AS350-B3 helicopter by a cable measuring 28.7 m shortened by wind resistance to approximately 27.7 m. Helicopter elevation was determined using a laser altimeter with backup barometric altimeter. The instrument was flown approximately 33 to 35 m above ground during both surveys. A high accuracy (±2 m) differential GPS was used to determine spatial location. Survey lines were oriented north-south and nominally spaced 50 m apart. Data were collected at a horizontal spatial frequency of 10 Hz producing soundings approximately every 3.5 meters. Recorded data consisted of inphase/quadrature amplitudes of the secondary magnetic field normalized by the primary field.

Survey areas did not overlap each year (Figure 3.4). The 2004 survey was flown to evaluate water quality changes and to evaluate data reproducibility. As such, the 2004 survey was smaller than the 2003 survey and was moved northward for anticipated CBNG development. Only data collected within the Quaternary aquifer boundary were retained in this study.

Table 3.2. Parameters for the 2003 and 2004 Fugro Airborne RESOLVE surveys at the study site.

Parameter	2003 Survey	2004 Survey
Coplanar Tx/Rx	387, 1700, 6536, 28120, 116300 Hz	391, 1801, 8162, 39130, 132640 Hz
Coaxial Tx/Rx	1413 Hz	3326 Hz
Line Direction	0-180º	0-180º
Line Spacing	50 m	50 m
Tx/Rx Height	35 m	33 m
Line Coverage	508.3 km	224.5 km
Sample Rate	10 Hz	10 Hz

Figure 3.3. The FUGRO Airborne RESOLVE system (photograph by Terry Ackman).

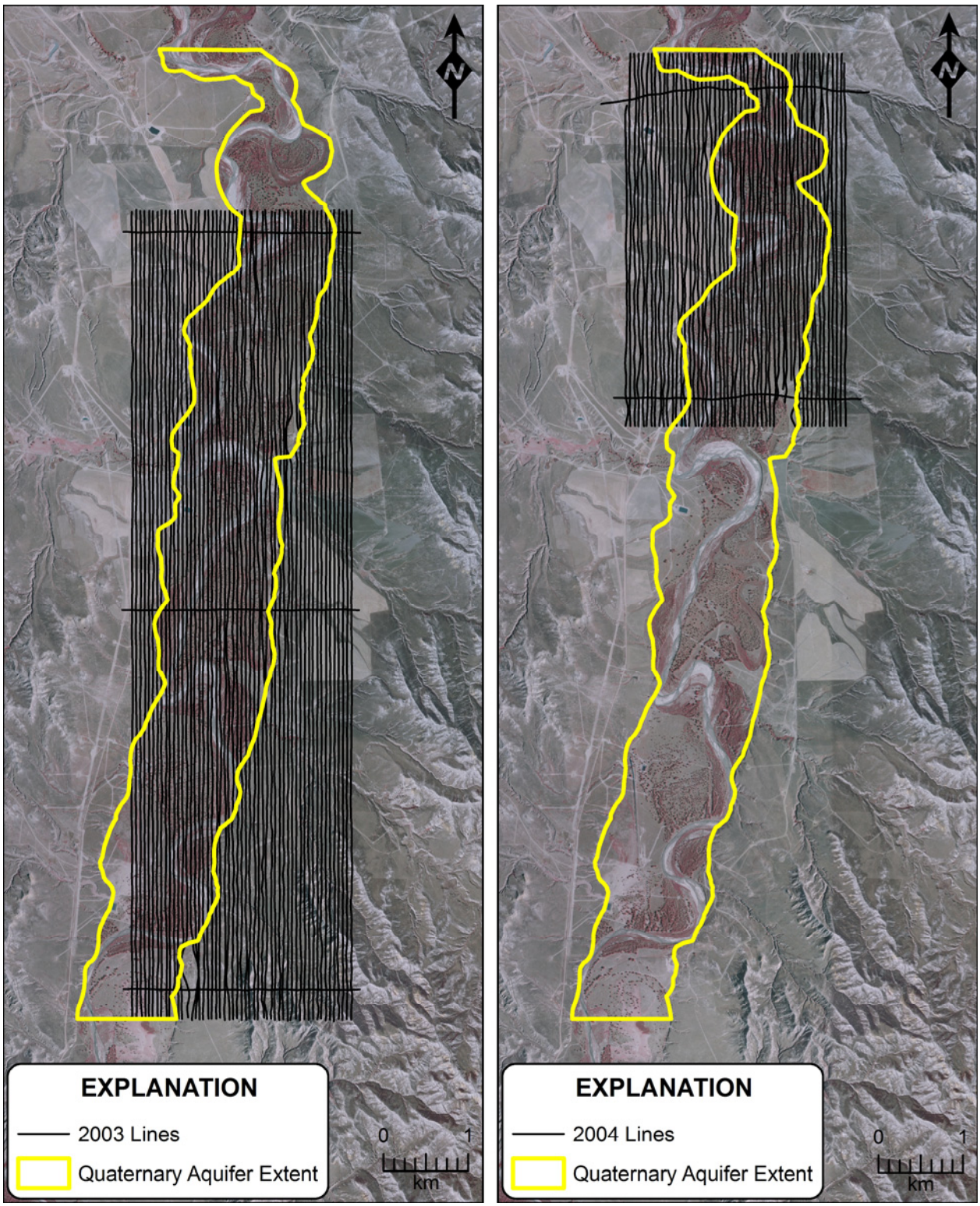

Figure 3.4. Flight lines for the 2003 and 2004 airborne electromagnetic surveys. Only data within the boundary of the Quaternary aquifer were evaluated.

3.3.2. System Calibration

The RESOLVE instrument was calibrated using the Fugro internal calibration procedure (Cain, 2003, 2004). Prior to the survey, at specified intervals during the survey, and after the survey, the instrument was flown to an altitude high enough that no ground effect was recorded. Any remaining signal was measured as the zero level and removed from the data until the next calibration. After zeroing the instrument, internal calibration coils were triggered. There is a calibration coil for each frequency for which the phase and amplitude response have been determined at the factory. The receiver phase angle and amplitude response to each calibration coil was compared to the factory calibrated response and phase/gain corrections were applied to adjust the instrument. In addition, transmitter output was continuously monitored during the survey and gains were applied to correct deviations. Because the internal calibration coils are calibrated at the factory, on-site ground calibrations using external coils are not necessary.

3.3.3. Quality Assurance and Quality Control

Standard quality assurance and quality control measures were implemented by the airborne data contractor prior to data delivery. Data were base leveled in the field to remove drift effects arising from temperature fluctuations. Low frequency spikes were removed using a spheric rejection median filter (Cain, 2003, 2004). High frequency noise was removed using a low pass spatial-domain filter with Hanning coefficients at the roll-off (Cain, 2003, 2004). Preliminary apparent resistivity maps were calculated using a proprietary pseudo-layer half-space model (Fraser, 1978). These preliminary maps were carefully inspected to identify line-to-line differences arising from subtle changes between in-flight calibrations. The inphase/quadrature data were micro-leveled to remove the resultant differences.

Further quality control measures were completed after data delivery to remove cultural noise. A high sensitivity cesium magnetometer was housed within the RESOLVE instrument that measured the total magnetic field with a sensitivity of 0.01 nT. This allowed for identification of well casings, pipelines, and other non-geologic features. Additionally, a coplanar power line monitor recorded the intensity of the secondary EM field at 60 Hz. Data were culled where

power line and magnetic anomalies occurred. The result was a leveled dataset free of known cultural interferences.

3.4. AIRBORNE ELECTROMAGNETIC DATA PROCESSING

3.4.1. Geophysical Inversion

Inversion algorithms were used to determine the subsurface electrical conductivity distribution at the site. The inverse problem involves determining the earth conductivity structure that produced observations measured by the RESOLVE system. Inversion were implemented utilizing EM1DFM software (UBC-GIF, 2000). EM1DFM uses an Occam's inversion routine; i.e. it attempts to fit a modeled response to the observed signal for a defined source/receiver while also computing an error term with a model smoothness constraint allowing for model evaluation (Constable et al., 1987). Inputs required for the program are the inphase and/or quadrature response of the secondary magnetic field, transmitter/receiver geometry, instrument altitude, and data error. The inversion is a one-dimensional (1D) scheme as data from adjacent soundings are not used. The 1D assumption is considered valid in sedimentary environments where lateral changes in geology are gradational. A reasonable pseudo-2D cross section can be formulated by stitching the soundings together as part of a post-processing routine. For a detailed summary of EM1DFM, please refer to http://www.eos.ubc.ca/ubcgif/iag/sftwrdocs/em1dfm/em1d-man.html.

The inversion problem is posed in EM1DFM as an optimization scheme mathematically defined as follows:

$$\Phi = \phi_d - \beta\phi_m$$

where:

Φ = model objective function
ϕ_d = model misfit
ϕ_m = model norm
β = tradeoff parameter

The model misfit is calculated as an l_2-norm (sum-of-squared differences) between computed and observed data. The model norm is used to determine the appropriate amount of model

structure. It can be adjusted to force the inversion to produce an earth model that contains only enough features to reproduce the observations, or it can be used to quantify a difference between a preconceived subsurface image in which case the computed model is similar to the user-supplied reference model. The tradeoff parameter (regularization parameter) balances opposing model tendencies to minimize the misfit and simplify the model.

The regularization parameter exerts the most significant influence on EM1DFM results. There are four methods of assigning β in EM1DFM: (1) fixed tradeoff (FTO), (2) discrepancy principle, (3) L-curve, and (4) Generalized Cross-Validation (GCV) criterion. The FTO method is implemented when the user assigns β. The discrepancy principle algorithm adjusts β until data misfit at each sounding is less than the number of observations. It is generally only used in theoretical studies where data errors are known (Farquharson and Oldenburg, 2004). In the L-curve method, EM1DFM creates a log-log plot of data misfit versus model norm and numerically finds the point of maximum curvature. This point is thought to correspond to equal emphasis of data misfit and model structure on the inversion (Farquharson and Oldenburg, 2004). The GCV-criterion algorithm computes the data misfit after leaving out each data point and assigns β as the value that produced the minimum misfit. The L-curve and GCV method produce similar results. However, the L-curve method can have convergence problems associated with numerical noise and the GCV criterion can "over-fit" data. Over-fitting occurs when data misfit is significantly less than the number of observations, which has been interpreted to result from abnormal conductivity models that represent noise instead of geologic information (Farquharson and Oldenburg, 2004). A suggested modeling approach is to complete trial inversions using the GCVcriterion, choose β from inversions where over-fitting is not observed, and then assign this value using the FTO algorithm for all inversions (Farquharson, 2005).

Several trial simulations were completed to determine a suitable regularization parameter and data error value before modeling the entire dataset. This process was completed for the 2003 and 2004 surveys, but only a description for 2003 is given. No prior information was known about the subsurface electrical structure at the site. As a result, the model norm components were set to fit the observations with the simplest model structure. This also ensured that starting/reference models had little impact on final results (because they are unknown). Trial runs indicated that β was in the range of 1 to 10. Because the misfit is a sum of squares term, differences can not be seen unless β is changed by an order of magnitude (Farquharson, 2005).

Therefore, simulations were completed with β set to 1, 10, and 100. Data errors were adjusted between 1%, 5%, and 10%. The inversions were performed on layered earth of 80, one meter thick layers. In addition to the inverted sections, a differential conductivity section was plotted by calculating the differential depth/conductivity pairs according to Huang and Fraser (1996) and then fitting a tension spline curve to these points. Data below the deepest differential depth point were culled in all conductivity sections.

Test inversions were evaluated by comparing the data misfit values (Table 3.3) and conductivity sections to the differential section (Figure 3.5, Figure 3.6, and Figure 3.7). The differential parameter method has been shown to give a good approximation of the true geoelectric distribution (Beamish, 2002; Huang and Fraser, 1996). Review of the various conductivity depth sections shows that the inversions are not overly sensitive to the adjusted parameters. The conductivity models have similar structures varying mostly in the range of computed values, but the data misfits reveal subtle differences. Average misfits are significantly more than the number of observations (10) for $\beta = 1$ with 1% error, $\beta = 10$ with 1% and 10% error, and $\beta = 100$ for all errors. Additionally, for $\beta = 1$ with 5% and 10% error, average misfits are significantly less than the number of observations indicating data over-fit. For $\beta = 10$ with 5% data error, average misfits are slightly less than the number of observations indicating optimal results. As a result, the final model parameters were $\beta = 10$ with 5% data error. A similar analysis on 2004 data revealed that $\beta = 10$ and 5% data error were the most appropriate values.

Table 3.3. Summary of misfit as the regularization parameter and data error were adjusted during EM1DFM inversions. The optimal results are highlighted.

β		Misfit (1%)	Misfit (5%)	Misfit (10%)
1	minimum	1.6	0.5	0.3
	maximum	816.4	37379.0	10.9
	average	16.3	1.6	1.1
10	minimum	5.8	1.5	24.6
	maximum	879.3	50.5	966.3
	average	25.4	9.7	77.9
100	minimum	25.3	4.4	4.4
	maximum	1088.2	222.0	180.5
	average	110.4	63.0	33.5

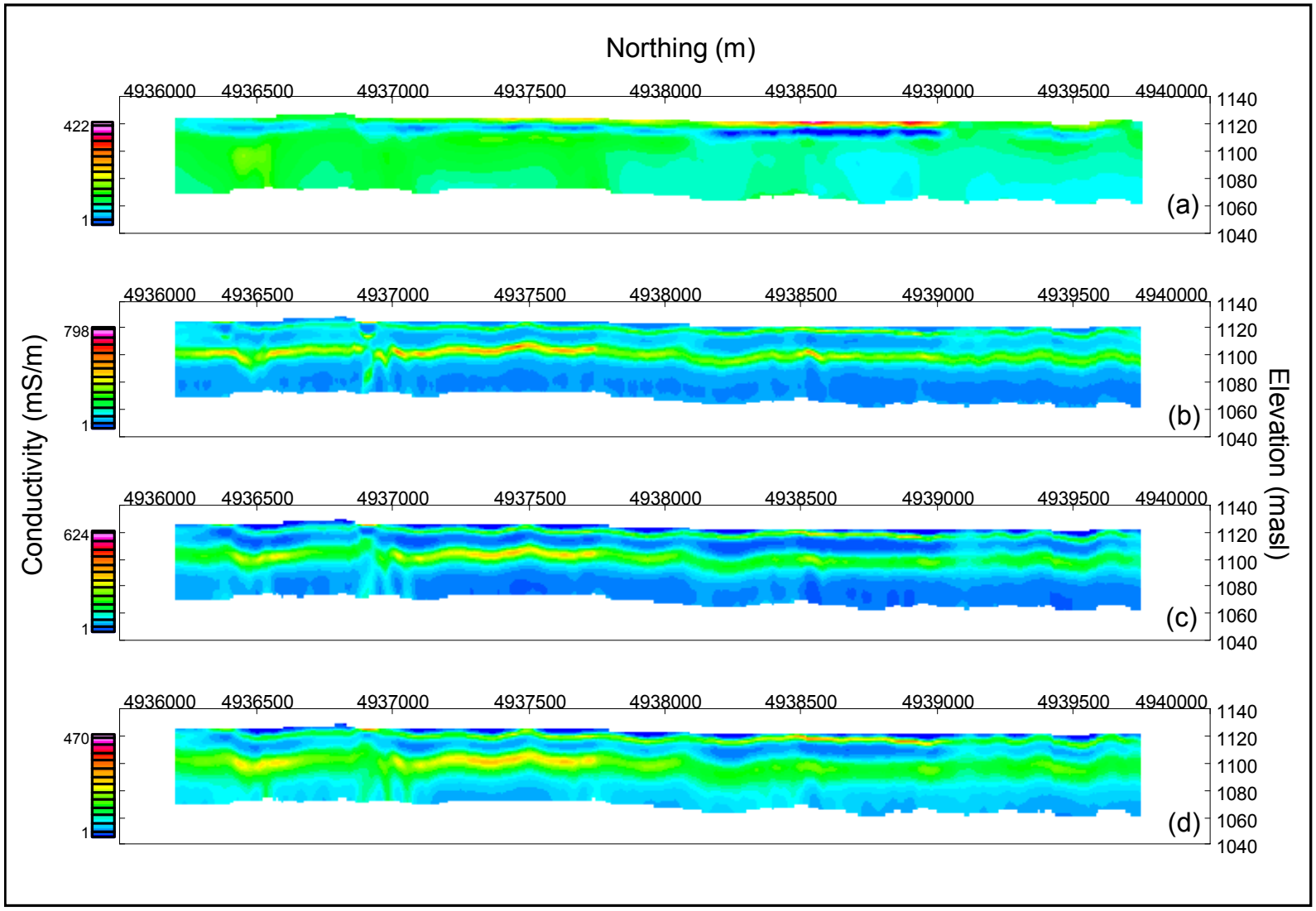

Figure 3.5. The effect of varying data error on model results for a fixed tradeoff parameter of 1. (a) Conductivity model constructed using the differential parameter method. (b) Conductivity model from EM1DFM with 1% data error. (c) Conductivity model from EM1DFM with 5% data error. (d) Conductivity model from EM1DFM with 10% data error.

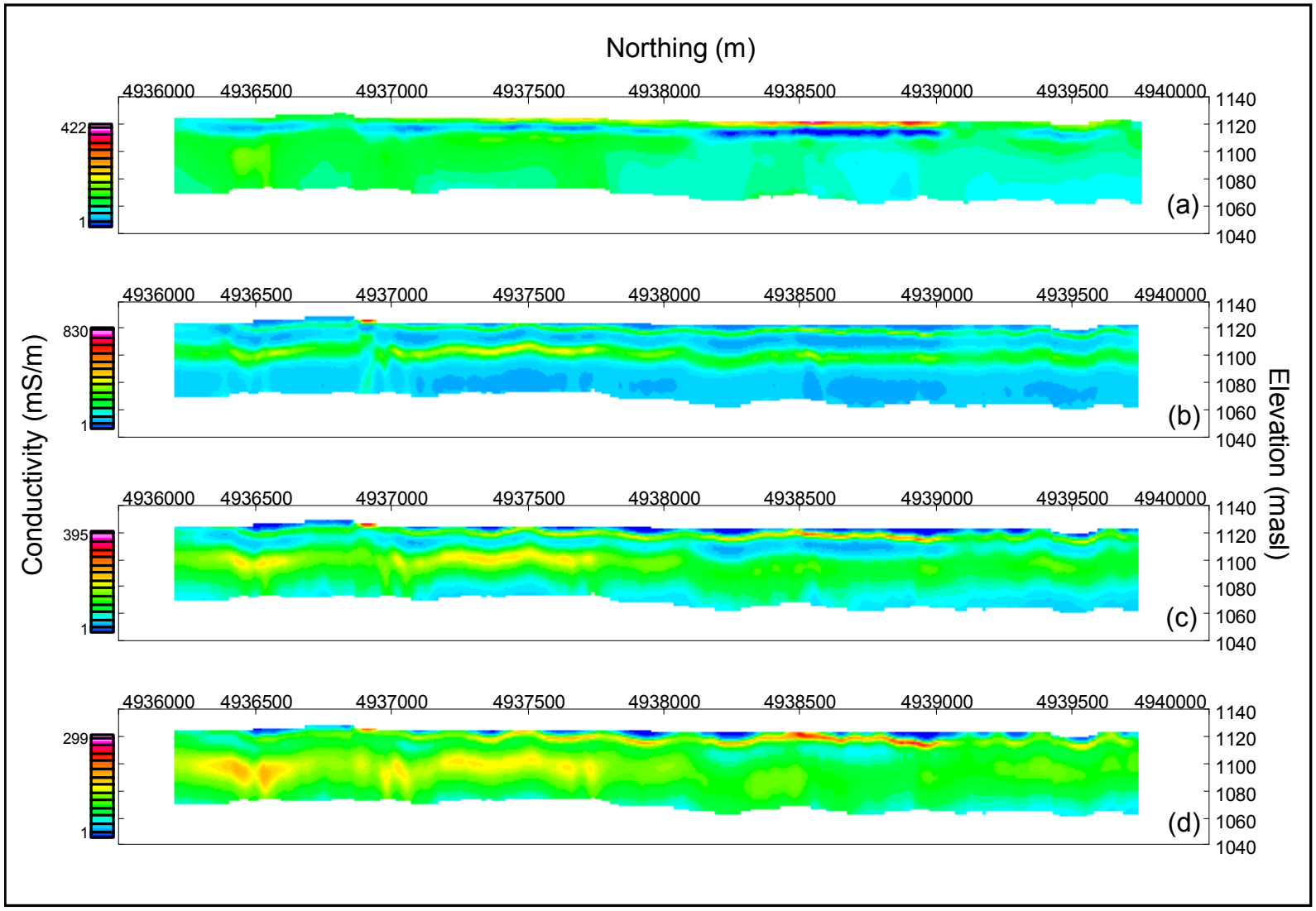

Figure 3.6. The effect of varying data error on model results for a fixed tradeoff parameter of 10. (a) Conductivity model constructed using the differential parameter method. (b) Conductivity model from EM1DFM with 1% data error. (c) Conductivity model from EM1DFM with 5% data error. (d) Conductivity model from EM1DFM with 10% data error.

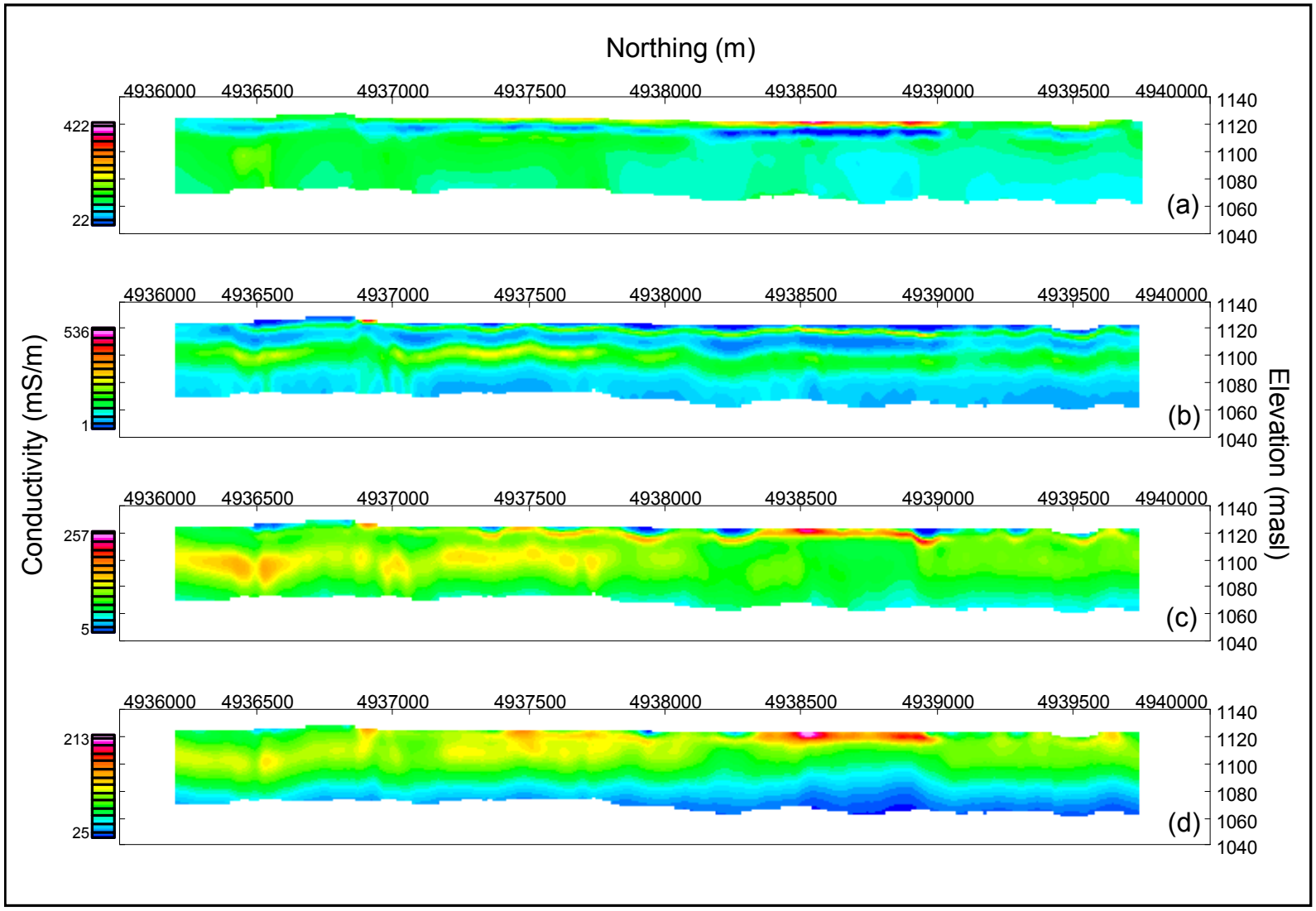

Figure 3.7. The effect of varying data error on model results for a fixed tradeoff parameter of 100. (a) Conductivity model constructed using the differential parameter method. (b) Conductivity model from EM1DFM with 1% data error. (c) Conductivity model from EM1DFM with 5% data error. (d) Conductivity model from EM1DFM with 10% data error.

3.4.2. Correlating Geophysical and Geochemical Data

AEM data were correlated to TDS levels by comparing inversion results to porewater electrical conductivity (EC) measured in several monitoring wells screened into the alluvial aquifer (Table 3.4 and Figure 3.8). Groundwater samples were collected within the study area on July 17-18, 2003 and September 29-30, 2004 by Pennaco Energy Incorporated (PEI). Although groundwater data were collected approximately two months after the 2004 flight, TDS levels changed by less than 5% from a May 28, 2004 sampling event. The formation conductivity at each well was taken as the peak inversion conductivity value within the saturated zone. The formation response was plotted against porewater EC measured during the corresponding groundwater sampling event (Figure 3.9a). Regression analysis was performed and an empirical relationship for each survey was developed. Additionally, measured porewater EC was correlated to measured TDS concentrations for the combined events (Figure 3.9b). The equations relating geophysical response to measured porewater EC for each survey and measured porewater EC to measured porewater salinity (TDS) using the data given in Table 3.4 are presented below:

2003 AEM:	$\sigma_w = 8.03\sigma_f^{1.14}$
2004 AEM:	$\sigma_w = 4.14\sigma_f^{1.42}$
Both Surveys	$TDS = 0.80\sigma_w$

where:

σ_w = porewater conductivity (μS/cm)
σ_f = formation conductivity (mS/m)
TDS = total dissolved solids (mg/L)

An important observation made when comparing the 2003 and 2004 AEM formation-to-porewater correlations is that there is a shift, or offset, between the two years (Figure 3.9a). One would expect the relationship for both years to fall on the same trend line. While the slopes for both years are approximately equal, their abscissa-intercept values are shifted. This indicates that the formation/salinity regression curves are specific to the respective flights. The shift may have resulted from a calibration difference between surveys

The site-specific formation conductivity/salinity relationships were used to convert model conductivities to inferred TDS values in the alluvial aquifer for the entire 2003 and 2004 surveys. The formation conductivity at each sounding was extracted from within the saturated zone of the alluvial aquifer (between the water table and bedrock surface as interpolated from site monitoring wells). The saturated zone was laterally defined as the eastern and western Kaycee escarpments (Figure 3.8). Calculated TDS values in the alluvial aquifer were interpolated to a 10 m grid using a modified Akima spline algorithm in Geosoft® for visualization.

Table 3.4. Water quality parameters measured from monitoring wells within the study area and corresponding formation conductivity derived from inversion of airborne geophysical survey data.

	2003 AEM Survey			2004 AEM Survey		
Well	σ_w (μS/cm)	TDS (mg/L)	σ_f (mS/m)	σ_w (μS/cm)	TDS (mg/L)	σ_f (mS/m)
J3W1	2310	1520	153	2970	1980	100
J3W2	2600	1780	209	3530	2520	113
J3W3	5290	4200	316	4190	3190	139
J3W4	6850	5300	359	5240	3870	166
J3W5	8080	6640	374	8010	6600	185
J5W1	3740	2780	212	3120	2250	123
J5W2	5090	4490	NA	OA	OA	OA
J5W3	2760	2080	140	2860	2190	94
J5W4	2650	1990	144	2640	2020	98
J5W5	3130	2430	230	3110	2410	109
J7W1	3080	2340	182	OA	OA	OA
J7W2	5530	4700	240	OA	OA	OA
J7W3	3130	2450	197	OA	OA	OA
J7W4	4910	4090	248	OA	OA	OA
NA	Not Available, AEM data were contaminated with power line noise					
OA	Out of Area, AEM survey did not extend this far south					

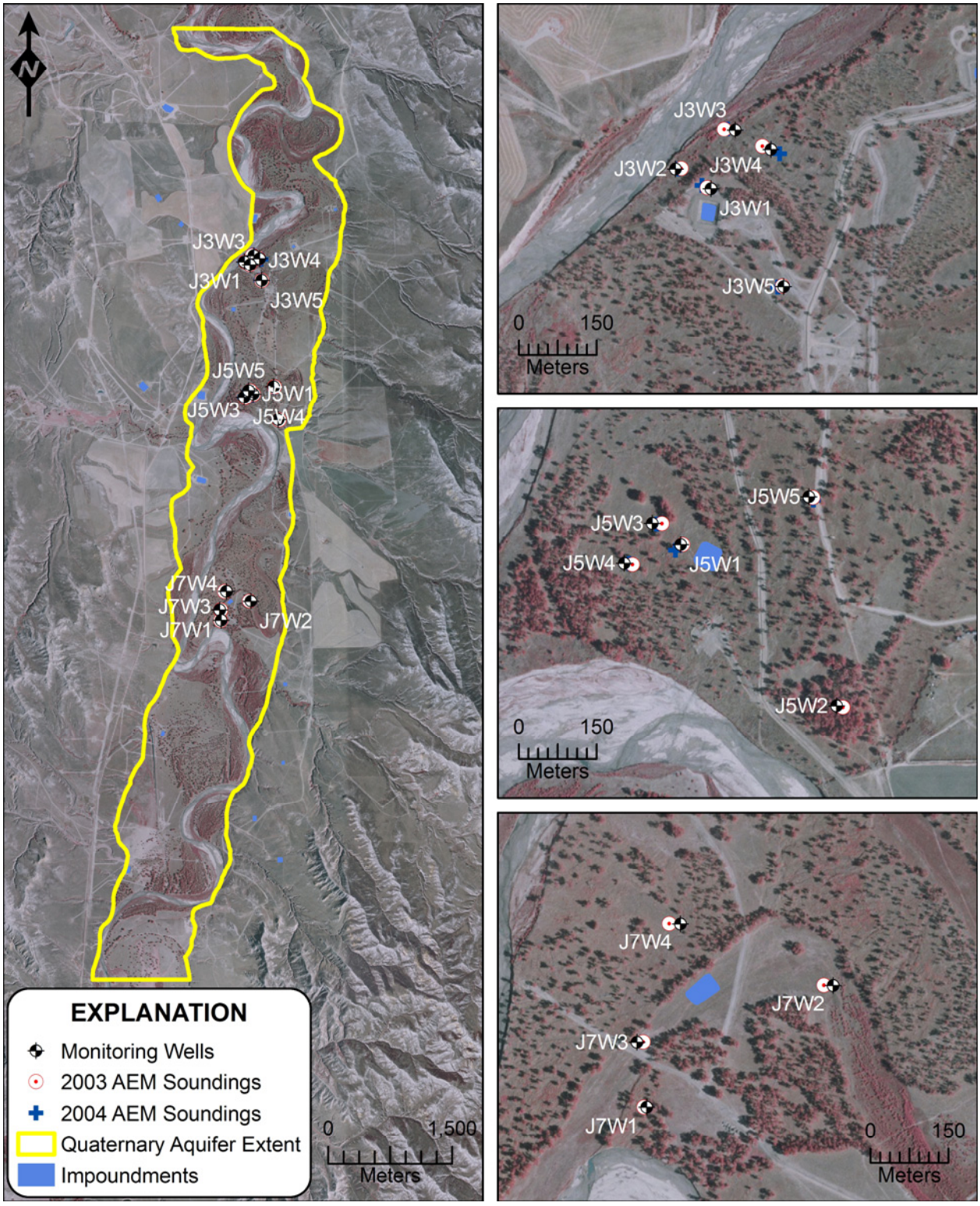

Figure 3.8. Location of monitoring wells and nearby AEM soundings for the 2003 and 2004 surveys.

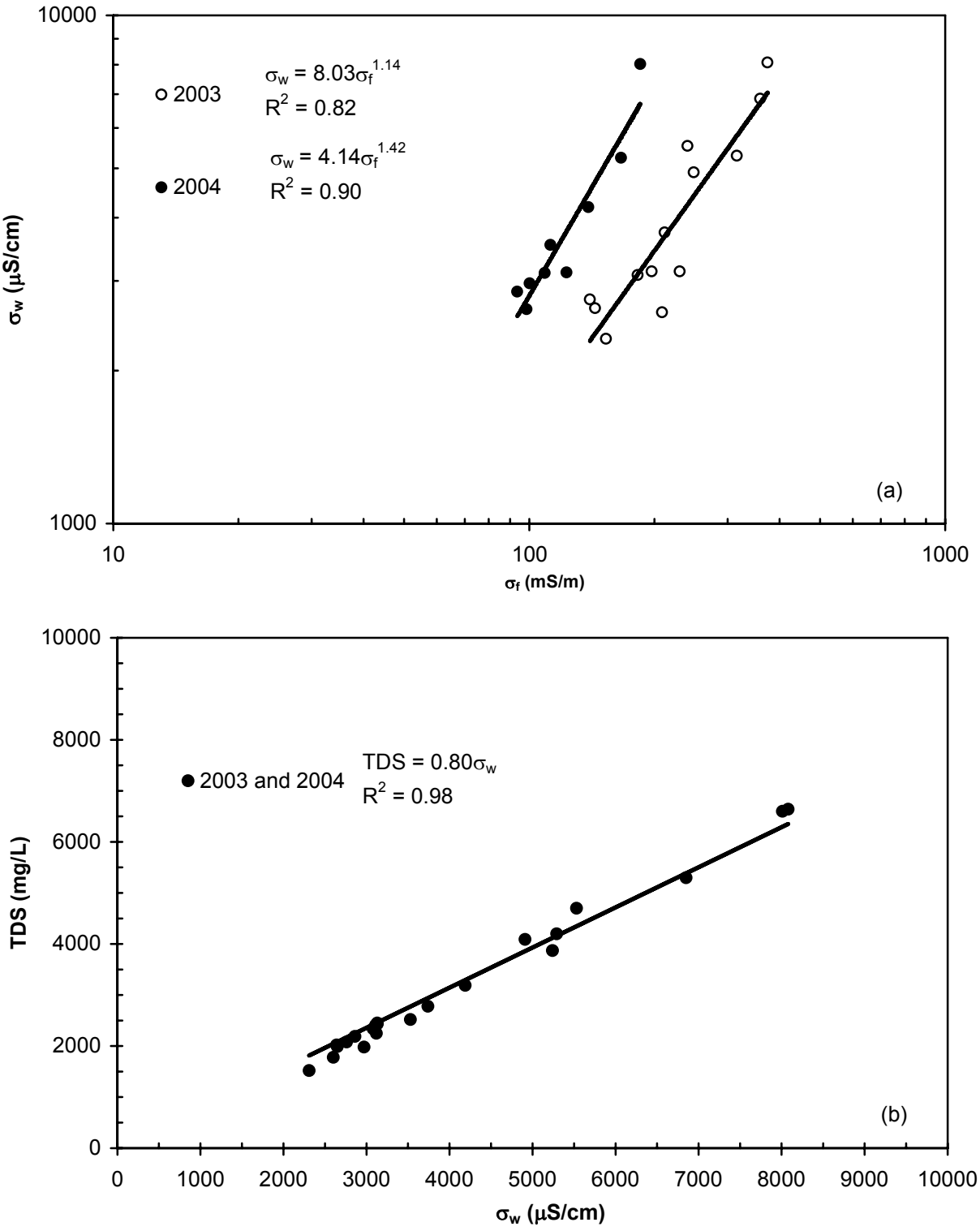

Figure 3.9. The relationship of airborne electromagnetic inversion results to water quality data collected in the study area. (a) Peak AEM formation conductivity within the saturated zone plotted against measured porewater conductivity for the 2003 and 2004 surveys. (b) Relationship between measured porewater conductivity and measured TDS concentrations for the 2003 and 2004 sampling events.

4. GEOCHEMICAL METHODS

4.1. INTRODUCTION

The second objective of this dissertation is to evaluate geochemical changes occurring in near surface aquifers receiving coalbed natural gas (CBNG) produced water. Traditional approaches involve using major ions to evaluate geochemical processes. Recently, isotope analyses have become routine in hydrogeologic field studies (Clark and Fritz, 1997; Frost et al., 2002; Frost and Toner, 2004; Gosselin et al., 2004; Negrel and Lachassagne, 2000; Negrel et al., 2004; Rhodes et al., 2002; Sharp et al., 2002). The radiogenic isotopes of strontium are particularly useful in hydrogeology because they are not affected by fractionation processes or partitioning (Clark and Fritz, 1997; Faure and Powell, 1972). Groundwater acquires strontium through mineral dissolution and/or ion exchange reactions yielding a strontium isotopic ratio that solely reflects water-rock interactions. As such, the strontium isotope method was used along with major ions to investigate CBNG water production and disposal.

4.2. STRONTIUM ISOTOPE METHOD

4.2.1. Strontium Chemistry

Strontium is classified as an alkaline earth metal along with beryllium, magnesium, calcium, barium, and radium. The alkaline earth metals commonly form divalent cations because they have two electrons in the *s* orbital. The ionic radius of Sr^{2+} is 1.13 Å while the ionic radius of Ca^{2+} is 0.99 Å and therefore Sr^{2+} readily replaces Ca^{2+} in calcium-bearing minerals (Faure and

Powell, 1972). Replacement commonly occurs in plagioclase feldspar, gypsum, anhydrite, calcite, dolomite, aragonite, and apatite (Capo et al., 1998). Additionally, Sr^{2+} can replace K^{+} in potassium feldspar when Al^{3+} has replaced Si^{4+} in the silica tetrahedral lattice (Faure and Powell, 1972). This replacement has also been observed in the clay minerals vermiculite and smectite (Capo et al., 1998).

Strontium has four naturally occurring isotopes and fourteen artificial radioactive isotopes. The stable isotopes and their abundances are as follows: ^{84}Sr 0.56%, ^{86}Sr 9.87%, ^{87}Sr 7.04%, and ^{88}Sr 82.53%. The amount of ^{87}Sr varies as it is formed form the β decay of ^{87}Rb (half life ~48.8 x 10^9 years). The relative abundance of ^{87}Sr is typically expressed as the ratio $^{87}Sr/^{86}Sr$. The common radioactive isotope ^{90}Sr is the product of uranium fission and is short lived in the environment (half life ~30 years).

4.2.2. Strontium Isotopes as Groundwater Tracers

The usefulness of the strontium isotope method in hydrogeologic investigations lies in the strong variation of the isotopic ratio throughout Phanerozoic time (Figure 4.1). In general, the curve depicts the relative contributions of strontium to the ocean from mid-ocean ridge hydrothermal alteration and continental weathering (Burke et al., 1982). The primordial $^{87}Sr/^{86}Sr$ ratio has been steadily increasing from 0.699 due to the decay of ^{87}Rb. Continental rocks are generally enriched in ^{87}Sr and have $^{87}Sr/^{86}Sr$ that range from 0.710 to 0.740 while basalts are somewhat depleted in ^{87}Sr with a $^{87}Sr/^{86}Sr$ of 0.703 (Clark and Fritz, 1997). The Late Cenozoic increase in the $^{87}Sr/^{86}Sr$ ratio is due to increased continental weathering rates from glaciation. The strong contrast in the $^{87}Sr/^{86}Sr$ ratio since the Cambrian is advantageous for hydrogeologic investigations of waters from multiple geologic regimes, such as at the study site.

Surface water inputs to groundwater systems are an important aspect to consider when using the strontium isotope method in hydrogeologic investigations. The two main inputs are typically stream discharge and precipitation. The strontium ratio in stream discharge is primarily controlled by drainage basin geology (Aberg, 1995; Wadleigh et al., 1985). The strontium ratio of small tributaries can vary significantly from the average watershed value due to localized variations in bedrock geology but the average watershed ratio will not be skewed by localized

departures from the predominant bedrock signature (Aberg, 1995; Wadleigh et al., 1985). Precipitation can depress the strontium ratio by simple dilution and by decreasing the residence time of soil water (Aberg, 1995).

Strontium isotopes can be used to determine mixing ratios between various reservoirs if they impart unique signatures. In a simple binary system, a plot of the $^{87}Sr/^{86}Sr$ ratio versus the inverse strontium concentration should yield a linear relationship. If you have water from two sources (for example, source *a* and source *b*), then the equation describing mixing of isotope ratios is as follows:

$$\left(\frac{^{87}Sr}{^{86}Sr}\right)_m = \frac{f_b[Sr]_b\left(\frac{^{87}Sr}{^{86}Sr}\right) + (1-f_b)[Sr]_a\left(\frac{^{87}Sr}{^{86}Sr}\right)}{f_b[Sr]_b + (1-f_b)[Sr]_a}$$

Note that the relationship is dependent on strontium concentrations.

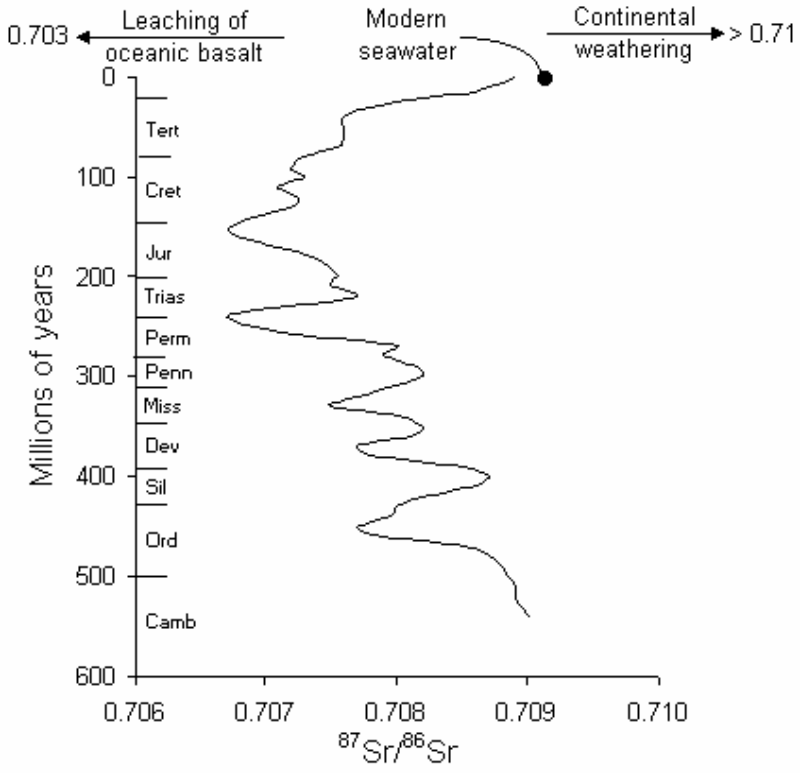

Figure 4.1. The strontium isotopic ratio curve measured in sedimentary rocks throughout Phanerozoic time (modified from Burke et al., 1982).

4.3. SAMPLE COLLECTION AND ANALYSIS

4.3.1. Pennaco Energy Sampling Events

Pennaco Energy Incorporated (PEI), a wholly owned subsidiary of Marathon Oil, regularly sampled monitoring wells, impoundments, and streams within the study area. Monitoring wells near J3 and J5 were sampled quarterly; however, several 1-inch piezometers near J3 and J5 were not sampled. Stream samples were collected quarterly from points upstream and downstream of the study area (Figure 4.2). Impoundments were never sampled directly, but impoundment outfalls were sampled periodically according to Wyoming Pollutant Discharge Elimination System (WYPDES) permitting requirements. Samples were not collected from J3 and J5 outfalls but they were collected from a nearby impoundment named NC7. All CBNG wells in the area are producing gas from the Anderson Coalbed. As such, the geochemistry of NC7 should adequately represent J3 and J5 water quality.

All locations (Figure 4.2) were sampled in July 2002, April 2003, and May 2004. Monitoring wells were purged by removing 3 to 5 well volumes using submersible pumps prior to sampling (Adams, 2004). Water from the Powder River and CBNG produced water outfalls were collected as grab samples. Electrical conductivity (EC) and pH were measured in the field by the sampler using instruments that were calibrated daily. Samples for dissolved metals were preserved to a pH < 2 using HNO_3. Trip and field blanks were used to ensure quality control of sampling techniques. All samples were field preserved on ice and shipped to Energy Laboratories in Gillette, Wyoming under normal chain-of-custody protocols.

PEI samples were analyzed by Energy Labs in Gillette, WY. Dissolved metals were analyzed using Inductively Coupled Plasma techniques (EPA method E200.7), anions were determined using an Ion Chromatograph (EPA method E300.0), bicarbonate was determined using Standard Methods 2320B, and dissolved solids were determined using Standard Methods 2540C. Field and trip planks were less than detection limits. These data were submitted yearly to the Wyoming Department of Water Quality (WYDEQ) and were obtained directly from the WDEQ upon request.

4.3.2. Isotope Sampling

Samples for isotopic and major cation analyses were collected on July 11-12, 2005 from the Powder River, produced water impoundments, monitoring wells, piezometers, and coalbed natural gas wells (Figure 4.3). All monitoring well and piezometer samples were collected using low flow sampling techniques with water purged using dedicated high density polyethylene tubing attached to a peristaltic pump. Outflow was directed to a flow-through cell where pH, temperature, and EC were monitored until they stabilized. Temperature and EC were measured using a YSI 3000 T-L-C meter while pH was measured using an Orion probe. All instruments were calibrated prior to use each day. Grab samples were collected from surface water locations and field parameters were measured *in-situ*. Produced water samples were collected from continuously pumped CBNG wells; therefore, purging was not necessary. All samples were field filtered using 0.45 μm syringe filters. Samples were separated into two 250 mL acid washed virgin high density polyethylene (HDPE) bottles; one was reserved for cation analyses and the other was reserved for isotopic analyses. Samples were preserved on ice and shipped by FedEx to the National Energy Technology Laboratory in Pittsburgh, PA on July 18, 2005. All samples were then preserved using ultrapure nitric acid to a pH < 2 at the University of Pittsburgh.

Water samples for isotopic analyses were processed at the University of Pittsburgh. Calcium, magnesium, sodium, potassium, and strontium concentrations were determined using a Spectro-Flame Modula, End-on-Plasma, Inductively-Coupled Plasma Atomic Emission Spectroscometer (ICP-AES) using EPA QA/QC protocol SW846. Total blanks were analyzed to measure contamination from sampling and preservation techniques and were less than detection limits.

Strontium was concentrated and purified using an ion exchange technique and SrSpec® resin in the Clean Laboratory at the University of Pittsburgh. Measured sample aliquots were dried in an acid-washed Teflon® vial and dissolved in 0.5 mL of purified 3N nitric acid. Cation exchange reactions were completed in quartz columns that were cleaned with 50% nitric acid and then rinsed with ultrapure water. Approximately 150 μl of SrSpec® resin was then injected into each column. This resin has been calibrated to separate strontium from other cations. The resin in each column was rinsed with subsequent additions of 1 mL ultrapure water, 1 mL 3N nitric acid, 0.5 mL ultrapure water, and 0.5 mL ultrapure water. The resin was then equilibrated using 0.5

mL ultrapure water. The sample was then introduced and unwanted cations were removed using three successive additions of 0.5 ml 3N nitric acid. Strontium was eluted and collected into Teflon vials by adding ultrapure water in 1 mL and 0.5 mL additions.

Isotopic abundances were determined using thermal ionization mass spectrometry (TIMS) techniques. Purified samples were dried and electroplated onto rhenium filaments with a tantalum activator solution. Samples were analyzed on a Finnigan MAT 262 TIMS. Strontium isotope data were normalized to an SRM987 value of 0.71025. In-run uncertainty was ±0.00001 and estimated external reproducibility was ±0.00002.

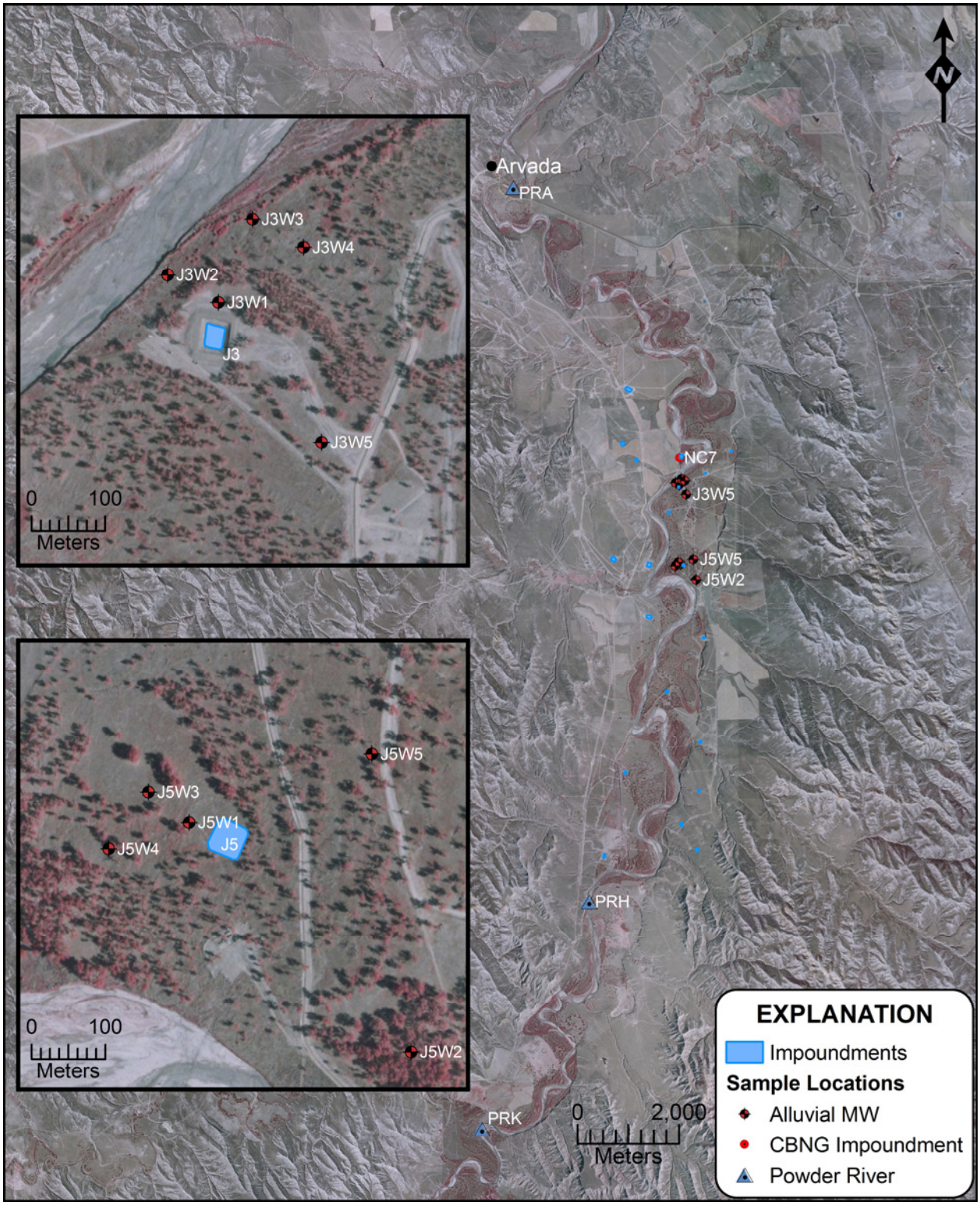

Figure 4.2. Water sample locations for the 2002, 2003, and 2004 PEI sampling events. The J3 and J5 CBNG produced water impoundments are enlarged. Note that MW = monitoring well.

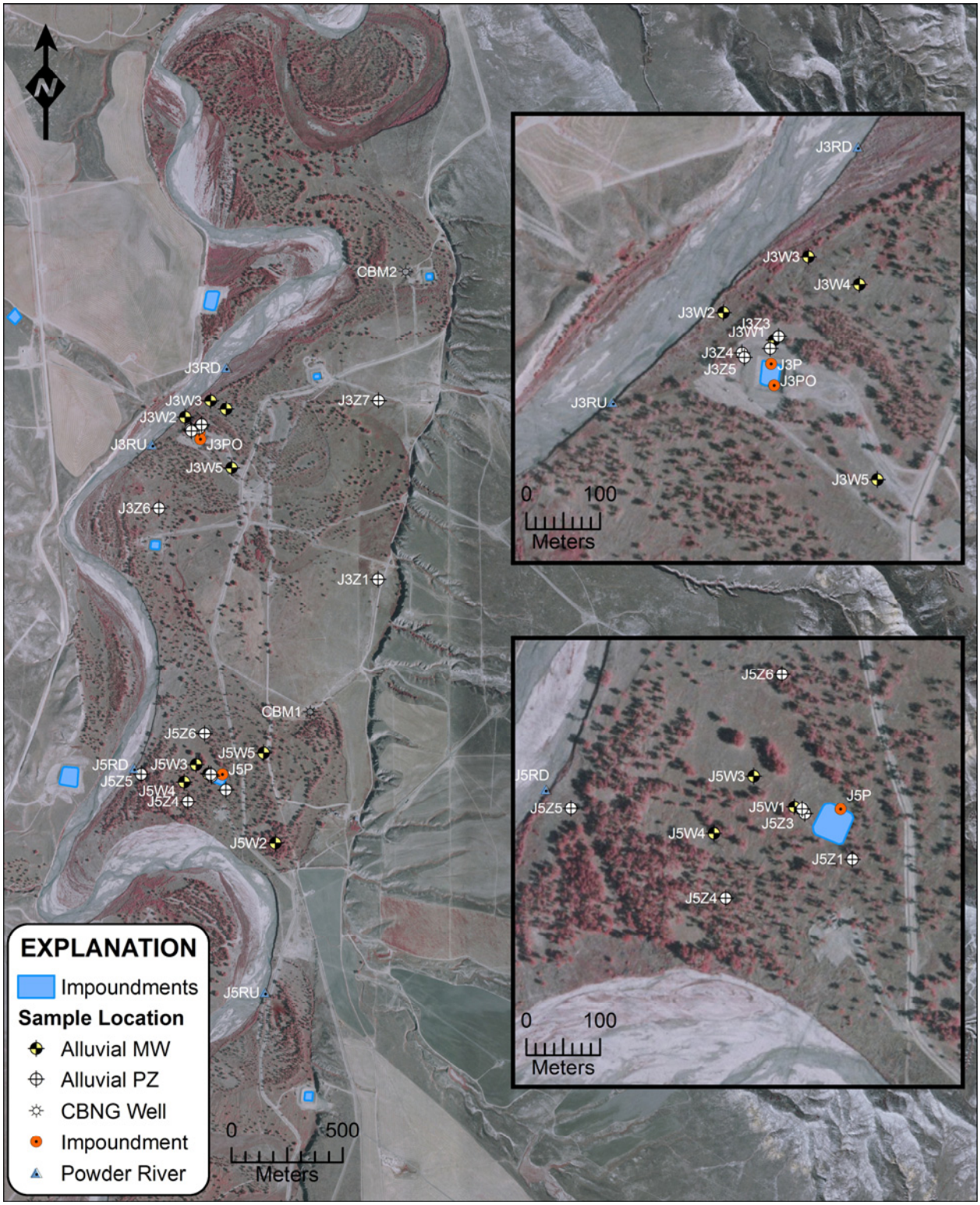

Figure 4.3. Water sample locations for the 2005 sampling event. The J3 and J5 CBNG produced water disposal impoundments are enlarged. Note that MW = monitoring well and PZ = piezometer.

5. AIRBORNE ELECTROMAGNETIC INVESTIGATION

5.1. INTRODUCTION

Rapid development of coalbed natural gas (CBNG) in the Powder River Basin (PRB) of Wyoming has focused national attention on produced water management strategies (Bartos and Ogle, 2002; BLM, 2003a, b; De Bruin et al., 2004; Frost et al., 2002; Stearns et al., 2005). Approximately 22,000 wells have been installed in Wyoming with as many as 40,000 more to be drilled within the next decade (BLM, 2003a). Production requires continuous groundwater extraction with each well producing approximately 34 m^3/day over a lifetime of 7 to 10 years (BLM, 2003a; De Bruin et al., 2004). The produced water is moderately saline and sodic (Bartos and Ogle, 2002; Rice et al., 2005; Rice et al., 2000). Current disposal methods include, but are not limited to, direct surface discharge, infiltration impoundments, containment impoundments, and land application (BLM, 2003a).

The potential environmental impacts associated with produced water disposal encompass water resource depletion, water quality degradation in surface water and groundwater systems, and damaged agricultural lands (Stearns et al., 2005). Production is expected to lower hydraulic head in PRB drinking water aquifers by approximately 60 to 120 m (BLM, 2003a). Research suggests that soils receiving CBNG produced water become more saline and sodic creating an environment conducive to exotic invasive plant species (Stearns et al., 2005). Results of research completed on an in-channel disposal reservoir concluded that infiltrating produced water created a perched aquifer with elevated total dissolved solids (TDS) concentrations (Rice et al., 2005). At the same site, airborne and ground-based geophysical methods were used to delineate the extent of produced water impact (Lipinski et al., 2004). This study demonstrated that geophysical methods may be very useful in evaluating produced water disposal.

Geophysical methods have become increasingly popular in hydrogeologic investigations (Rubin and Hubbard, 2005). These methods allow researchers to complete non-invasive subsurface investigations over scales that range from sub-meter to watershed. The advantage of geophysical methods is that they can help fill data gaps left by incomplete monitoring networks at a fraction of the cost. Within the PRB, a geophysical method to map water quality on a sub-watershed scale is needed. The Airborne Electromagnetic (AEM) method is the best available geophysical technique suited for this application.

AEM geophysical surveys were originally developed in Canada for mineral exploration and have been used sparingly in hydrogeologic investigations (Fountain, 1998). Early hydrogeologic applications included saltwater intrusion mapping (Sengpiel, 1983) and groundwater prospecting (Sengpiel, 1986). More recently, AEM was used to map saltwater intrusion at various depths in the Florida Everglades by relating chloride concentrations to geophysical response (Fitterman and Deszcz-Pan, 1998). AEM also proved useful during a hydrogeologic site characterization at Oak Ridge Reservation, Tennessee to map buried drums, fold geometry, and karst features (Doll et al., 2000). Additionally, AEM was used at the Sulphur Bank Mercury Mine in northern California to delineate a groundwater plume near Clear Lake where traditional characterization methods had failed (Hammack and Mabie, 2002). Oilfield salinization influence along the Red River alluvial terrace in Texas was quantified using AEM (Paine, 2003). Large scale lithologic variations within the Edwards Aquifer, Texas were mapped using AEM as well (Smith et al., 2003).

The purpose of this study is to determine the efficacy of AEM surveys to map water quality in an alluvial aquifer receiving CBNG produced water discharge from several infiltration impoundments. AEM techniques were expected to provide a higher spatial resolution of water quality visualization than could be attained using traditional ground-based geochemical sampling approaches. This would allow broad scale interpretations of hydrogeologic and geochemical processes at the site. If successful, AEM could be used to evaluate subsurface processes controlling water quality within the aquifer and potentially aid impoundment location strategies for future development.

5.2. SITE DESCRIPTION

5.2.1. Geologic Setting

Regionally, the study site is located within the Powder River Basin (Figure 5.1). It is an intermontane asymmetric structural and sedimentary basin covering over 57,000 km^2 of Montana and Wyoming. CBNG exploration and development is focused within the Paleocene Fort Union Formation and to a lesser extent in the Eocene Wasatch Formation. Both units crop out in the study area and consist of sandstone interbedded with siltstone, mudstone, carbonaceous shale, and coal deposited in fluvial systems fed by ancestral uplifts (Flores, 1986). The most widespread CBNG development is within the Wyodak-Anderson coal zone of the Fort Union Formation. This zone contains eleven named coalbeds with up to six located at any given location displaying complex stratigraphic relationships. The Anderson coalbed, which is part of the Wyodak-Anderson coal zone, is the production target within the study area occurring approximately 230 m below grade.

Locally, the study site is located along the Powder River approximately 5 km south of Arvada, Wyoming (Figure 5.2a). Quaternary alluvium of the Powder River can be summarized into four units (Figure 5.2b). The oldest unit is the Arvada Formation characterized by highly weathered gravelly sand stained red with yellow-brown cobbles (Leopold and Miller, 1954). The Ucross Formation disconformably overlies the Arvada Formation and is composed of rounded gravels derived from igneous and metamorphic rocks of the Bighorn Mountains. The upper one meter is impregnated with calcium carbonate and gypsum interpreted to be a paleosol (Leopold and Miller, 1954). The Kaycee Formation overlies the Ucross Formation and is generally classified as mixed colluvium/alluvium. It contains a clearly developed soil layer underlain by well sorted silt-sized quartz grains. The Lightning Formation is the most recent alluvium consisting of tan fine to medium sand with some fine gravel devoid of bedding planes (Leopold and Miller, 1954). The alluvium overlies thick, blue-gray clay, which in turn overlies bedrock. Climatically controlled erosion created three prominent terraces within alluvium named the Kaycee, Moorcroft, and Lightning terraces (Figure 5.2b).

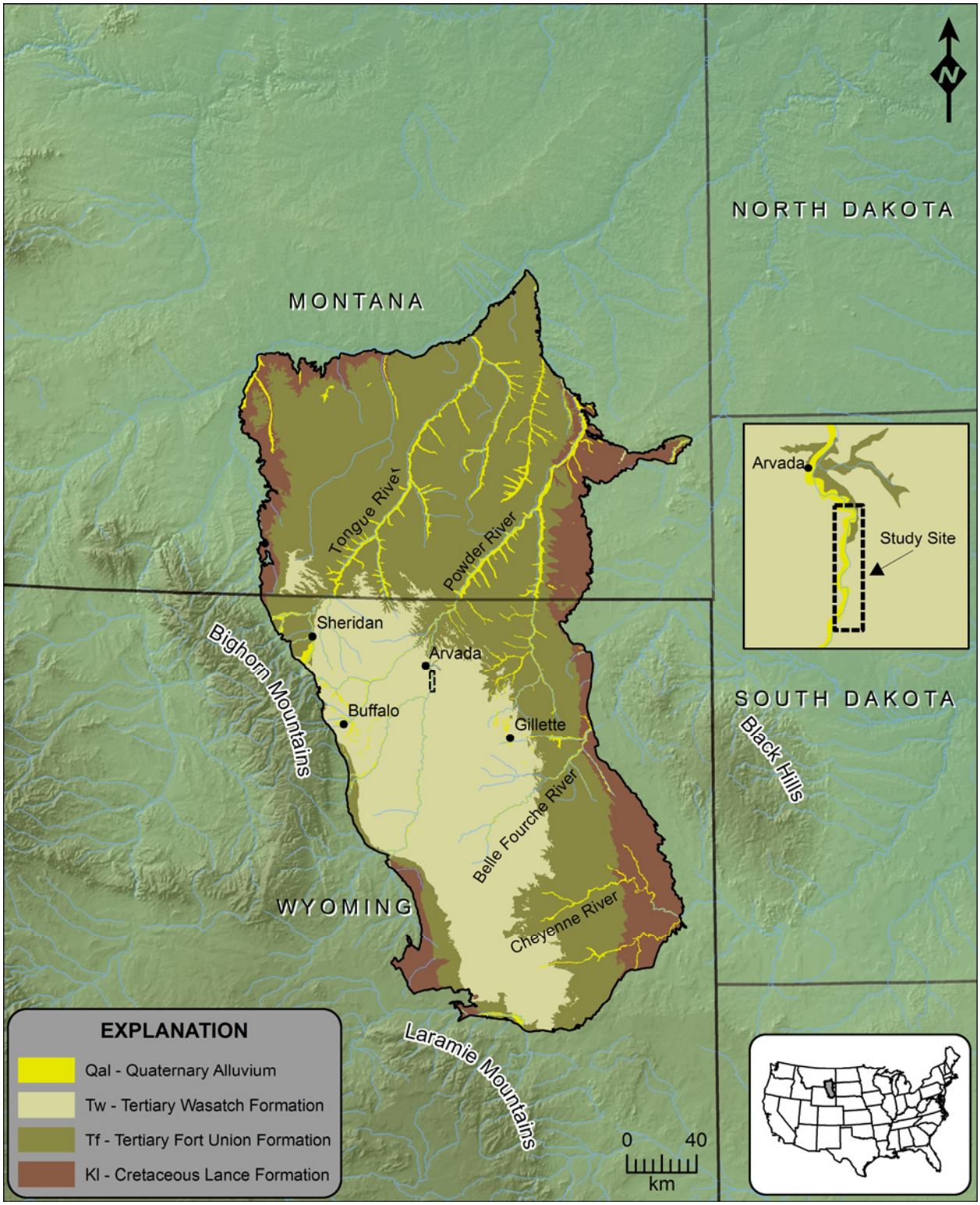

Figure 5.1. The generalized bedrock geology of the Powder River Basin depicted in relation to major physiographic features. Small rectangle approximately 5 km south of Arvada, Wyoming outlines the study area.

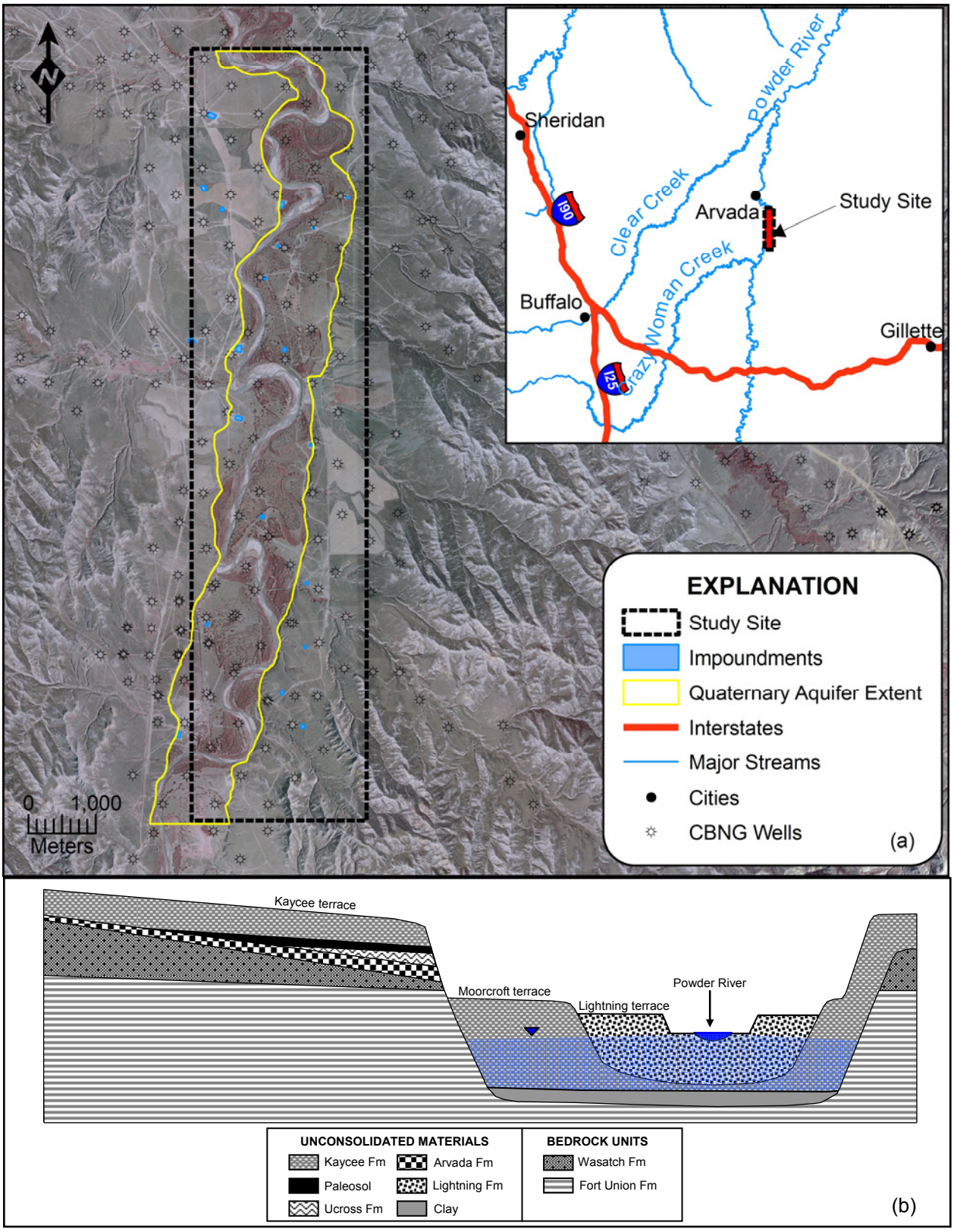

Figure 5.2. Study site (a) location along the Powder River and (b) schematic cross-section depicting the Powder River alluvial valley. Note the extent of the alluvial aquifer is depicted on both figures.

5.2.2. Hydrogeologic Setting

The Wasatch and Upper Fort Union Formations contain the Tongue-River-Wasatch (TRW) aquifer. This regional unit is actually composed of many sub-regional aquifers with limited lateral extent. Aquifers are contained within highly permeable sandstones, coalbeds, and conglomerates, but are confined by interbedded mudstone and shale units. The Wyodak-Anderson coal zone occurs in the TRW aquifer and is considered the most continuous hydrogeologic unit in the PRB (BLM, 2003a). The TRW aquifer is mainly confined except near recharge and discharge areas where localized water table conditions exist. Recharge occurs in topographically high areas and discharge is mainly to large stream systems, such as the Tongue River (Hinaman, 2005). Groundwater within bedrock aquifers generally flows to the northwest (Daddow, 1986).

Quaternary alluvium at the study site contains a thin, unconfined aquifer (Figure 5.2b). Alluvium ranges in thickness from about 3 to 15 m, but averages 6 m. The aquifer occurs approximately 2 to 3 m below the ground surface and extends laterally to the bedrock erosional surface along the Kaycee terrace (Figure 5.2a) and vertically downward to the clay layer overlying bedrock (Figure 5.2b). As such, groundwater within the aquifer generally flows northward at the site mimicking the bedrock topography. The main source of recharge to the alluvial aquifer is the Powder River but additional recharge is provided by CBNG infiltration impoundments (Figure 5.2a). The Powder River is a losing stream throughout the study area, which is typical for a semi-arid climate (Ringen and Daddow, 1990). Impoundments have been receiving produced water discharge under Wyoming Pollution Discharge Elimination System Permits (WYPDES) since late 2001 and early 2002. Discharge rates into each pond have steadily decreased from approximately 150-200 m^3/s in April 2002 to 1-5 m^3/sec in June 2006. Produced water has TDS levels approximately one order of magnitude less than native alluvial water, which should provide an adequate target for electromagnetic geophysical techniques throughout the study area.

5.3. METHODS

5.3.1. Data Collection

Fugro Airborne Surveys collected airborne electromagnetic (AEM) data within the study area on July 25, 2003 and July 31, 2004 using the RESOLVE system (Cain, 2003, 2004). The system consists of five coplanar transmitter/receiver coils one coaxial transmitter/receiver coil. Coplanar frequencies during the 2003 survey were 387 Hz, 1.7 kHz, 6.54 kHz, 28.1 kHz, and 116 kHz while the coaxial frequency was 1.41 kHz. Coplanar frequencies during the 2004 survey were 391 Hz, 1.8 kHz, 8.18 kHz, 39.1 kHz, and 132.6 kHz while the coaxial frequency was 3.33 kHz. Survey lines were oriented north-south and nominally spaced 50 m apart. The instrument was flown approximately 33 to 35 m above ground during both surveys. The system also houses a coplanar power line monitor and high sensitivity cesium magnetometer to identify cultural features that may contaminate EM data.

The survey areas did not completely overlap each year (Figure 5.3). The 2004 survey was flown to evaluate water quality changes and to evaluate reproducibility of the 2003 data. As such, the 2004 survey was approximately one-half the spatial extent of the 2003 survey. It was also moved northward for anticipated CBNG development. Data outside the Quaternary aquifer boundary were not analyzed because there are no near surface-aquifers within these sediments. Additionally, data contaminated with power line and magnetic noise were culled.

5.3.2. Data Processing

The subsurface electrical conductivity distribution was determined using the Occams inversion program EM1DFM (UBC-GIF, 2000). Input required for the program is the inphase and/or quadrature response of the secondary magnetic field, transmitter/receiver geometry, instrument altitude, and data error. Data were inverted to a uniform, 80-layered earth with 1 meter layer thicknesses. Inversions were completed using the fixed tradeoff parameter algorithm with $\beta=10$ after trial inversions indicated this was the optimal value. Data error values were determined to

be approximately 5%, which is consistent with previous research (Tølbøll and Christiansen, 2006).

AEM data were correlated to water quality by comparing inversion results to water quality data measured from several monitoring wells screened into the alluvial aquifer (Figure 5.3). Samples were collected on July 17-18, 2003 and September 29-30, 2004 and analyzed for electrical conductivity (EC) and total dissolved solids (TDS). Groundwater EC within each well was correlated to formation conductivity values at nearby AEM soundings. The formation conductivity value used was the peak EM1DFM value within the phreatic zone. Regression analysis was performed and an empirical relationship for each survey was developed below:

$$\sigma_w = 8.03\sigma_f^{1.14} \quad (R^2 = 0.82;\ 2003\ data)$$

$$\sigma_w = 4.14\sigma_f^{1.42} \quad (R^2 = 0.90;\ 2004\ data)$$

where:

σ_w = porewater conductivity (μS/cm)
σ_f = formation conductivity (mS/m)

Groundwater EC is related to TDS using the following site-specific relationship:

$$TDS = 0.80\sigma_w \quad (R^2 = 0.99)$$

where:

σ_w = porewater conductivity (μS/cm)
TDS = total dissolved solids (mg/L)

TDS levels within the alluvial aquifer at all AEM soundings were then calculated using the formation conductivity determined from EM1DFM within the phreatic zone and the above equations. Vertical resolution of TDS can not be achieved because the aquifer is approximately 3 m below grade and only 4 to 6 m thick limiting interpretations to two-dimensions. Plan view maps were created by interpolating geophysically inferred TDS levels at each AEM sounding to a 10 m grid using a modified Akima spline bi-directional gridding algorithm in Geosoft®. These maps represent the inferred TDS levels within the unconfined aquifer; they do not represent surface water quality within the river or the CBNG impoundments themselves.

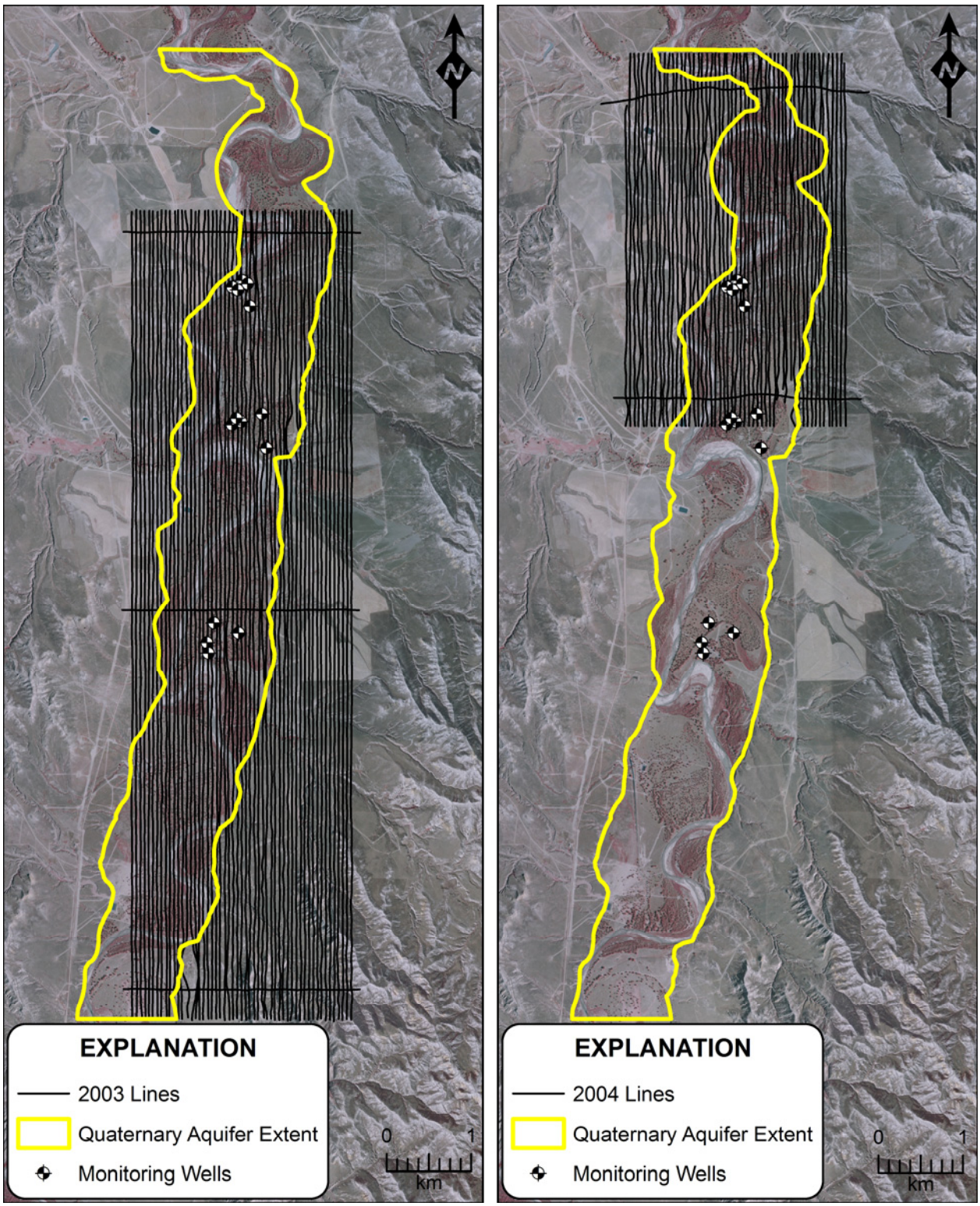

Figure 5.3. Flight lines for the 2003 and 2004 airborne electromagnetic survey along the Powder River. Only data from within the boundary of the Quaternary aquifer were evaluated. Observed TDS and EC readings from monitoring wells were used to correlate AEM response to water quality.

5.4. RESULTS AND DISCUSSION

5.4.1. Overall Observations

Geophysical results indicate that inferred aquifer TDS levels varied from 780 to 9900 mg/L in 2003 and from 820 to 8300 mg/L in 2004 (Figure 5.4). In general, the spatial TDS distribution within the aquifer is characterized by relatively low TDS water (~1,500 mg/L) along the Powder River with higher TDS levels (up to 9900 mg/L) away from the river. This pattern indicates the stream is losing throughout the area with low salinity Powder River water feeding the alluvial aquifer where evapotranspiration elevates TDS concentrations. This observation is consistent with previous research that evaluated gauging data and water quality results for samples collected along the Powder River (Clark and Mason, 2006; Ringen and Daddow, 1990).

Geomorphology is interpreted to control the geophysically inferred TDS distribution. There is an interpreted correlation between stream paleochannels and high TDS levels, which may represent variation in water quality or lithologic differences that masked water quality information (Figure 5.5). Paleochannels form oxbow lakes where silt and clay eventually deposit; clay is an electrically conductive material. However, these features also collect rainfall and runoff because they are topographically low. Evaporation of water stored in these depressions could concentrate dissolved solids prior to infiltration thereby increasing aquifer salinity levels. Additionally, aquifer TDS concentrations are characteristically lower in point bars associated with high amplitude, short wavelength stream meanders (Figure 5.5). Considering the Powder River flows north, it is interpreted that in these point bars, Powder River water flows into the feature and remerges as baseflow on the northern end creating a gaining stream section. Groundwater residence time is short because dissolved constituents are not concentrated.

5.4.2. Survey Comparisons

Evaluation of coincident survey areas reveals that there were not significant differences among successive years and that data were reproducible (Figure 5.6). Standard deviation (-1, 0, 1) plots support this conclusion (Figure 5.6). The major features observed in the 2003 survey were

reproduced in the 2004 results. There are subtle differences in water quality near the CBNG impoundments, but this is expected considering the transient nature of water disposal.

5.4.3. Impoundment Influences

Produced water influence from infiltration impoundments in the alluvial aquifer is apparent. Three conceptual models were developed after evaluating the results (Figure 5.7): (1) impoundments locally increase TDS levels within the alluvial aquifer, (2) impoundments locally dilute TDS levels in the alluvial aquifer, and (3) impoundments do not appreciably alter aquifer TDS levels. These are purely a result of location and background aquifer quality. An example of each is discussed below.

Impoundment NC7 is approximately 4400 m^2 and has been receiving produced water since 2001. As imaged with AEM, there is an interpreted salinity plume emanating from the pond (Figure 5.7 and Figure 5.8b). This feature is most likely due to vadose zone salt dissolution by infiltrating CBNG water. Depth to water in this point bar is approximately 1 m, which is readily available for vegetation to use and subsequently concentrate soluble salts in the root zone. White nodules interpreted to be concentrated salt (perhaps gypsum) were observed in hand auger samples collected downgradient of NC7. The interpreted plume appears to discharge into the Powder River directly downgradient of the impoundment. Supporting this interpretation are field reconnaissance photographs taken on June 16, 2006 that depict a saturated layer along the stream bank and potential salt accumulation near the geophysically interpreted discharge (Fugure 5.9. These features were not observed outside of the interpreted plume.

Impoundment J3 is approximately 750 m^2 and has been receiving produced water since late 2001. Observed groundwater flow in the alluvial aquifer is northeast but it has been altered into a radial pattern around the impoundment (Figure 5.8c). Native water immediately upgradient of J3 is moderately saline with TDS levels ranging from approximately 5,000 to 7,000 mg/L. Conductivity measurements taken from J3 pond water indicate that TDS levels are on the order of 1,500 to 2,000 mg/L. Infiltrating produced water is interpreted to have created a dilution anomaly within the underlying aquifer surrounding the impoundment with TDS levels similar to impoundment water quality (Figure 5.7 and Figure 5.8c). Vadose zone salt dissolution was not

interpreted from the AEM results. The difference between J3 and NC7 is that depth to water is approximately 3 m at J3 making water more difficult for plants to obtain essentially limiting root zone salt accumulation. Evaluation of the spatial distribution of TDS levels coupled with hydraulic potential information reveals that the J3 impoundment may have created a small gaining stream section in the Powder River through groundwater mounding. Supporting this interpretation are field reconnaissance photos that depict the presence of apparent groundwater discharge along the bank of the Powder River hydraulically down gradient of J3 (Figure 5.10).

Impoundment J5 is approximately 2,000 m^2 and has been receiving produced water since 2001. Interpretation of the AEM results surrounding J5 is not as clear as NC7 or J3 (Figure 5.7 and Figure 5.8d). The pond is located near a large amplitude, low wavelength stream meander. This meander is interpreted to be a preferential pathway for Powder River water, which has TDS levels ranging from 1,500 to 2,000 mg/L. Native alluvial aquifer water upgradient of J5 is moderately saline with TDS levels approximately 2,000 mg/L. J5 impoundment water has TDS levels ranging from 1,500 to 2,000 mg/L and downgradient levels within the alluvial aquifer are approximately 2,500 mg/L. Subsequently, minimal salt dissolution occurred as CBNG water infiltrated, and the contrast between TDS background levels and infiltrating produced water levels is not enough to readily discern a distinct plume.

5.5. CONCLUSIONS AND RECOMMENDATIONS

Water quality within an alluvial aquifer receiving produced water discharge from coalbed natural gas extraction was successfully mapped using airborne electromagnetic geophysical surveys. Three classes of water within the alluvial aquifer were interpreted based the geophysically inferred total dissolved solids concentrations; (1) Powder River water, (2) native alluvial groundwater, and (3) infiltrated produced water. Geophysical discrimination of each class was highly dependent on location because groundwater dominated by the Powder River signature and produced water had similar TDS levels. Where these two classes were in close proximity, there was no way to geophysically distinguish them.

Several important conclusions can be drawn from the research contained in this paper that may not have been readily apparent based on traditional hydrological investigations. Main regulatory concerns of produced water disposal are that TDS and sodium adsorption (SAR) levels in groundwater and surface water TDS will increase. Stream meanders appear to be preferential flow paths for river water where the stream loses water to the point bar, the hydraulic potential field forces the water to migrate through the meander, and then it reemerges as baseflow downstream. Impoundments located within these features will be hydraulically connected to the stream. Also, infiltrating produced water was interpreted to have dissolved vadose zone salts in point bars before reaching the phreatic zone. This observation was reported in another area of the Powder River Basin to a more extreme extent (Rice et al., 2005). Additionally, impoundments located too close to losing sections of the stream may locally reverse fluid potential creating gaining stream sections. This may act to increase TDS loads in the river by displacing native saline water into the river and increase river SAR levels when produced water eventually migrates to the stream.

Recommendations for infiltration impoundments can be drawn from this research. Considering that produced water is characterized by high SAR levels and that infiltrating produced water will often increase in TDS, an engineering step may be needed during impoundment construction to eliminate these problems. Impoundments are essentially constructed as a raised berm on grade leaving approximately 2 to 3 m of native soil between the impoundment base and the water table. Alternatively, one could excavate the native soil and replace it with clean sand, which would promote infiltration and eliminate vadose zone salt dissolution. To circumvent sodium problems, the producer should consider gypsum and sulfur amendments as completed in other regions of the basin (Ganjegunte et al., 2005). Additionally, impoundments should be placed as far away from the river as possible to eliminate natural flow regime modifications (gaining vs. losing), which may potentially change the surface water chemistry in an undesirable fashion.

5.6. ACKNOWLEDGMENTS

This work was supported by the National Energy Technology Laboratory of the Department of Energy. The author would like to thank Pennaco Energy (subsidiary of Marathon Oil, Inc.) for access to their wells. Additionally, the author would like to thank Phil Kuhn (landowner) for access to his property. Lastly, this work could not have been completed without access to the UBC-GIF inversion code EM1DFM. The author is grateful for use of the code and for the many discussions with Colin Farquharson while modeling the data.

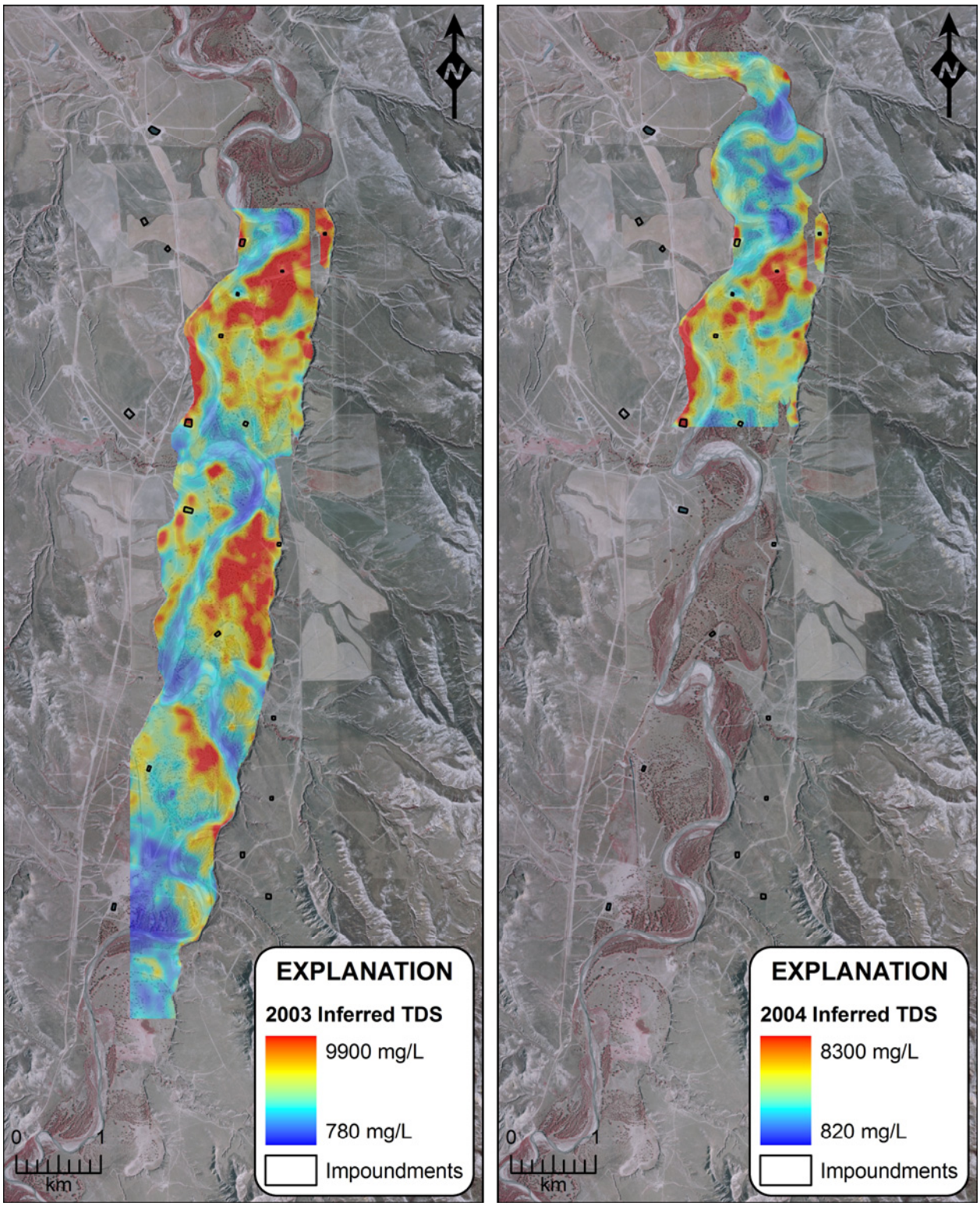

Figure 5.4. Geophysically inferred TDS levels in the Powder River alluvial aquifer for July 25, 2003 and July 31, 2004. A standard deviation color stretch with 50% transparency was applied to the TDS images.

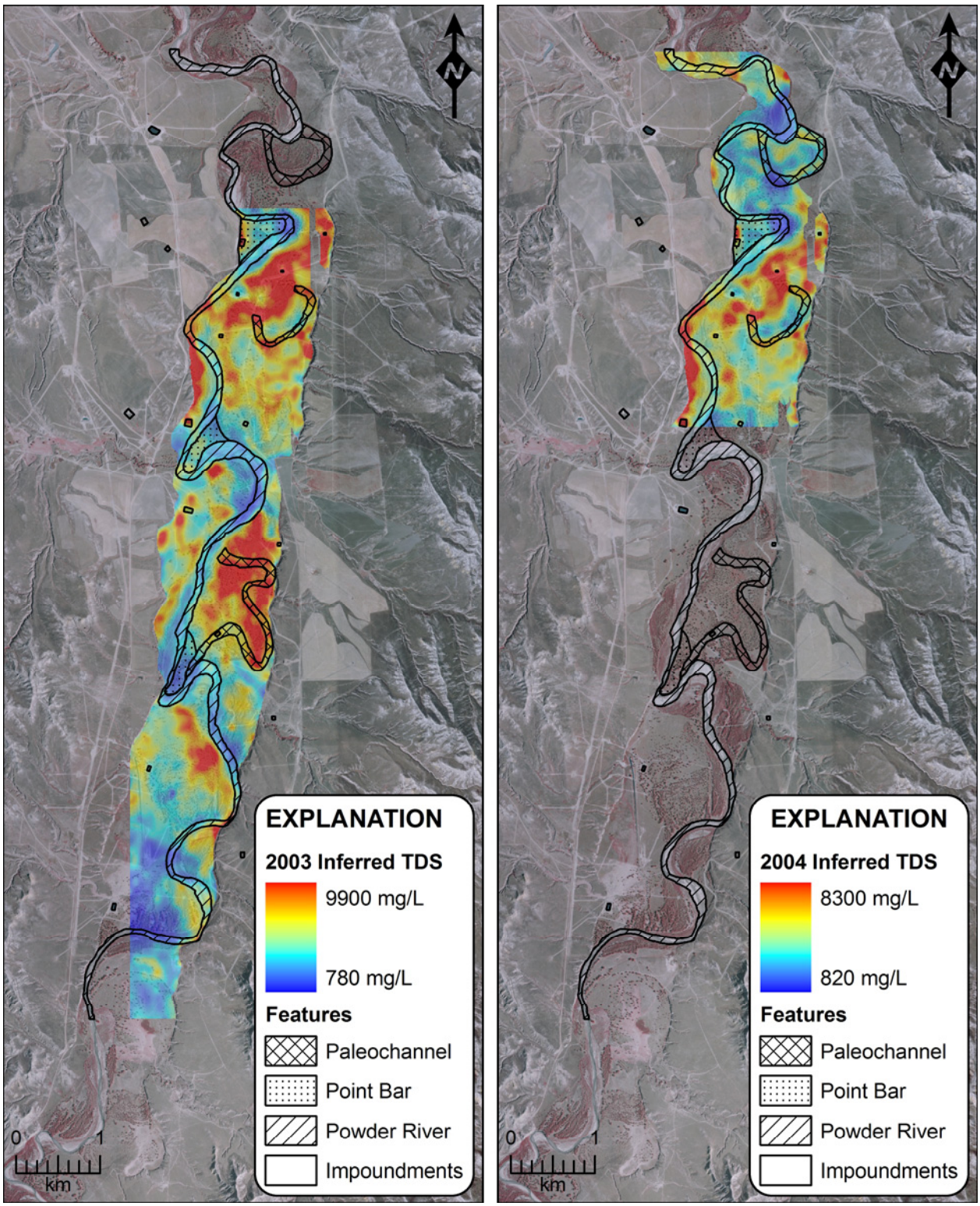

Figure 5.5. Relationship of inferred aquifer TDS to observed geomorphologic features. Note the apparent correlation of high TDS to paleochannels and low TDS to point bars within high amplitude, short wavelength stream meanders. A standard deviation color stretch with 50% transparency was applied to the TDS images.

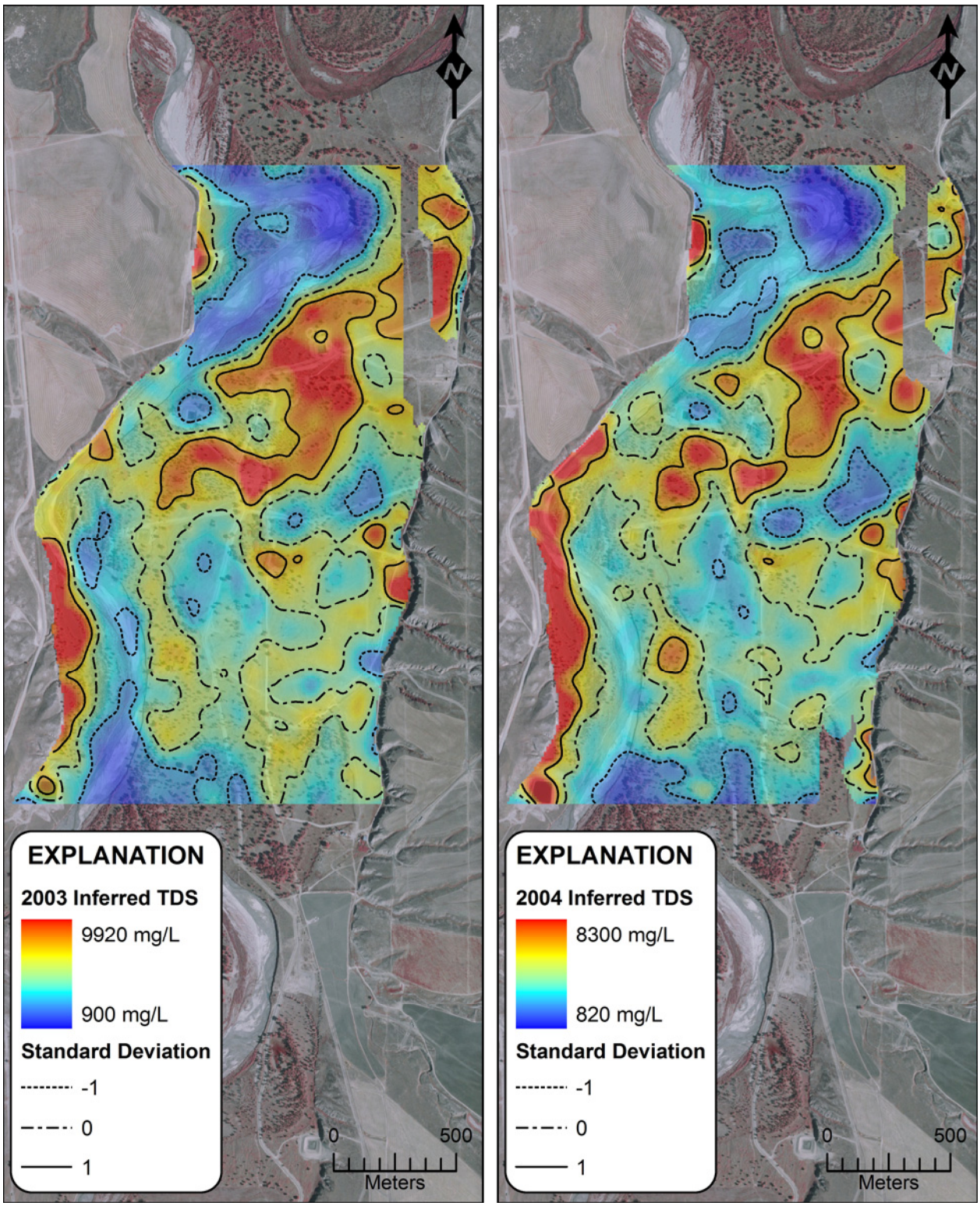

Figure 5.6. Comparison of the 2003 and 2004 geophysically inferred TDS distributions in the overlapping survey regions. Contours represent one standard deviation below (-1) and above (1) the mean (0). A standard deviation color stretch with 50% transparency was applied to the TDS images.

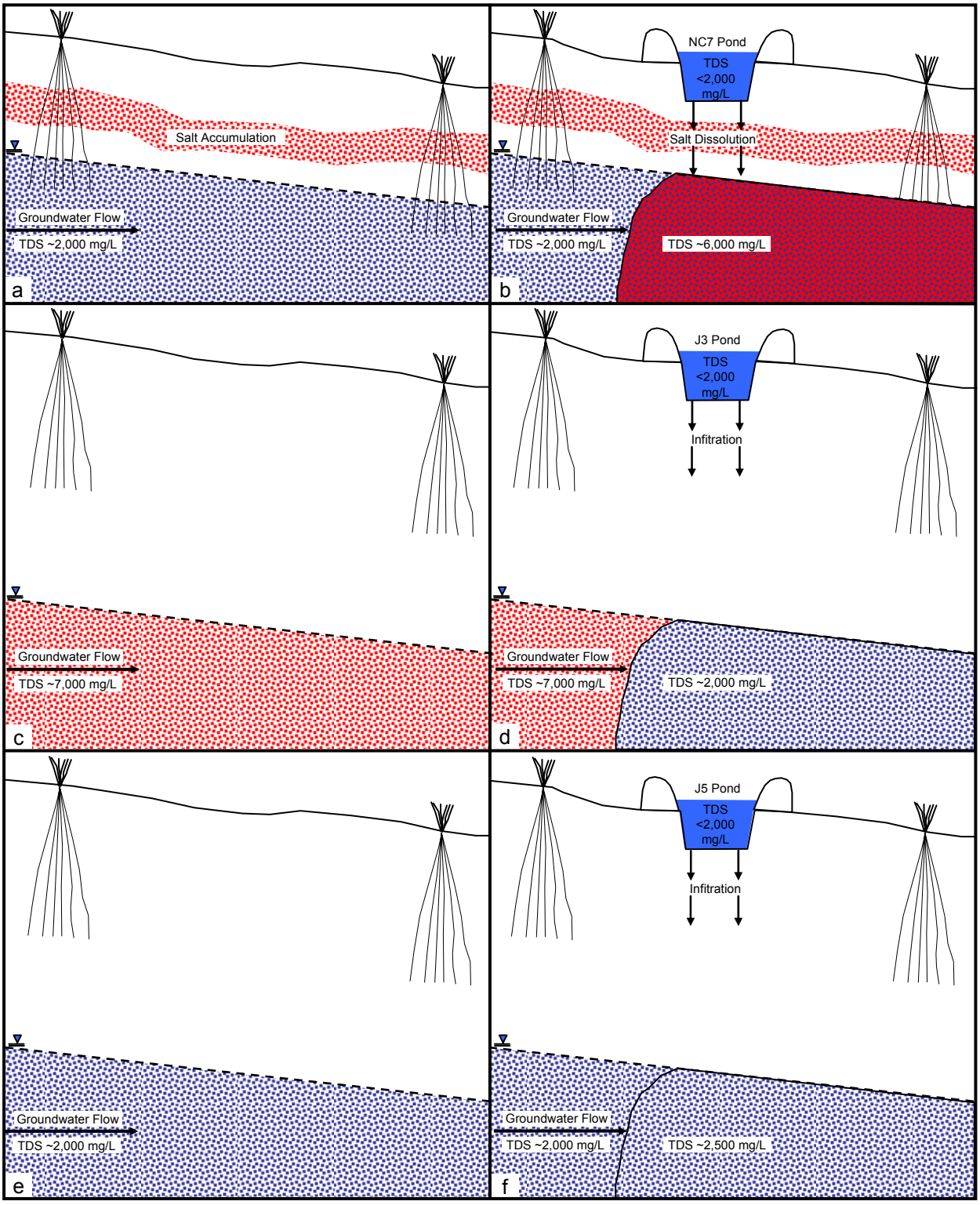

Figure 5.7. Conceptual representation of CBNG impoundment influence on aquifer water quality. (a) Site NC7 prior to pond installation and (b) after disposal. (c) Site J3 prior to pond installation and (d) after disposal. (e) Site J5 prior to pond installation and (f) after disposal. Note the interpreted control of water table depth on vadose zone salt accumulation. Also note the affect of background water salinity levels on the ability of AEM to map CBNG water influence.

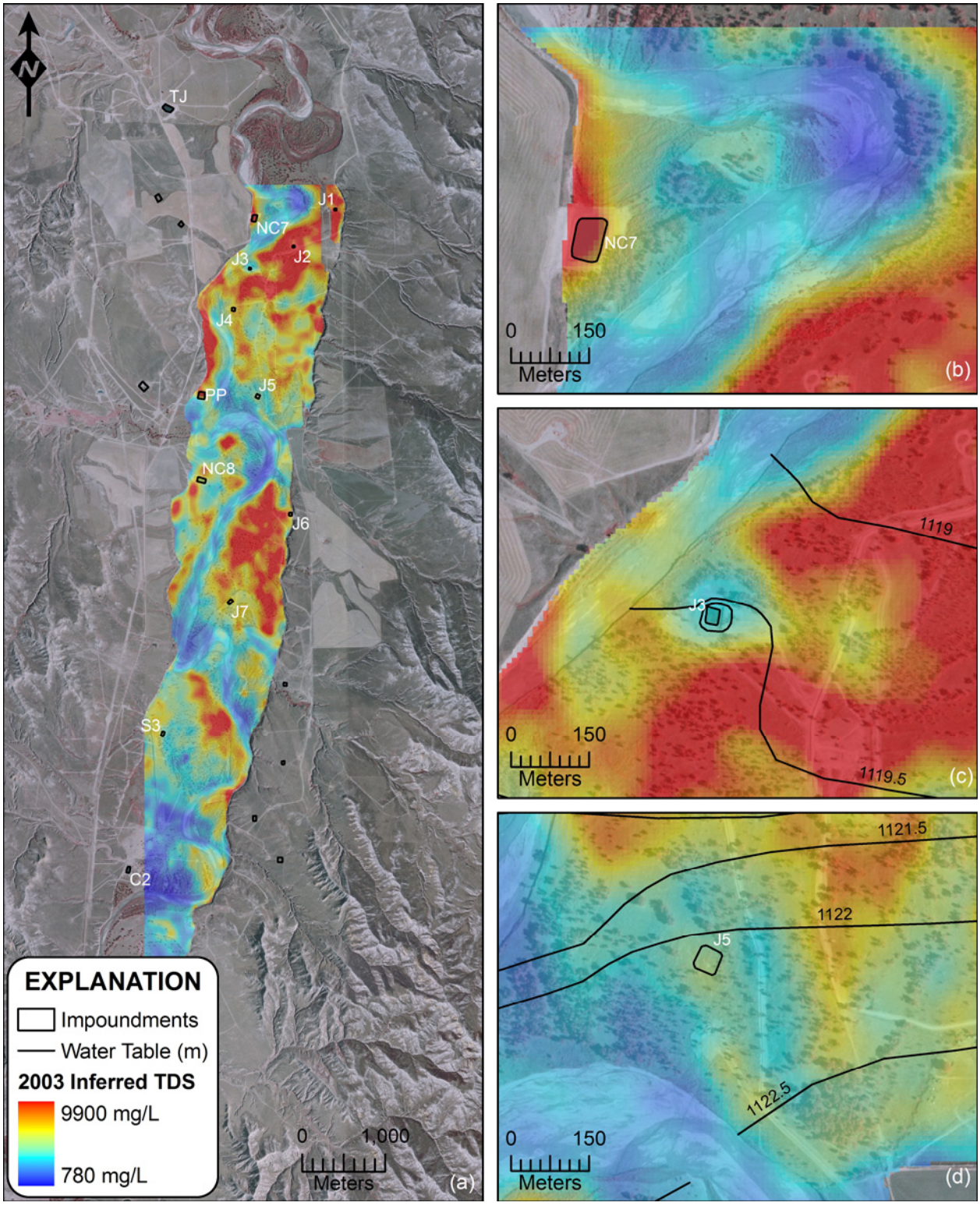

Figure 5.8. Geophysically inferred TDS levels in the alluvial aquifer on July 25, 2003 for (a) the entire site, (b) impoundment NC7, (c) impoundment J3, and (d) impoundment J5. A standard deviation color stretch with 50% transparency was applied to the TDS images.

Figure 5.9. Field photographs of apparent groundwater discharge along the Powder River bank downgradient of the NC7 produced water disposal impoundment. (a) View of the bank approximately 3 m from stream with interpreted groundwater discharge. (b) White crust interpreted to be accumulated salts adjacent to (a). Photograph by James Sams.

Figure 5.10. Field photograph of Powder River in vicinity of J3 produced water impoundment. (a) View depicting the relative location of J3 with respect to the stream. (b) Stream bank with apparent groundwater discharge depicted. Photograph by Bruce D. Smith.

6. GEOCHEMICAL INVESTIGATION

6.1. INTRODUCTION

Natural gas consumption is expected to increase by 50% in the next 20 years and methane extracted from coal is expected to help fill this demand (ARI, 2002). On a national level, coalbed natural gas (CBNG) currently accounts for approximately 7% of natural gas production (ARI, 2002; USGS, 2003). CBNG development is occurring in several basins throughout the United States, but the most rapid development is in the Powder River Basin (PRB) of Wyoming and Montana where approximately 22,000 coalbed natural gas (CBNG) wells have been installed since 1997 (WOGCC, 2006). It is anticipated that as many as 40,000 more wells will be drilled within the next decade (BLM, 2003a). Estimates of recoverable gas volumes vary, but range from 4.3 trillion cubic feet (TCF) to 39 TCF in the PRB (ARI, 2002; De Bruin et al., 2004; Flores et al., 2004), which is approximately 16% of US CBNG reserves (Limerick, 2004).

CBNG production requires dewatering coalbeds to allow methane desorption and extraction (De Bruin et al., 2004). PRB wells have some of the highest water/gas production ratios of current CBNG fields. For example, each PRB well produces 1.9 barrels (bbls) per 1000 cubic feet (MCF) gas, while San Juan Basin CBNG wells produce approximately 0.031 bbls water per MCF gas (DOE, 2003). Each PRB well produces approximately 34 m^3 water per day over a 7 to 10 year life span, but volumes decrease over the production history (BLM, 2003a). Groundwater associated with methane bearing coalbeds have a distinct geochemical character being effectively devoid of calcium, magnesium, and sulfate (Rice et al., 2000; Van Voast, 2003). Previous research indicates that water from PRB coalbeds is generally typified by total dissolved solids (TDS) concentrations ranging from 270 to 2720 mg/L with the sodium adsorption ratio (SAR) ranging from 5 to 32 (Rice et al., 2000).

Produced water quality is the main determinant for deciding water management strategies in the Powder River Basin. It is currently managed through direct surface discharge, land application systems, evaporation ponds, and unlined impoundments (ARI, 2002; BLM, 2003a). Subsurface injection is problematic because production occurs from multiple zones at varying depths and can involve several companies (BLM, 2003a). Direct surface disposal permits were issued along the eastern basin margin where CBNG water salinity and SAR levels are less than that of ambient water, but this practice has since stopped. Land application is risky because PRB soils contain montmorillonite, a clay mineral that is subject to dispersion from sodicity (Ganjegunte et al., 2005; Stearns et al., 2005). Land application also increases soil salinity, which in turn reduces the ability of plants to extract soil nutrients. This creates an environment conducive to exotic invasive species, such as salt cedar (Stearns et al., 2005). Lined impoundments are used to store water for treatment with ion exchange or reverse osmosis prior to disposal. In the northern and western part of the basin where salinity and SAR levels are higher than ambient levels, CBNG producers have turned to infiltration impoundments designed to promote near surface aquifer recharge.

Environmental impacts associated with infiltration impoundments are not very well understood. Rice et al. (2005) observed a highly saline plume within unconsolidated materials downgradient of a CBNG water impoundment in Wyoming. Input TDS levels were approximately 3,000 mg/L while samples from downgradient monitoring wells had TDS concentrations on the order of 80,000 to 100,000 mg/L. The authors concluded that infiltrating CBNG water dissolved vadose zone salts (Rice et al., 2005). Water disposal was stopped after contamination was observed in a drinking water aquifer approximately 30 m beneath the impoundment (McKinley, 2004). However, water remained in the impoundment for at least 6 months after disposal ceased, which was attributed to reduced soil permeability from clay dispersion and swelling (Healy, 2006). Considering that there are over 1100 permitted impoundments in Wyoming, research is needed to mitigate future problems.

The main purpose of this study is to evaluate the effects of CBNG produced water disposal using infiltration impoundments. The objectives include: (1) using major ions from multiple sampling events to identify geochemical changes within an alluvial aquifer receiving produced water discharge and (2) using strontium isotopes as produced water tracers. The research is expected to help understand processes responsible for observed geochemical changes

in near surface aquifers. The research is applicable to anticipated CBNG development in other parts of the PRB and other CBNG producing regions throughout the United States.

6.2. SITE DESCRIPTION

The Powder River Basin (PRB) is an intermontane asymmetric structural and sedimentary basin covering over 57,000 km^2 of Montana and Wyoming (Figure 6.1). CBNG exploration and development is focused within the Paleocene Fort Union Formation and to a lesser extent in the Eocene Wasatch Formation. Both units crop out in the study area and consist of sandstone interbedded with siltstone, mudstone, carbonaceous shale, and coal deposited in fluvial systems fed by ancestral uplifts (Flores, 1986). Widespread CBNG development occurs within the Wyodak-Anderson coal zone of the Fort Union Formation, which contains eleven named coalbeds. This coalbed also serves as a regional aquifer (BLM, 2003a) where groundwater flow is generally to the northwest (Daddow, 1986). The Anderson coalbed, which is part of the Wyodak-Anderson coal zone, is the production target within the study area occurring approximately 230 m below grade.

The study site is located along the Powder River approximately 5 km south of Arvada, Wyoming (Figure 6.2a). Quaternary alluvium in this area is comprised of four units (Figure 6.2b). The Arvada Formation contains highly weathered gravelly sand stained red with yellow-brown cobbles (Leopold and Miller, 1954). The Ucross Formation disconformably overlies the Arvada Formation and is composed of rounded gravels of igneous and metamorphic rocks. The upper one meter is impregnated with calcium carbonate and gypsum interpreted to be a paleosol (Leopold and Miller, 1954). The Kaycee Formation generally contains mixed colluvium/alluvium consisting of a clearly developed soil layer underlain by well sorted silt-sized quartz grains. The Lightning Formation consists of tan fine to medium sand with some fine gravel devoid of bedding planes (Leopold and Miller, 1954). The alluvium overlies thick, blue-gray clay overlying bedrock (Ringen and Daddow, 1990). Climatically controlled erosion created the Kaycee, Moorcroft, and Lightning terraces flanking the stream.

A thin, unconfined aquifer occurs within the Kaycee and Lightning Formations (Figure 6.2b). Alluvium ranges in thickness from about 3 to 15 m, but averages 6 m. The aquifer occurs approximately 2 to 3 m below the ground surface and extends laterally away from the Powder River until intersecting the bedrock erosional surface along the Kaycee terrace (Figure 6.2). A thick, blue-gray clay prevents vertical migration of alluvial water into underlying bedrock aquifers (Ringen and Daddow, 1990). As such, groundwater within the aquifer generally flows northward along the bedrock erosional surface. The main source of recharge to the alluvial aquifer is the Powder River but additional recharge is provided by CBNG infiltration impoundments (Figure 6.2a). The impoundments were installed by Pennaco Energy Inc. (PEI) and have been receiving produced water discharge under Wyoming Pollution Discharge Elimination System Permits since late 2001. The specific impoundments investigated in this research are named J3 and J5. Discharge rates into each pond have steadily decreased from approximately 150-200 m^3/s in April 2002 to 1-5 m^3/sec in June 2006.

6.3. METHODS

6.3.1. PEI Sampling and Analysis

Pennaco Energy Inc, (PEI) collected samples from monitoring wells, impoundment outfalls, and the Powder River at varying time intervals from 2001 to present (Figure 6.3). For the purposes of this study, all locations were sampled in July 2002, April 2003, and May 2004, which would allow for comparison of produced water, alluvial groundwater, and stream water chemistry. Monitoring wells were purged by removing 3-5 well volumes using a submersible pump (Adams, 2004). Surface water samples were collected as grab samples. Impoundments J3 and J5 were not sampled during the course of the study, but impoundment NC7 was sampled monthly as part of permit requirements. This impoundment should adequately represent J3 and J5 water quality because all three ponds receive production water from the Anderson Coalbed. Electrical conductivity (EC) and pH were measured in the field with instruments that were calibrated daily.

All samples were shipped on ice to Energy Laboratories in Gillette, Wyoming under normal chain-of-custody protocols. Samples for metal analyses were preserved to pH < 2 using HNO_3. Dissolved metals were analyzed using an ICP-AES (EPA method E200.7), anions were determined using an IC (EPA method E300.0), bicarbonate was determined using Standard Methods 2320B, and dissolved solids were determined using Standard Methods 2540C.

6.3.2. Isotope Sampling and Analysis

Samples were collected on July 11-12, 2005 from the Powder River, produced water impoundments, alluvial aquifer monitoring wells and piezometers, and coalbed natural gas wells for cation and strontium isotope analyses (Figure 6.4). Alluvial groundwater samples (piezometers and monitoring wells) were collected using low flow sampling techniques (Puls and Barcelona, 1996). Groundwater was purged using dedicated high density polyethylene (HDPE) tubing attached to a peristaltic pump directed to a flow-through cell where pH, temperature, and electrical conductivity (EC) were monitored until they stabilized. CBNG produced water samples were collected from continuously pumped gas wells; therefore, purging was not necessary. All samples were field filtered using 0.45 μm syringe filters and separated into two 250 mL acid washed virgin HDPE bottles; one was reserved for cation analyses and the other was used for isotopic analyses. Samples were packed and shipped on ice and further preserved at the University of Pittsburgh using ultrapure nitric acid to a pH < 2.

Cations were analyzed in the geochemistry laboratory at the University of Pittsburgh using a Spectro-Flame Modula, End-on-Plasma, ICP-AES. EPA QA/QC protocol SW846 was followed. Total blanks were analyzed to measure contamination from sampling and preservation techniques and were less than detection limits.

Strontium isotope samples were concentrated and purified using ion exchange and SrSpec® resin under clean laboratory conditions. Purified samples were loaded onto rhenium filaments with a tantalum activator solution. Samples were analyzed on a Finnigan MAT 262 Thermal Ionization Mass Spectrometer. Strontium isotope data were normalized to a SRM987 value of 0.71025. In-run uncertainty was ±0.00001 and estimated external reproducibility was ±0.00002.

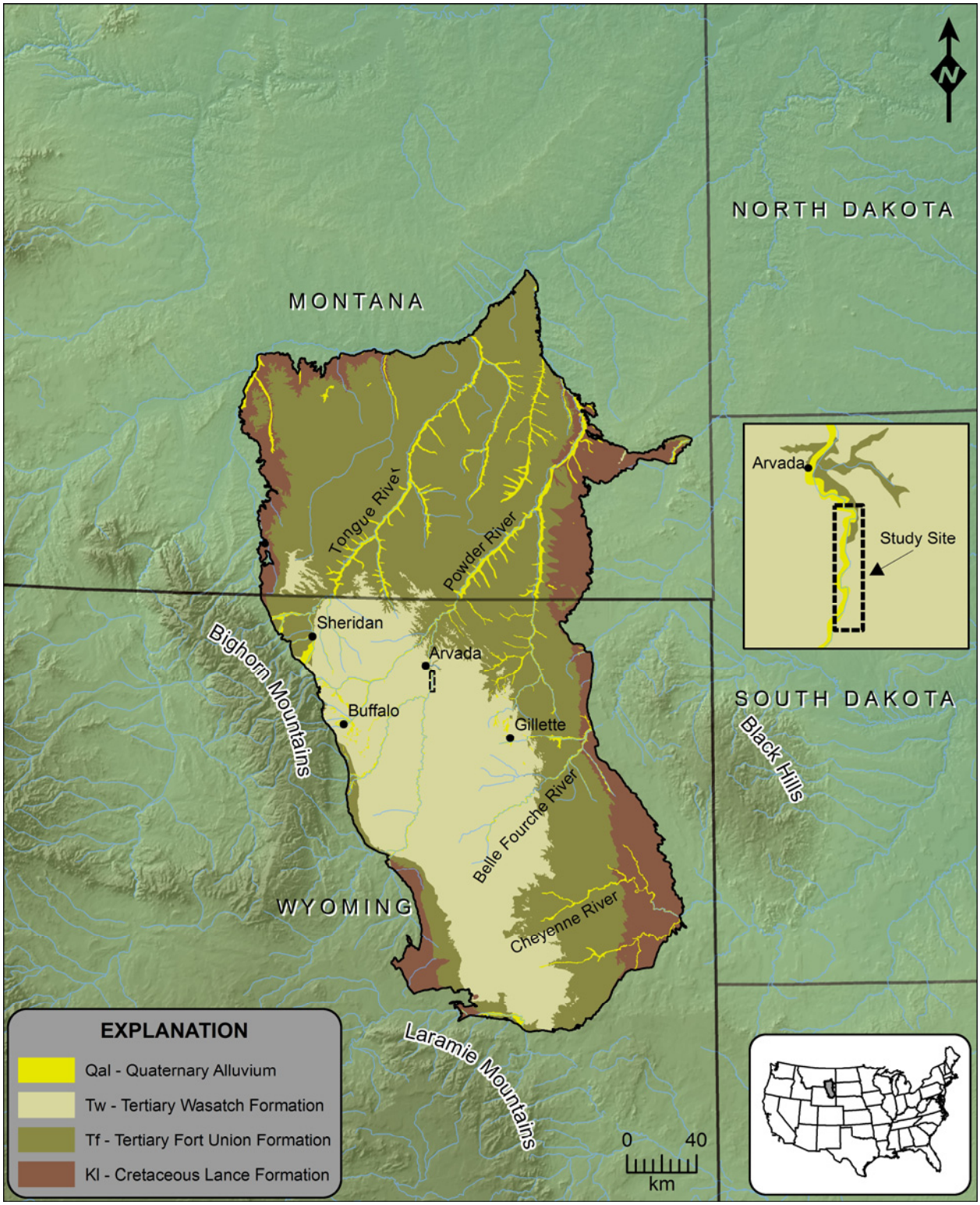

Figure 6.1. The generalized bedrock geology of the Powder River Basin depicted in relation to major physiographic features. Small rectangle approximately 5 km south of Arvada, Wyoming outlines the study area.

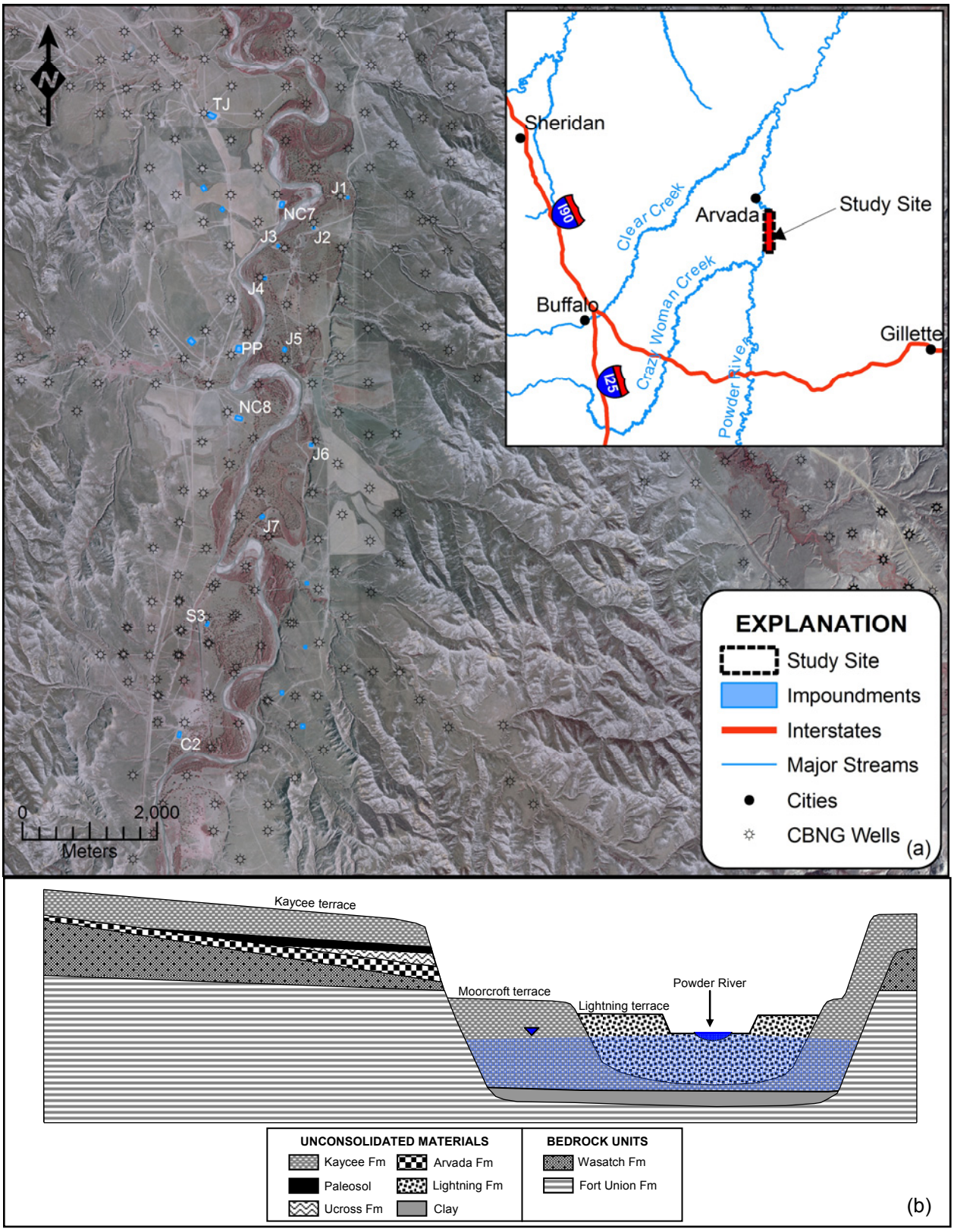

Figure 6.2. Study site (a) location along the Powder River and (b) schematic cross-section depicting Quaternary deposits within the Powder River alluvial valley.

6.4. RESULTS AND DISCUSSION

6.4.1. Trends Major Ions

Discernable trends within the raw major ion data are difficult to detect (Table 6.1) but Piper diagrams reveal distinct characteristics for the various samples (Figure 6.5). In general, produced water is characterized as sodium-bicarbonate type with little calcium and magnesium and little to no detectable levels of sulfate. It contains total dissolved solid concentrations (TDS) less than 2000 mg/L, but SAR levels are high ranging from 25.9 to 30.7. Based on the salinity-SAR relationship developed by the USDA (1954), CBNG water at the site is classified as C3-S4, corresponding to high salinity hazard with a very high sodium hazard. These results are consistent with other studies (Bartos and Ogle, 2002; Ganjegunte et al., 2005; Rice et al., 2000; Van Voast, 2003). The SAR values preclude its use as irrigation water because it will most likely cause clay dispersion with subsequent reduction in soil permeability, which is the reason it is managed using infiltration impoundments at this site.

River samples generally fall within the sodium-sulfate facies. TDS levels were consistent during each sampling event, but varied between separate events from approximately 3320-3650 mg/L in 2002, 1740-1770 mg/L in 2003, and 960-2070 mg/L in 2004. SAR levels also were also consistent during each sampling event but varied between separate events from 8.8-9.5 in 2002, 4.3-5.4 in 2003, and 6.8-7.5 in 2004. Both TDS and SAR in the Powder River are highly controlled by discharge levels. The 2002 sampling event occurred in July when Powder River discharge is near its yearly minimum while the other two sampling events occurred in April and May when spring snowmelt dilutes TDS levels. These results are consistent with reported data (Clark and Mason, 2006; Lindner-Lunsford et al., 1992).

Alluvial groundwater samples generally fall within the sodium-calcium-sulfate facies (Figure 6.5). TDS and SAR levels vary spatially throughout the alluvial aquifer but were consistent amongst each sampling event. TDS ranged from approximately 1300 to 6800 mg/L within the alluvium while SAR ranged from approximately 4.2-12.8.

Montana has set strict standards regulating EC and SAR in Powder River water, which applies to discharge entering the state from Wyoming. From November 1 to March 1, the

monthly average EC standard is 2500 µS/cm and no sample may exceed an EC value of 2500 µS/cm. The monthly average SAR standard during this period is 6.5 and no sample may exceed a SAR value of 9.75. From March 2 to October 31, the monthly average EC standard is 2000 µS/cm and no sample may exceed an EC value of 2500 µS/cm. The monthly average SAR standard during this period is 5.0 and no sample may exceed a SAR value of 7.5. Based on these standards, all Powder River samples were out of compliance during the 2002 and 2004 sampling events for EC and SAR. However, observations made by the United States Geological Survey (USGS) at gauging stations along the Powder River indicate that before CBNG development occurred, historical EC and SAR levels within the Powder River have been above these levels (Clark and Mason, 2006). Additionally, sample PRA is located downstream of the study site and water quality at this location is similar to that from locations PRH and PRK, which are upstream of the impoundments.

6.4.2. Interpreted Process Major Ions

Cation exchange processes play an important role in water quality at the site. A plot of molar Na^+ versus Cl^- supports this interpretation (Figure 6.6a-c). If halite dissolution controlled sodium concentrations, the data would plot along a 1:1 line. Brine inputs would cause the data to fall below the 1:1 line reflecting increased chloride concentrations. However, all data plot above the 1:1 mixing line indicating that cation exchange is likely increasing Na^+ levels in water samples. Additionally, a plot of $Ca^{2+}+Mg^{2+}$ versus $SO_4^{2-}+HCO_3^-$ can also be used to support the interpretation. If calcite, dolomite, and gypsum dissolution were the dominant reactions in a system, then samples would plot on a 1:1 line, but if cation exchange were the dominant process, then points would be shifted below the 1:1 line due to the removal of Ca^{2+} and Mg^{2+} from solution through cation exchange. All samples plot below the 1:1 line on the $Ca^{2+}+Mg^{2+}$ versus $SO_4^{2-}+HCO_3^-$ graph (Figure 6.6d-f).

Produced water is enriched in sodium and bicarbonate. Sodium enrichment is interpreted to result from cation exchange reactions as water migrates through Fort Union rocks, which has been observed by others (Bartos and Ogle, 2002; Van Voast, 2003) and is supported this research (Figure 6.6). Others have hypothesized that sodium enrichment within Fort Union strata could be

enhanced by calcite/dolomite precipitation in the presence of high bicarbonate concentrations (Van Voast, 2003). At bicarbonate concentrations above 1,000 mg/L, which are typical in methane bearing coalbeds, the solubility of calcium and magnesium is less than 25 mg/L (Van Voast, 2003). Bicarbonate concentrations increase during sulfate reduction as methane is produced (Bartos and Ogle, 2002; Rice et al., 2000; Rice and Claypool, 1981; Van Voast, 2003).

Powder River water geochemistry at the site is controlled by stream provenance. Approximately 50% of discharge originates in the Bighorn Mountains while the other 50% originates within the plains. The alpine component of discharge increases during spring snow melt. Discharge contributed from the mountains is generally sodium-bicarbonate facies reflecting Paleozoic limestone sources in the Bighorn Mountains (Clark and Mason, 2006; Lindner-Lunsford et al., 1992). As this water enters the foothills, it interacts with Mesozoic marine sandstone and shale units, where gypsum dissolution alters it to calcium-sulfate type (Clark and Mason, 2006; Lindner-Lunsford et al., 1992). As the water enters the plains, it presumably interacts with sodium rich shale. Sodium enrichment is due to displacement of Na^{+} into solution and uptake of Ca^{2+} and Mg^{2+} ions by cation exchange reactions with clays (Clark and Mason, 2006; Lindner-Lunsford et al., 1992). Additional sodium is provided from oilfield brine effluent in Salt Creek, a tributary of the Powder River approximately 80 km south of the study site (Clark and Mason, 2006; Lindner-Lunsford et al., 1992).

Alluvial water quality is similar to the Powder River because it is a losing stream throughout the study area. As a result, sodium-sulfate river water recharges the alluvial aquifer where TDS concentrations increase due to evaporative processes. The major cation composition of the river water also alters within the aquifer as calcium levels increase. Reverse cation exchange would increase Ca^{2+} and Mg^{2+}, but it would only be expected if Ca^{2+} and Mg^{2+} concentrations were very low with respect to sodium. White nodules interpreted to be gypsum have been observed in borehole logs from within the study area making gypsum dissolution the likely process controlling this interpretation.

Mixing processes are reflected in the major ion data during all three sampling events (Figure 6.5). Conceptually, produced water infiltrates the alluvial aquifer where it mixes with alluvial groundwater. Piper diagram interpretations indicate mixing between sodium-bicarbonate and sodium-calcium-sulfate waters in wells downgradient of both impoundments. As such, data from 2003 and 2004 were arbitrarily classified based on visual inspection of the Piper diagrams

into four classes: (1) sodium-bicarbonate, (2) sodium-sulfate, (3) sodium-calcium-sulfate, and (4) mixed (1 and 3). These data were plotted as a post map with water table contours to aid interpretations (Figure 6.7 and Figure 6.8).

At J3, groundwater generally flows north and northeast; therefore, we would expect produced water influence to potentially affect wells J3W1 to J3W4. CBNG influence was observed at these downgradient monitoring wells (Figure 6.7 and Figure 6.8). In 2004, produced water is interpreted to have reached J3W4 (Figure 6.8). This conclusion is important because CBNG water is interpreted to be migrating towards the Powder River. If CBNG water continues to be disposed in J3, it could eventually reach the Powder River, if it has not already.

At J5, groundwater generally flows northwest; therefore, we would expect produced water to affect J5W1, J5W3, and potentially J5W4. CBNG influence was observed at J5W1 and was also observed in J5W3 during the 2004 sampling event (Figure 6.7 and Figure 6.8). CBNG from J5 could potentially reach the Powder River, but more data are needed to verify this interpretation.

6.4.3. Trends Strontium Isotopes

Strontium isotope ratios determined for filtered water samples collected during the 2005 season are markedly different for the various sample types. Produced water samples (J3, J3O, J5, CBM1, CBM2) have strontium isotope ratios that range from 0.71188 to 0.71366 (Table 6.2). Powder River water samples have a strontium isotopic composition of 0.71082 throughout the study area. Alluvial groundwater samples have strontium ratios that vary spatially and range from 0.71049 to 0.71123. Differences are greater than estimated data error (± 0.00002) indicating that these samples may provide insight into subsurface water-rock interactions or cation exchange processes at the site.

6.4.4. Interpreted Processes Strontium Isotopes

Produced water samples have strontium isotopic values that are not consistent with Wyodak-Anderson coalbeds at this location within the PRB. Fort Union sandstones near Gillette,

Wyoming contain labile strontium in carbonate cement, which imparts a strontium isotope ratio to coalbed water of approximately 0.7126 to 0.7127 on a relatively short time scale that is not appreciably altered by increased water-rock interaction (Frost et al., 2002). Organic matter from Fort Union coals have a $^{87}Sr/^{86}Sr$ of approximately 0.7157 (Frost et al., 2002). Recharge water along the eastern basin margin should gradually acquire the coalbed strontium isotope ratio as it flows downgradient (towards the basin center and northwestward) due to increased water-rock interactions. Samples collected within the study site are near the center of the basin and should have $^{87}Sr/^{86}Sr$ ratios similar to the Fort Union coalbed (0.7157). As samples representing the Anderson coalbed ranged from 0.7119 to 0.71376, it is interpreted that these CBNG wells are producing mixed CBNG/sandstone water. Additionally, this interpretation assumes that surrounding sandstone aquifers have strontium isotope ratios that are less than that observed in eastern Fort Union sandstones (Frost et al., 2002), which is likely considering that previously reported values were collected over 60 km to the east of our study site and that the Fort Union formation contains highly heterogeneous strata. Dewatering of the Anderson coalbed may likely be the cause of reported dry artesian wells in Arvada, Wyoming (Vanvig, 2006).

A major objective of this research was to evaluate the utility of strontium isotopes to trace CBNG water after it is disposed in infiltration impoundments. Major ion data were successful at identifying produced water influence downgradient of impoundments J3 and J5. For strontium isotopes to be successful, the strontium ratio within impoundments and alluvium should be different. The $^{87}Sr/^{86}Sr$ ratio in J3 was 0.7124 while upgradient alluvial wells were approximately 0.7108 (Figure 6.9). The $^{87}Sr/^{86}Sr$ ratio of J5 was 0.7137 while upgradient alluvial wells were approximately 0.7109 (Figure 6.10). These differences are greater than data uncertainties indicating that this method is viable. Based on the observed alluvial and impoundment strontium ratios, one would expect elevated $^{87}Sr/^{86}Sr$ near the impoundments that gradually decreased to levels characteristic of the alluvial aquifer further downgradient. This spatial distribution is not observed at either impoundment (Figure 6.9 and 6.10). Additionally, these data do not plot on a binary mixing line when $^{87}Sr/^{86}Sr$ is plotted against 1/Sr (Figure 6.11). Subsequently, mixing was not observed at J3 or J5 using strontium isotope data.

The observed distribution of strontium isotope ratios infers that infiltrating impoundment water acquired the alluvium strontium signature rapidly. This could be the result of two processes: (1) dissolution of strontium salts in the vadose zone or (2) cation exchange reactions.

Dissolution of vadose zone salts is possible, but is likely to be insignificant as TDS levels downgradient of both impoundments did not increase after produced water disposal began. Additionally, these data were collected approximately four years after disposal started. Therefore, quickly dissolving salts, such as gypsum, should have been leached from the vadose zone underlying the impoundment at the time samples were collected. This leaves cation exchange reactions as the most likely process that produced the observations. Previous research indicates that even with low montmorillonite clay percentages (1%), the retardation factor of strontium can be on the order of ~1000 (Johnson and DePaolo, 1997a, b). In the presence of high SAR water, sodium will displace calcium and strontium from cation exchange sites on clays. The exchanged strontium will have the strontium isotope ratio of the alluvial sediments, which will buffer the strontium isotope ratio of infiltrating produced water.

6.5. CONCLUSIONS AND RECOMMENDATIONS

Waters from the various sample regimes display distinct geochemical characteristics that result from several geochemical processes. Produced water is characteristically sodium-bicarbonate type resulting from cation exchange processes that enrich sodium and sulfate reduction that enriches bicarbonate. Powder River water at the site is characteristically sodium-sulfate type water, which is the product of gypsum dissolution and cation exchange processes that occur from its origin in the Bighorn Mountains and Great Plains along its flow path. Alluvial water is characteristically sodium-calcium-sulfate type water that is altered Powder River water with increased salinity due to evapotranspiration processes and increased calcium due to water-rock interactions. Disposal of produced water into infiltration impoundments creates water that is a mix between sodium-bicarbonate and sodium-calcium-sulfate type waters. With time, these produced water plumes have gradually migrated downgradient.

Impoundment location may have a profound impact on the ultimate fate of produced water. Impoundments placed too close to the Powder River run the risk of altering the stream from losing to gaining, forcing mixed alluvial/produced water into the Powder River. Considering Montana has set strict standards on EC and SAR and that historical data from pre-

CBNG development indicate that native Powder River water may sometimes violate these standards, additional input of high EC and high SAR water could be detrimental. Situating the impoundment further from the stream will prevent this problem and could potentially allow SAR levels to decrease through increased water-rock interaction time in the alluvial sediments.

Strontium isotopes revealed insight into several geochemical processes at the site. First, strontium isotope data coupled with results presented in previous research (Frost et al., 2002) indicate that the Anderson Coalbed is dewatered at this site. Additionally, strontium isotope data indicate that Powder River alluvial sediments have a high cation exchange capacity. Distinct isotopic end members were present between produced water and alluvial water; however mixing was not observed using strontium data while it was readily apparent in major ion data. This implies that high SAR water forces strontium, calcium, and magnesium adsorbed to clays into solution where they are replaced by sodium. Ultimately, replacement of divalent cations with monovalent cations will cause clay minerals to expand and disperse, thereby reducing their infiltration capacity. This could create infiltration impoundments that essentially become lined with impermeable clay, which would lower their designed disposal capabilities.

6.6. ACKNOWLEDGEMENTS

This work was supported by the National Energy Technology Laboratory of the Department of Energy. The author would like to thank the Wyoming Department of Environmental Quality for their assistance in field logistics and Marathon Oil Company for access to their wells. Additionally, the author would like to thank Brian K. Games for his expert assistance with all aspects of sample processing.

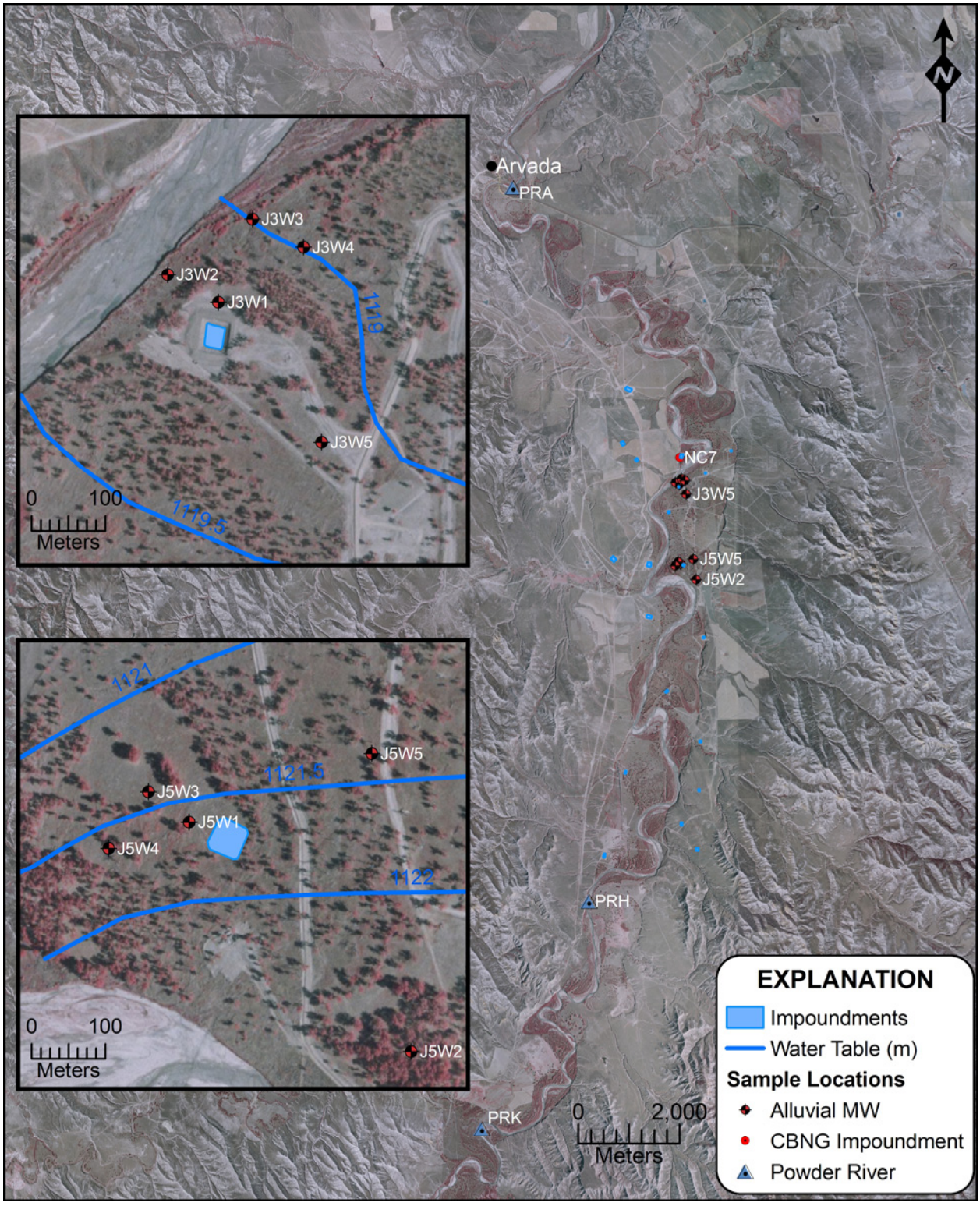

Figure 6.3. Sample locations for the 2002, 2003, and 2004 PEI sampling events. Water table contours are from July 2005.

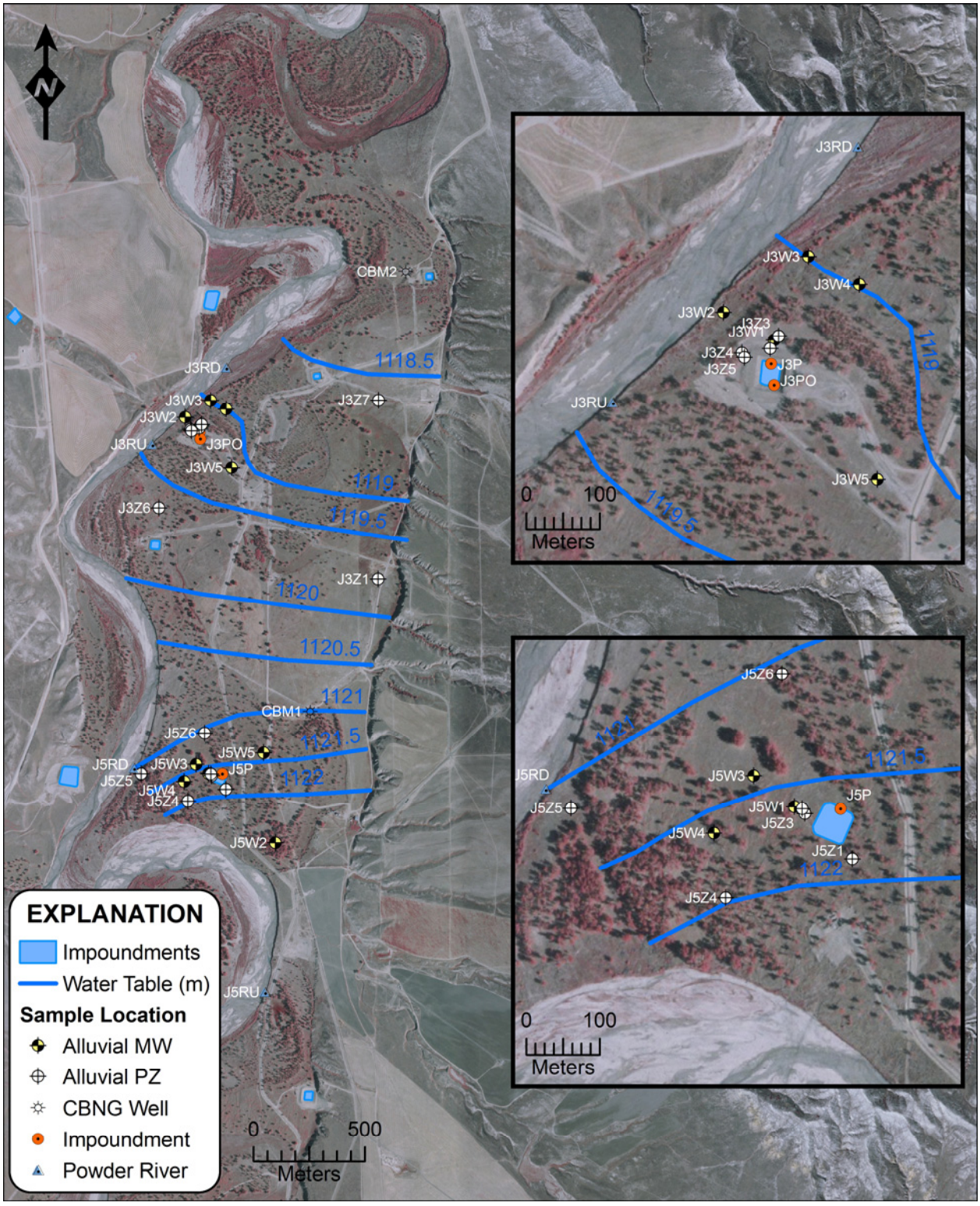

Figure 6.4. Strontium isotope sample locations surrounding the J3 and J5 CBNG produced water disposal impoundments for July 2005. Water table contours are from this sampling event.

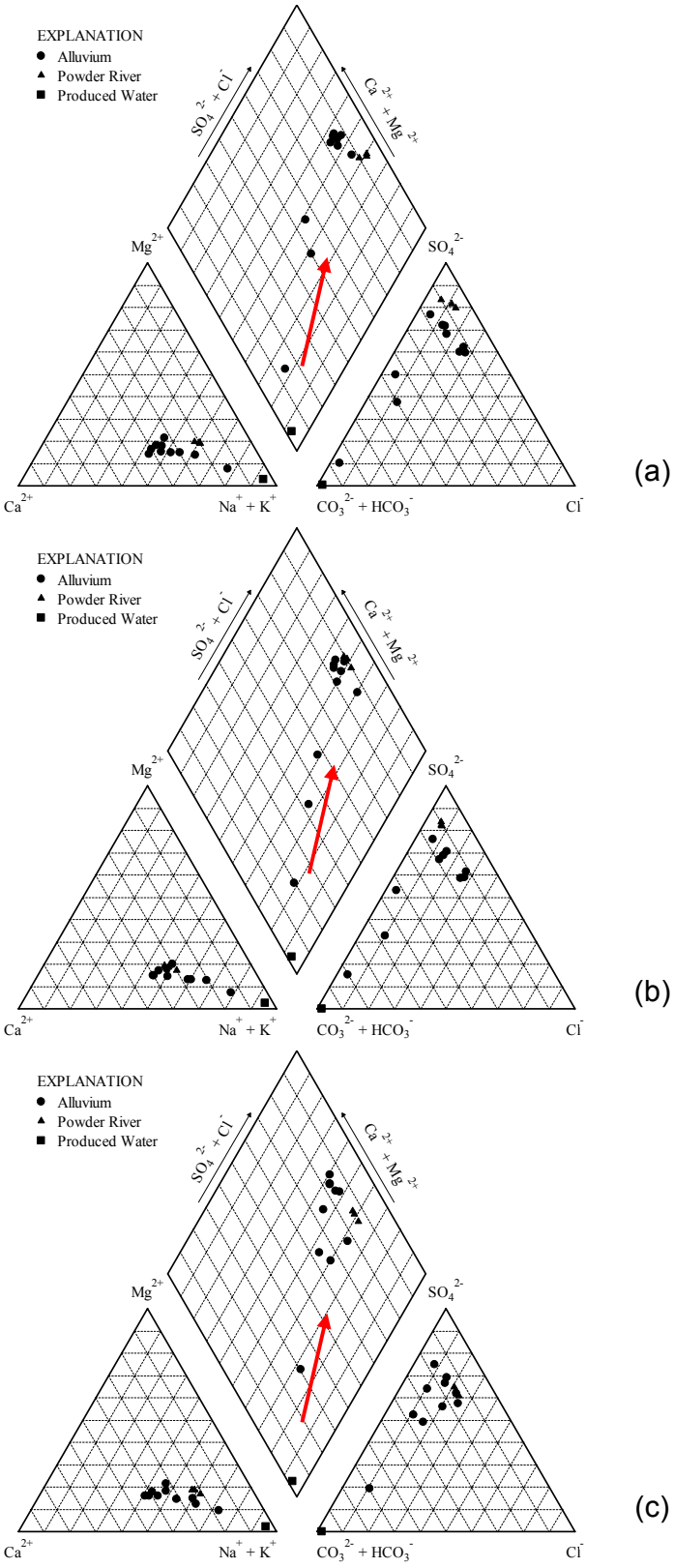

Figure 6.5. Piper diagrams of the PEI sampling results for (a) 2002, (b) 2003, and (c) 2004. Mixing is depicted with red line.

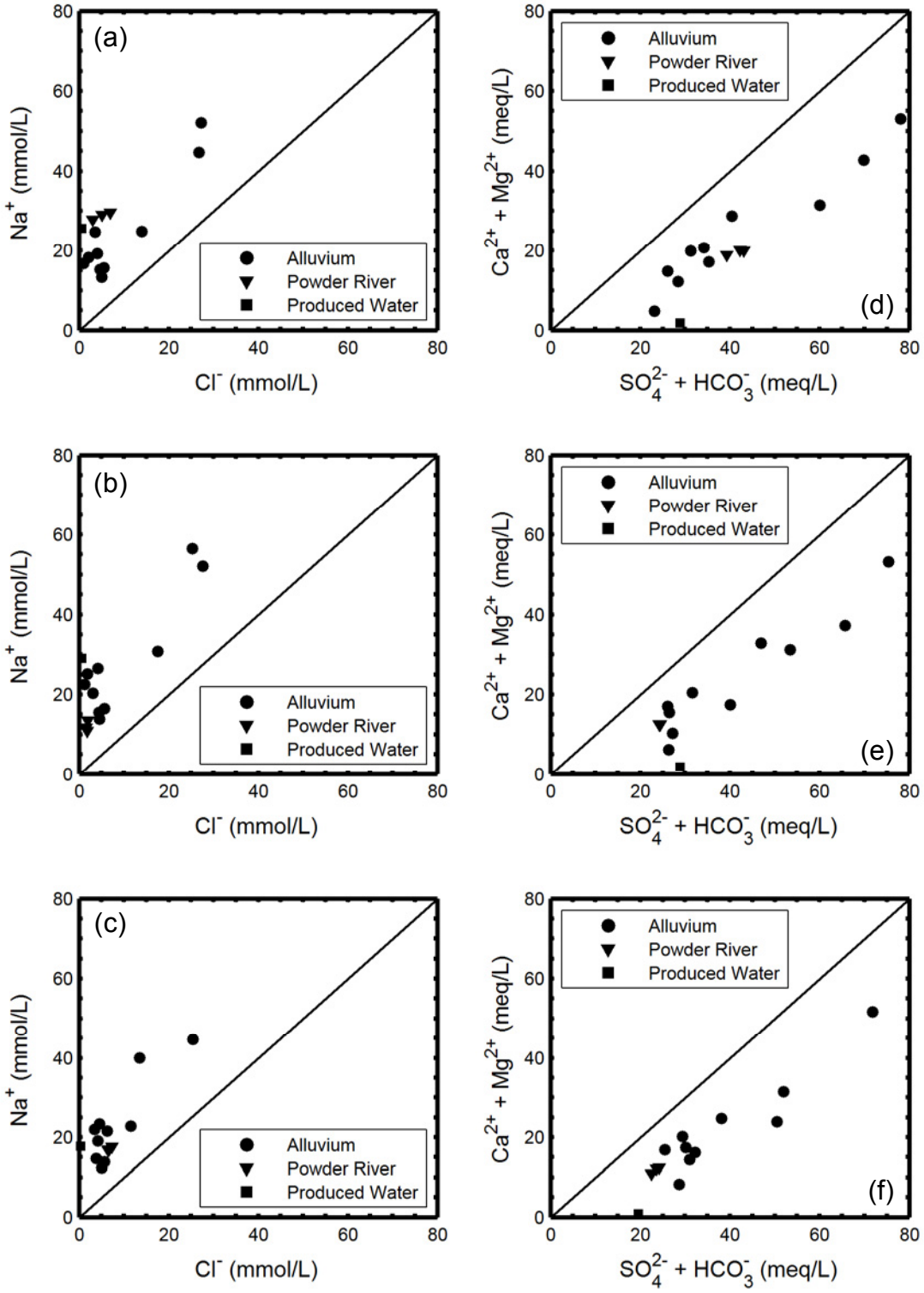

Figure 6.6. Relationship between Na^+ and Cl^- for the (a) 2002, (b) 2003, and (c) 2004 sampling events and the relationship between $Ca^{2+} + Mg^{2+}$ and $SO_4^{2-} + HCO_3^-$ for the (d) 2002, (e) 2003 and (f) 2004 sampling events.

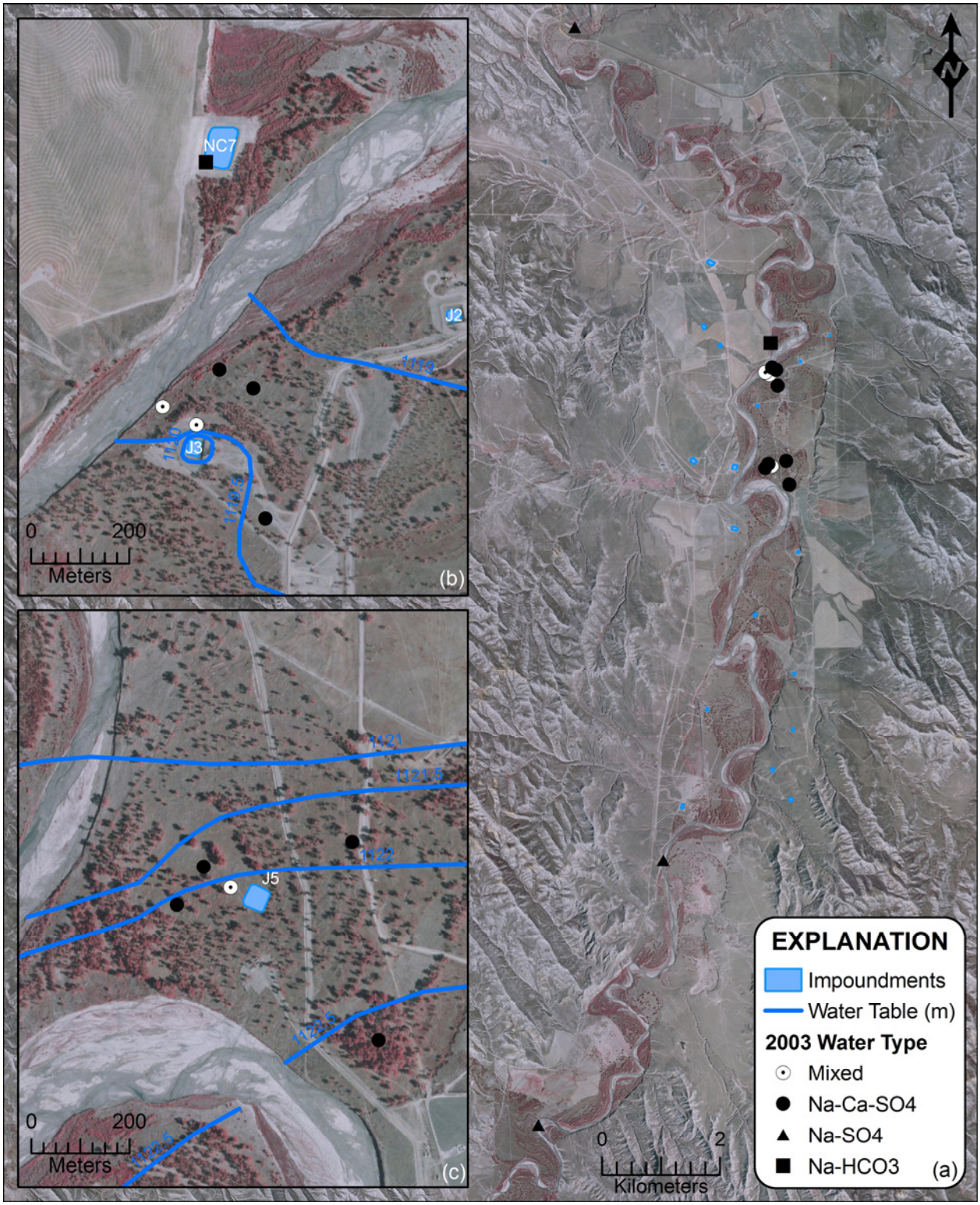

Figure 6.7. Classified 2003 geochemical data for (a) the entire study site, (b) the J3 site, and (c) the J5 site.

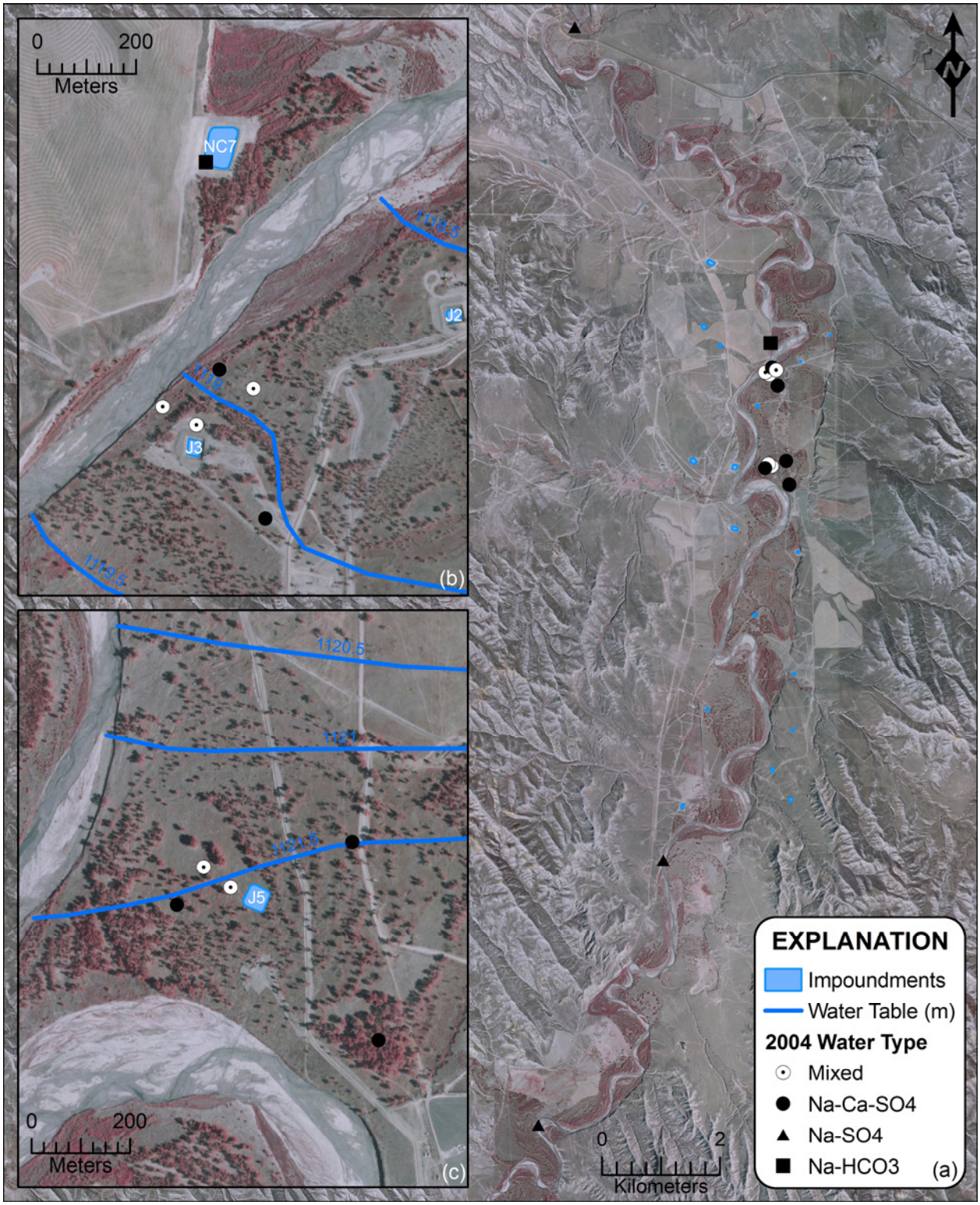

Figure 6.8. Classified 2004 geochemical data for (a) the entire study site, (b) the J3 site, and (c) the J5 site.

Figure 6.9. Strontium isotope ratios at sample locations near the J3 impoundment.

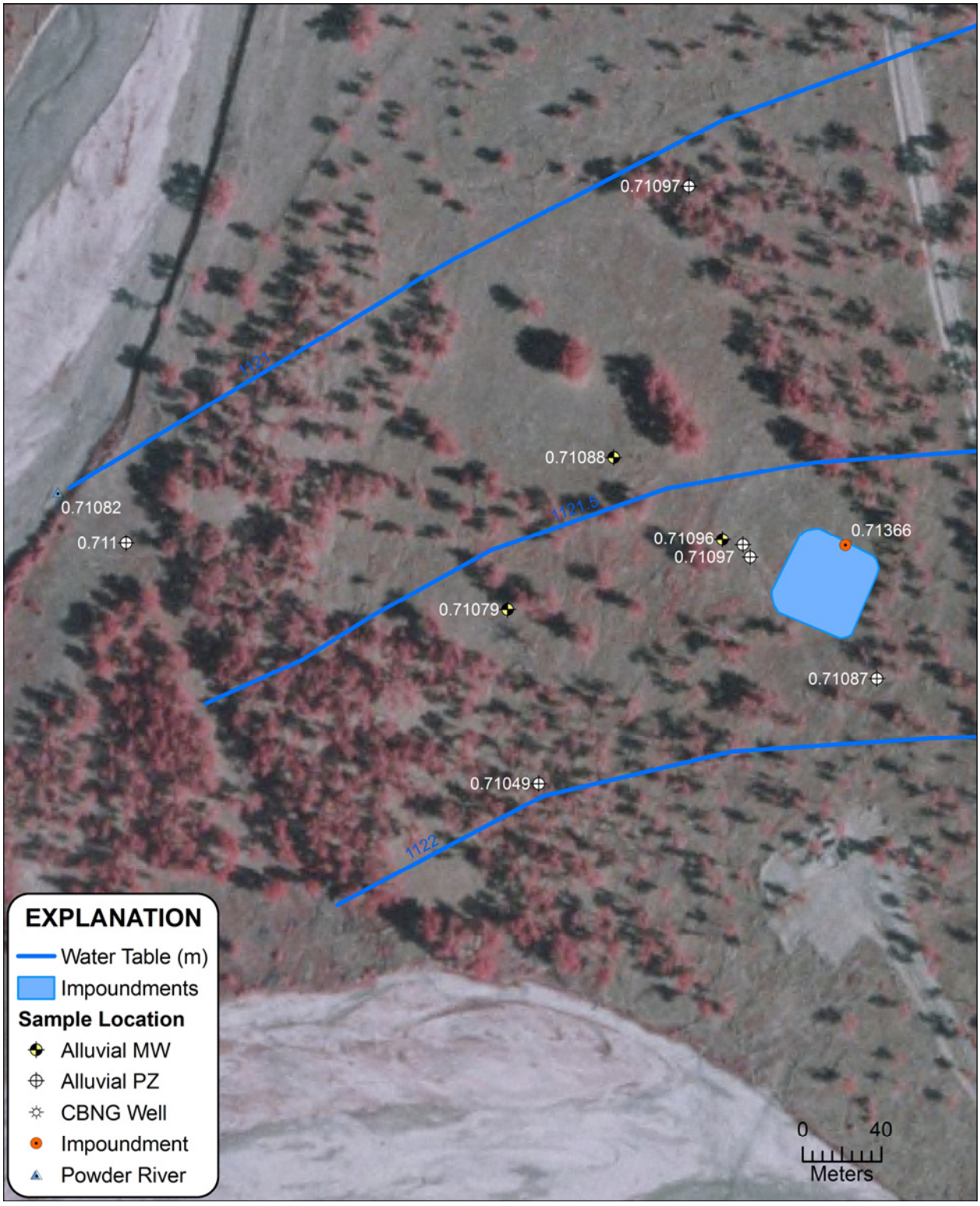

Figure 6.10. Strontium isotope ratios at sample locations near the J5 impoundment.

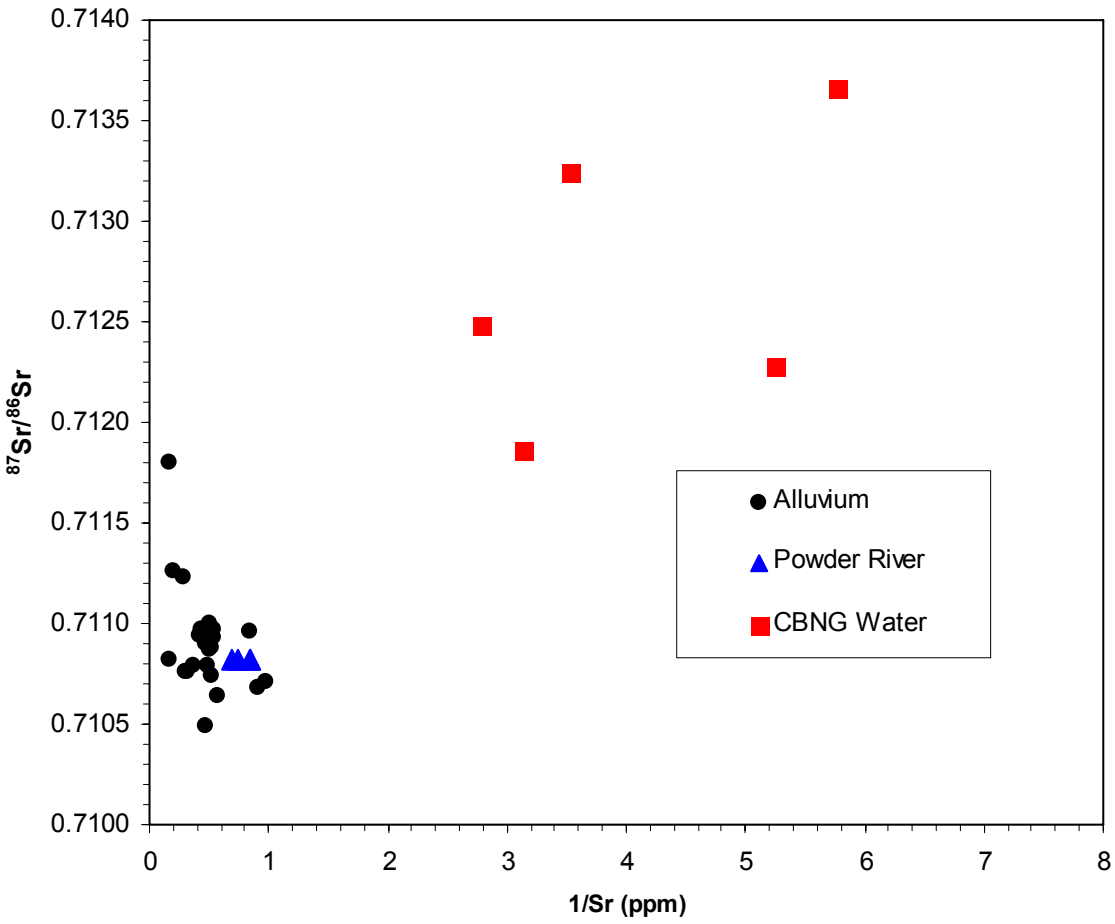

Figure 6.11. Relationship between $^{87}Sr/^{86}Sr$ and 1/Sr for samples collected within the Powder River alluvial aquifer near the J3 and J5 impoundments.

Table 6.1. Geochemical analyses of water samples collected from the study area by PEI during three events.

Site	Date	Ca^{2+} mg/l	Mg^{2+} mg/l	Na^{+} mg/l	K^{+} mg/l	HCO_3^{-} mg/l	Cl^{-} mg/l	SO_4^{2-} mg/l	TDS mg/l	EC µS/cm	SAR unitless	pH s.u.
J3W1	07/09/02	65	20	387	5	1260	33	117	1320	2060	10.8	7.64
J3W2	07/09/02	157	54	445	8	993	143	581	1950	2870	7.8	7.29
J3W3	07/09/02	384	117	574	10	402	493	1630	3530	4560	6.6	7.17
J3W4	07/09/02	576	171	1200	13	731	962	2790	6410	7980	11.3	7.01
J3W5	07/09/02	639	258	1030	16	939	946	3020	6710	7960	8.7	7.04
J5W1	07/09/02	238	65	421	7	1020	71	892	2200	2980	6.2	7.34
J5W2	07/09/02	425	126	570	12	689	123	2350	4110	4680	6.2	7.15
J5W3	07/09/02	212	53	308	7	299	178	1020	1590	2610	4.9	7.25
J5W4	07/09/02	301	61	351	9	335	163	1240	2310	2930	4.8	7.05
J5W5	07/09/02	297	73	361	8	354	193	1370	2570	3280	4.9	7.19
PRA	07/08/02	205	118	682	22	201	247	1920	3650	4770	9.4	8.56
PRH	07/08/02	215	115	641	20	286	105	1810	3460	4590	8.8	8.53
PRK	07/08/02	195	112	669	22	195	181	1740	3320	4470	9.5	8.29
NC7	07/01/02	20	10	590	8	1750	20	5	1922	2470	26.9	8
J3W1	04/09/03	82	26	520	7	1350	40	201	1540	2350	12.8	7.52
J3W2	04/09/03	130	48	470	8	1060	107	473	1770	2610	8.9	7.38
J3W3	04/09/03	430	140	710	13	445	621	1910	4170	5250	7.6	7.21
J3W4	04/09/03	500	150	1300	16	746	894	2580	6010	7580	13.1	7.09
J3W5	04/09/03	640	260	1200	19	940	975	2890	6830	8040	10.1	7.1
J5W1	04/09/03	240	68	580	9	1090	63	1070	2600	3400	8.5	7.43
J5W2	04/09/03	430	120	610	13	592	146	2110	3880	4420	6.7	7.2
J5W3	04/09/03	220	56	360	9	354	155	996	2140	2740	5.6	7.29
J5W4	04/09/03	250	56	320	9	311	159	1010	2130	2670	4.8	7.22
J5W5	04/09/03	300	68	380	9	331	199	1260	2550	3150	5.2	7.2
PRA	04/06/03	160	55	270	10	162	56	1050	1740	2260	4.7	8.20
PRH	04/06/03	160	56	250	9	174	62	1030	1780	2290	4.3	8.24
PRK	04/06/03	160	54	310	11	172	69	1040	1770	2300	5.4	8.24
NC7	04/01/03	20	10	669	9	1760	19	0	1906	2450	30.7	7.86
J3W1	05/27/04	110	35	508	7	1370	121	297	1790	2810	10.8	7.36
J3W2	05/27/04	182	66	498	8	777	219	879	2300	3310	8.0	7.16
J3W3	05/27/04	325	105	526	9	465	405	1470	3190	4330	6.5	7.07
J3W4	05/27/04	321	97	922	11	904	477	1720	4180	5550	11.6	7.03
J3W5	05/27/04	622	251	1030	15	977	899	2690	6170	7990	8.8	7.04
J5W1	05/27/04	223	63	440	7	811	144	911	2290	3160	6.7	7.3
J5W2	05/27/04	435	120	538	10	591	158	2040	3780	4530	5.9	7
J5W3	05/27/04	247	63	340	7	521	132	1040	2220	2940	5.0	7.27
J5W4	05/27/04	247	57	285	7	318	176	979	2050	2740	4.2	7.18
J5W5	05/27/04	297	67	320	7	323	198	1160	2370	3140	4.4	7.12
PRA	05/29/04	138	67	387	11	268	227	955	2070	2920	6.8	8.26
PRH	05/29/04	134	66	391	12	272	236	923	2020	2890	6.9	8.25
PRK	05/29/04	123	58	405	12	266	261	874	1960	2890	7.5	8.27
NC7	06/01/04	11	5	409	5	1190	12	0	1346	1730	25.8	7.8

Table 6.2. Geochemical analyses of water samples collected from the study area in July 2005.

Location	Date	Na^+ mg/L	K^+ mg/L	Ca^{2+} mg/L	Mg^{2+} mg/L	SAR unitless	Sr^{2+} mg/L	$^{87}Sr/^{86}Sr$
Coalbed Natural Gas Well Samples								
CBM1	7/12/05	404	10	14	7	21.7	0.28	0.71324
CBM2	7/12/05	444	10	14	7	24.5	0.32	0.71188
Impoundment Samples								
J3P	7/11/05	626	14	5	8	40.3	0.19	0.71228
J3O	7/11/05	517	11	17	8	25.6	0.36	0.71248
J5P	7/12/05	532	12	4	7	36.2	0.17	0.71366
Alluvial Aquifer Samples								
J3W1	7/11/05	693	16	239	79	9.9	2.15	0.71090
J3W2	7/11/05	450	12	195	73	7.0	1.73	0.71064
J3W3	7/11/05	452	14	329	109	5.5	2.66	0.71079
J3W4	7/11/05	788	16	252	72	11.3	1.89	0.71074
J3W5	7/11/05	1054	29	696	287	8.5	5.76	0.71082
J3Z1	7/11/05	666	20	544	292	5.7	6.02	0.71180
J3Z2	7/11/05	481	10	108	37	10.2	1.09	0.71068
J3Z3	7/11/05	551	11	107	33	11.9	1.01	0.71071
J3Z4	7/11/05	821	17	390	139	9.1	3.32	0.71076
J3Z5	7/11/05	850	18	360	117	10.0	3.20	0.71076
J3Z6	7/11/05	593	14	245	62	8.8	1.86	0.71093
J3Z7	7/11/05	1012	26	550	409	8.0	5.10	0.71126
J5W1	7/12/05	218	8	172	52	3.7	1.18	0.71096
J5W2	7/12/05	498	11	481	91	5.5	3.51	0.71123
J5W3	7/12/05	339	5	287	28	5.1	1.91	0.71088
J5W4	7/12/05	302	8	331	64	4.0	2.02	0.71079
J5W5	7/12/05	334	11	340	71	4.3	2.28	0.71097
J5Z1	7/12/05	344	11	287	74	4.7	1.97	0.71087
J5Z2	7/12/05	437	8	338	89	5.5	2.42	0.71094
J5Z3	7/12/05	560	9	335	104	6.9	2.31	0.71097
J5Z4	7/12/05	352	9	272	65	5.0	2.11	0.71049
J5Z5	7/12/05	370	9	293	63	5.1	1.95	0.71100
J5Z6	7/12/05	468	11	287	56	6.6	1.85	0.71097
River Samples								
J3RU	7/11/05	240	11	111	56	4.6	1.18	0.71082
J3RD	7/11/05	219	11	111	54	4.3	1.18	0.71082
J5RU	7/12/05	307	13	143	58	5.5	1.46	0.71082
J5RD	7/12/05	281	12	134	56	5.1	1.34	0.71082

Strontium isotope data were normalized to SRM987 = 0.71025. In-run uncertainty is ~0.00001 and estimated external reproducibility is ±0.00002.

7. INTEGRATING GEOPHYSICS AND GEOCHEMISTRY

7.1. INTRODUCTION

Geophysical methods have been successfully applied to hydrogeologic problems in the past (Aaltonen and Olofsson, 2002; Asprion and Aigner, 1999; Corona and Mavko, 1999; Fitterman and Deszcz-Pan, 1998; Fitterman et al., 1991; Hubbard et al., 2001; Hubbard and Rubin, 2000; Hubbard et al., 1999; Hyndman and Gorelick, 1996; Hyndman and Harris, 1996; Land et al., 2004; Lesmes et al., 2002; Robineau et al., 1997; Scanlon et al., 1999; Smith et al., 2003; Tronicke et al., 2002; Wynn and Liner, 2002). These methods can be used to quantify hydrogeologic parameters, monitor subsurface processes, and map water quality with a higher degree of spatial resolution than traditional characterization methods. However, case histories of geophysical methods applied to hydrogeologic problems larger than plume scale are limited, which is in part due to cost and technology considerations (Fitterman and Deszcz-Pan, 2002; Fitterman et al., 1991; Love et al., 2005; Sengpiel, 1983, 1986; Smith et al., 2004). Advances in airborne electromagnetic (AEM) methods over the past decade coupled with sophisticated and readily available processing algorithms have created a niche for AEM in hydrogeologic investigations. Past AEM research includes applications in water quality mapping (Fitterman and Deszcz-Pan, 1998; Lipinski et al., 2004; Lipinski et al., 2006; Sengpiel, 1983, 1986) and inferring regional scale lithologic variations (Smith et al., 2003; Smith et al., 2004). These studies demonstrate that geophysical applications may be cost effective tools for sub-watershed to watershed scale problems.

The rapid development of coalbed natural gas (CBNG) from Tertiary coals in the Powder River Basin (PRB) of Wyoming and Montana since 1997 has created water management problems that could be aided by AEM. CBNG production involves dewatering coalbeds to allow methane desorption and extraction (De Bruin et al., 2004). Each PRB well produces

approximately 34 m^3 water per day over a 7 to 10 year span with produced water volumes decreasing over the well production history (BLM, 2003a). PRB wells have some of the highest water/gas production ratios of current CBNG fields. For example, each PRB well produces 1.9 barrels (bbls) per 1000 cubic feet (MCF) gas, while San Juan Basin CBNG wells produce approximately 0.031 bbls water per MCF gas (DOE, 2003). Over 4.1 billion barrels (Bbbls) have been produced from approximately 22,000 wells since development began in 1997 (WOGCC, 2006). There are expected to be approximately 40,000 additional wells in the Wyoming PRB.

Groundwater associated with methane bearing coalbeds is classified as sodium bicarbonate type with moderate salinity (Rice et al., 2000; Van Voast, 2003). It is also typified as being sodic; it contains elevated levels of sodium relative to magnesium and calcium, which is quantified by the sodium adsorption ratio (SAR). The major disposal mechanism of PRB produced water is through infiltration impoundments. Geophysical studies were proposed to better understand the hydrology related to CBNG produced water disposal.

A detailed airborne EM study was previously completed at an area consisting of several infiltration impoundments along the Powder River (Lipinski et al., 2007b). In this study, geophysical response was correlated to aquifer salinity levels and used to infer processes associated with infiltration impoundments. While airborne EM depicts water quality at a large spatial scale, it only depicts total dissolved solids concentrations; therefore, major ions and strontium isotopes were used to evaluate geochemical processes in the same aquifer (Lipinski et al., 2007a). These data were used to determine geochemical changes occurring in an alluvial aquifer receiving CBNG water. In this study, the main objective is to integrate the previous geophysical and geochemical results to enhance understanding of processes associated with produced water disposal through infiltration impoundments.

7.2. SITE DESCRIPTION

The study site is located approximately 5 km south of Arvada, Wyoming within the Powder River Basin (PRB) (Figure 7.1a) and was described in detail in previous papers (Lipinski et al., 2007a; Lipinski et al., 2007b). CBNG exploration at this site is focused within the Anderson

Coalbed of the Fort Union Formation, which occurs approximately 230 m below the surface. Production water is brought to the ground surface and discharged into several infiltration impoundments located in the Powder River alluvial valley (Figure 7.1a). Powder River alluvium is composed of four units (Figure 7.1b). The Arvada Formation contains highly weathered gravelly sand (Leopold and Miller, 1954). The Ucross Formation is composed of rounded gravels of igneous and metamorphic rocks and the upper portion is impregnated with calcium carbonate and gypsum interpreted to be a paleosol (Leopold and Miller, 1954). The Kaycee Formation contains a clearly developed soil layer underlain by well sorted silt-sized quartz grains. The Lightning Formation consists of fine to medium sand devoid of bedding planes (Leopold and Miller, 1954). Underlying these sediments is a thick, blue-gray clay overlying bedrock that is pervasive throughout the area (Ringen and Daddow, 1990). The alluvium contains a thin, unconfined aquifer that occurs approximately 2 to 3 m below the ground surface and extends laterally to the bedrock erosional surface along the Kaycee terrace and vertically downward to the clay layer overlying bedrock (Figure 7.1). Impoundments were installed by Pennaco Energy Inc. (PEI) and have been receiving produced water discharge under Wyoming Pollution Discharge Elimination System Permits since late 2001. Discharge rates into ponds have steadily decreases from approximately 150-200 m^3/s in April 2002 to 1-5 m^3/sec in June 2006.

7.3. METHODS

The primary goal of this research is to integrate research presented in two previous papers (Lipinski et al., 2007a; Lipinski et al., 2007b). As such, the reader is referred to these articles for a detailed description of data collection and analysis. However, a brief description of each is provided below.

7.3.1. AEM Data Collection and Processing

Fugro Airborne Surveys collected airborne electromagnetic (AEM) data within the study area on July 25, 2003 and July 31, 2004 using the RESOLVE system (Cain, 2003, 2004). The system

consists of five coplanar transmitter/receiver coils one coaxial transmitter/receiver coil. Coplanar frequencies during the 2003 survey were 387 Hz, 1.7 kHz, 6.54 kHz, 28.1 kHz, and 116 kHz while the coaxial frequency was 1.41 kHz. Coplanar frequencies during the 2004 survey were 391 Hz, 1.8 kHz, 8.18 kHz, 39.1 kHz, and 132.6 kHz while the coaxial frequency was 3.33 kHz. Data outside the Quaternary aquifer boundary were not analyzed as part of this study. Additionally, data were culled form areas with power line and magnetic interference. Filtered and leveled data were subject to geophysical inversion using the UBC-GIF program EM1DFM. Formation conductivity values computed from the inversion were related to porewater salinity using field data collected from monitoring wells in the study area. Results were interpolated to a regular grid for visualization in plan view. Vertical resolution of porewater salinity is not attainable because the aquifer is only approximately 4 to 6 m thick.

7.3.2. Water Quality Sampling

Pennaco Energy, Incorporated (PEI) collected samples from various locations in the study area at regular intervals from 2001 to present. Data were available for April 2003 and May 2004 from alluvial monitoring wells, the Powder River, and an impoundment for comparison with the June 2003 and July 2004 airborne EM data. Samples were analyzed for major ions by Energy Labs in Gillette, Wyoming under normal chain-of-custody protocols. These data were submitted to the Wyoming Department of Environmental Quality (WYDEQ) and were provided to the author upon request.

Samples were collected on July 11-12, 2005 from the Powder River, produced water impoundments, alluvial monitoring wells, alluvial piezometers, and coalbed natural gas wells for cation and strontium isotope analysis. Cations were analyzed in the geochemistry laboratory at the University of Pittsburgh using a Spectro-Flame Modula, End-on-Plasma, ICP-AES according to EPA QA/QC protocol SW846. Strontium isotope samples were concentrated and purified using ion exchange and SrSpec® resin under clean laboratory conditions. Samples were analyzed on a Finnigan MAT 262 Thermal Ionization Mass Spectrometer. Strontium isotope data were normalized to a SRM987 value of 0.71025. In-run uncertainty was ±0.00001 and estimated external reproducibility was ±0.00002.

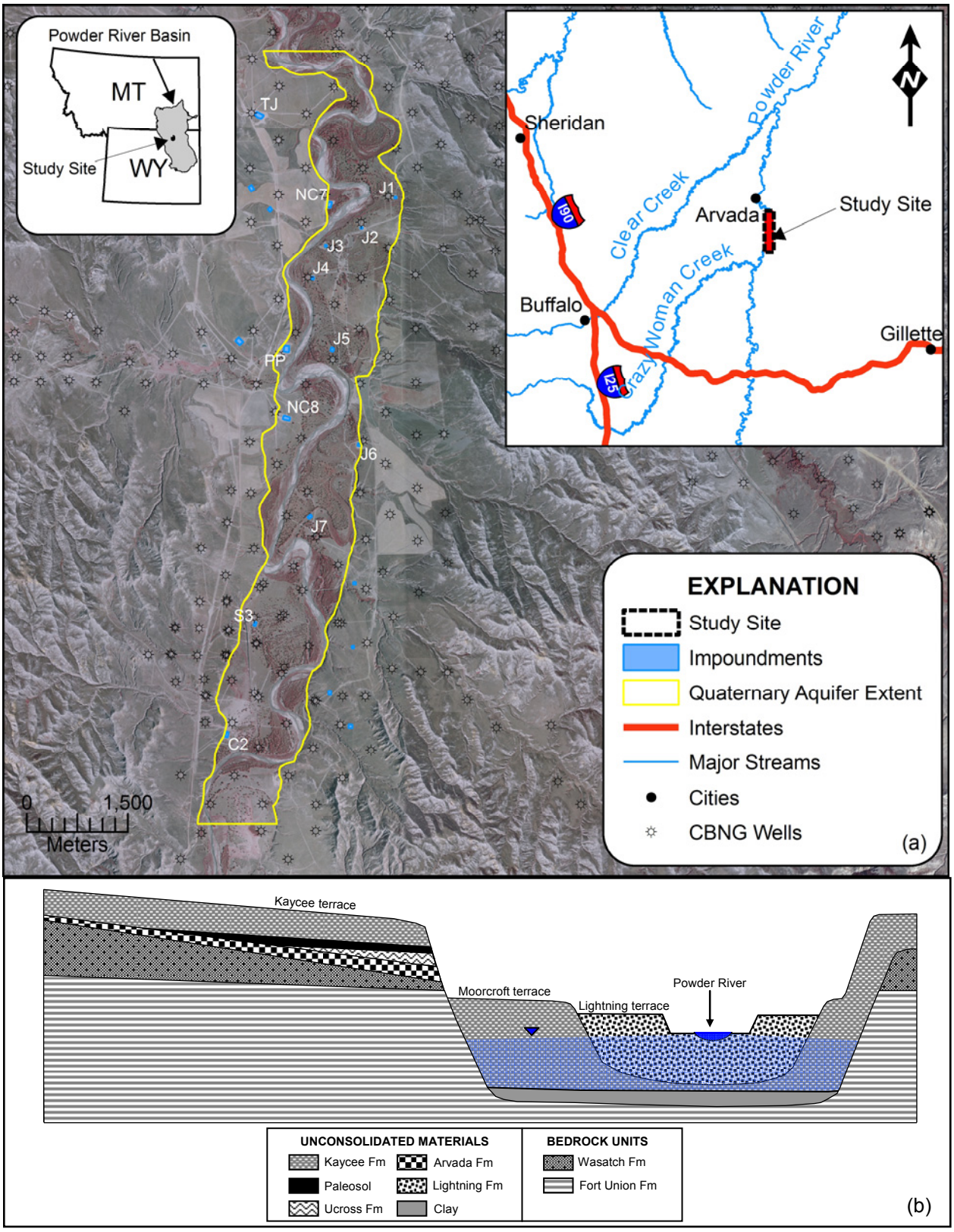

Figure 7.1. Study site (a) location along the Powder River and (b) schematic cross-section depicting Quaternary deposits within the Powder River alluvial valley.

7.4. RESULTS AND DISCUSSION

7.4.1. Observations

Geochemical and geophysical results were coupled to provide a clearer picture of underlying processes at the site. Results from the 2003 and 2004 sampling events were classified based on their previously reported major ion chemistry (Lipinski et al., 2007a). Stream samples are prototypically sodium-sulfate type, produced water is prototypically sodium-bicarbonate type, and unaltered alluvial groundwater is typically sodium-calcium-sulfate type. Additionally, a class consisting of mixed produced water and alluvial water was created to account for the observed mixing near impoundments. These classes were plotted as a post map underlain by geophysically inferred porewater TDS concentrations (Figures 7.2 and 7.3).

Observed dilution of geophysically inferred alluvial groundwater TDS concentrations at impoundment J3 is most likely due to produced water (Figures 7.2 and 7.3). Wells immediately downgradient of the impoundment contain mixed produced/alluvial water. Additionally, produced water influence has extended further downgradient from 2003 to 2004, which is not readily apparent in the geophysical data alone. Additionally, spatial distribution of TDS coupled with the interpreted hydraulic head distribution infers that produced water most likely has migrated to the Powder River at this location.

Observed patterns of geophysically inferred alluvial groundwater TDS concentrations at impoundment J5 is due in part to CBNG water (Figures 7.2 and 7.3), but this determination could not definitively be made using geophysical data. The proximity of the impoundment to the meander where low TDS Powder River water continually flushes the system has created a natural dilution zone at this site compared to other regions of the aquifer where dissolved salts are concentrated by evapotranspiration. Infiltrating produced water has similar TDS levels as the alluvial water, but the major ion chemistry is markedly different. This is only apparent in the geochemical results. Produced water has migrated further downgradient from 2003 to 2004 (Figures 7.2 and 7.3), which is also not apparent based upon the interpretations of AEM geophysical data.

A major concern of regulatory agencies is that produced water will alter stream water quality. Geochemical and geophysical data indicate that produced water has migrated to the Powder River at two sites, NC7 and J3 (Figures 7.2 and 7.3). However, geochemical analyses of samples collected from the Powder River upstream and downstream of these impoundments indicate that there is no impact on the overall stream geochemistry (notably electrical conductivity and the sodium adsorption ratio (SAR) are similar for samples collected upstream and downstream of CBNG impoundments).

7.4.2. System Conceptual Model

Coupling the geophysical results to the geochemical results allows for a clearer conceptual model to describe observations at the site (Fugure 7.4). From geophysical data and field observations, it was interpreted that vadose zone salt dissolution created a salinity plume downgradient of NC7. Shallow groundwater can create vadose zone salt accumulation through high evapotranspiration. While no groundwater data were available, we can infer from J3 and J5 interpretations that the major ion composition of groundwater reflects mixed conditions. At J3 and J5 it was interpreted from major ion data and strontium isotope data that cation exchange reactions were a major controlling factor on the concentration of sodium relative to calcium and magnesium in infiltrating produced water (Lipinski et al., 2007a). Additionally, major ion data indicated that CBNG has mixed with native alluvial water downgradient of impoundments. Groundwater at J3 and J5 was deeper than at NC7, therefore, vadose zone salt accumulation is not interpreted to occur here. These observations allow for an overall update to the conceptual model of produced water disposal within Quaternary alluvium of the Powder River (Figure 7.4).

7.5. CONCLUSIONS AND IMPLICATIONS FOR FUTURE DEVELOPMENT

Geophysical data were not collected prior to CBNG water disposal. Subsequently, the undisturbed pattern of TDS concentrations with the alluvial groundwater was unknown. Anomalous features within the geophysical data can be correlated to anomalous features in the

geochemical data. Completing these comparisons allows geochemical data to confirm or refute interpretations made from the geophysical data. Additionally, the inferred processes controlling produced water distribution within the alluvial aquifer gleaned from geochemical analyses can be used to provide insight into other processes observed in areas where only geophysical information is available.

Results from the coupled geochemical and geophysical investigation have provided significant insight into processes resulting from produced water disposal using infiltration impoundments. Impoundment location is an important consideration prior to construction and subsequent use in CBNG development. In this area, impoundments should be located within the alluvial valley as far away from the river as possible because native alluvial water (with high TDS levels) could be forced into the stream by reversing the hydraulic head field. Additionally, stream meanders serve as poor locations because they are essentially in direct communication with the Powder River. Point bars may also have significant vadose zone salt accumulations from evapotranspiration by dense vegetation and a shallow water table, which infiltrating CBNG water will dissolve creating TDS plumes. Cation exchange processes act to lower sodium levels of infiltrating produced water but this process may ultimately reduced the sediment permeability by clay dispersion decreasing the designed disposal capacity of the impoundment.

Observations made at this study site are important for proposed development in other portions of the basin. The Powder River alluvial aquifer water quality is generally considered poor and it is not typically used for irrigation or even stock watering. However, alluvial sediments of the Tongue River northwest of the study area contain water that has low TDS levels (<1,000 mg/L) and low SAR levels (<4) (Nimick, 2002) because the Tongue River has its origin in the Bighorn Mountains and is a gaining stream throughout Wyoming. Disposal of produced water in a similar manner as that observed at the study site may have profoundly different effects. Produced water would essentially increase SAR and EC levels in the aquifer potentially rendering them unusable for their designated use class. Also, impoundments would essentially be in hydraulic communication with the Tongue River. Tongue River alluvial sediments are coarser than those encountered at the study site; therefore their cation exchange capacities may be much lower. As such, there will be little opportunity for sodium concentrations to decrease as the infiltrated water migrates to the stream. However, this setting might prove useful to reevaluate strontium isotopes as CBNG water tracers.

AEM surveys could be successfully used to monitor produced water disposal within alluvial valleys of the Powder River Basin if they are enhanced by geochemical studies. For this strategy to be successful, pre-development airborne EM surveys should be completed. The geophysical data can then be evaluated to determine potentially suitable impoundment locations. Field investigations could be completed at these sites that included soil sampling and laboratory analyses to determine grain size distributions, cation exchange capacities, and soluble salt concentrations. These would provide government and corporate stakeholders with information needed to predict the behavior of solutes within the subsurface after disposal. Post-development surveys could then be used to focus ground-based water quality investigations to verify geophysical interpretations. Additionally, the airborne geophysical data can be used in cases where ground-based studies are logistically prohibitive.

7.6. ACKNOWLEDGEMENTS

This work was supported by the National Energy Technology Laboratory of the Department of Energy. The author would like to thank the Wyoming Department of Environmental Quality for their assistance in field logistics and for their data sharing practices. The author is also thankful to Marathon Oil Company for access to their monitoring wells.

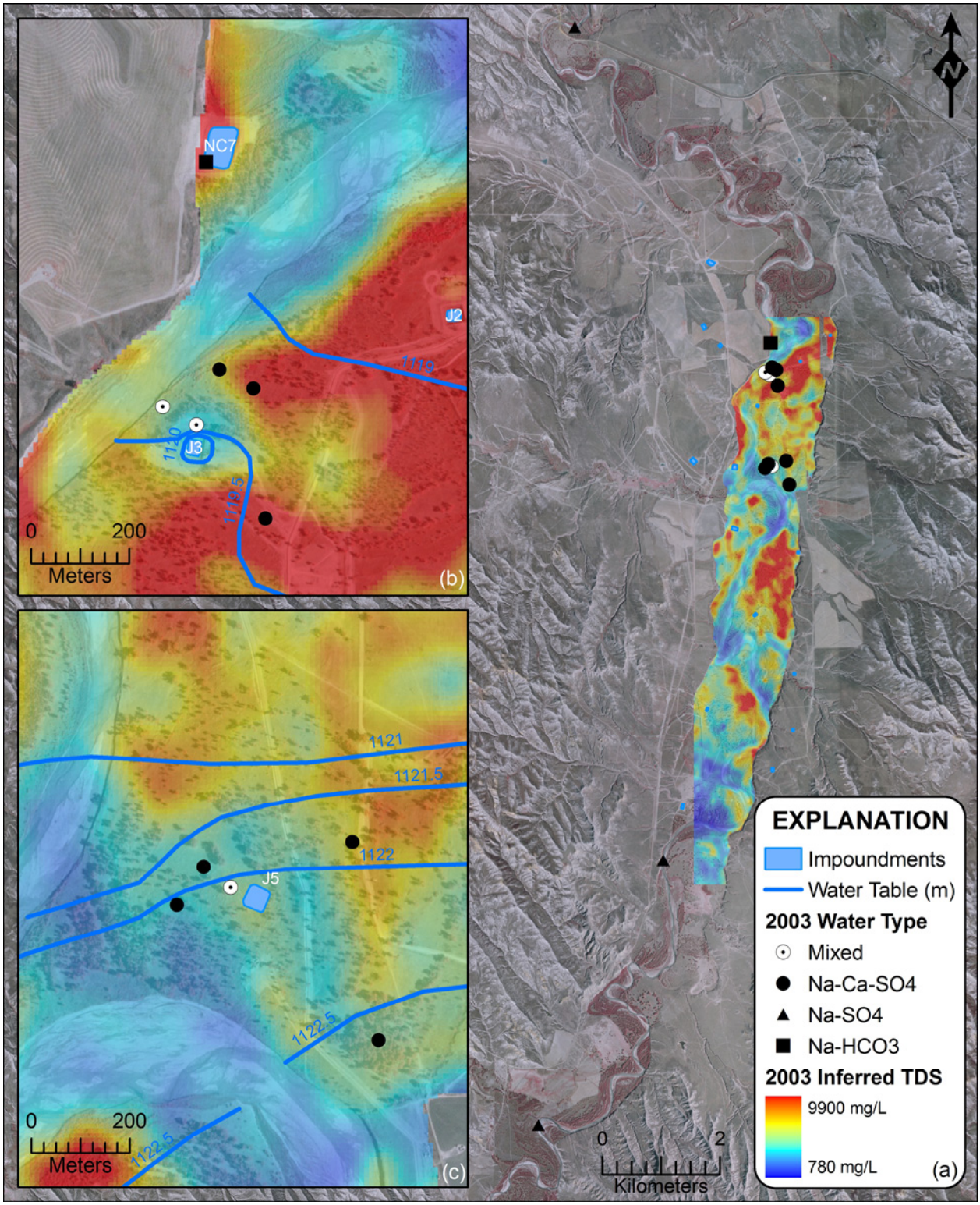

Figure 7.2. Groundwater sample types interpreted from major ion data plotted over the geophysically inferred porewater TDS map for (a) the entire study site, (b) near impoundment J3, and (c) near impoundment J5. Groundwater data are from April 2003 and AEM data are from July 2003. Mixed samples represent mixed alluvial and CBNG produced water.

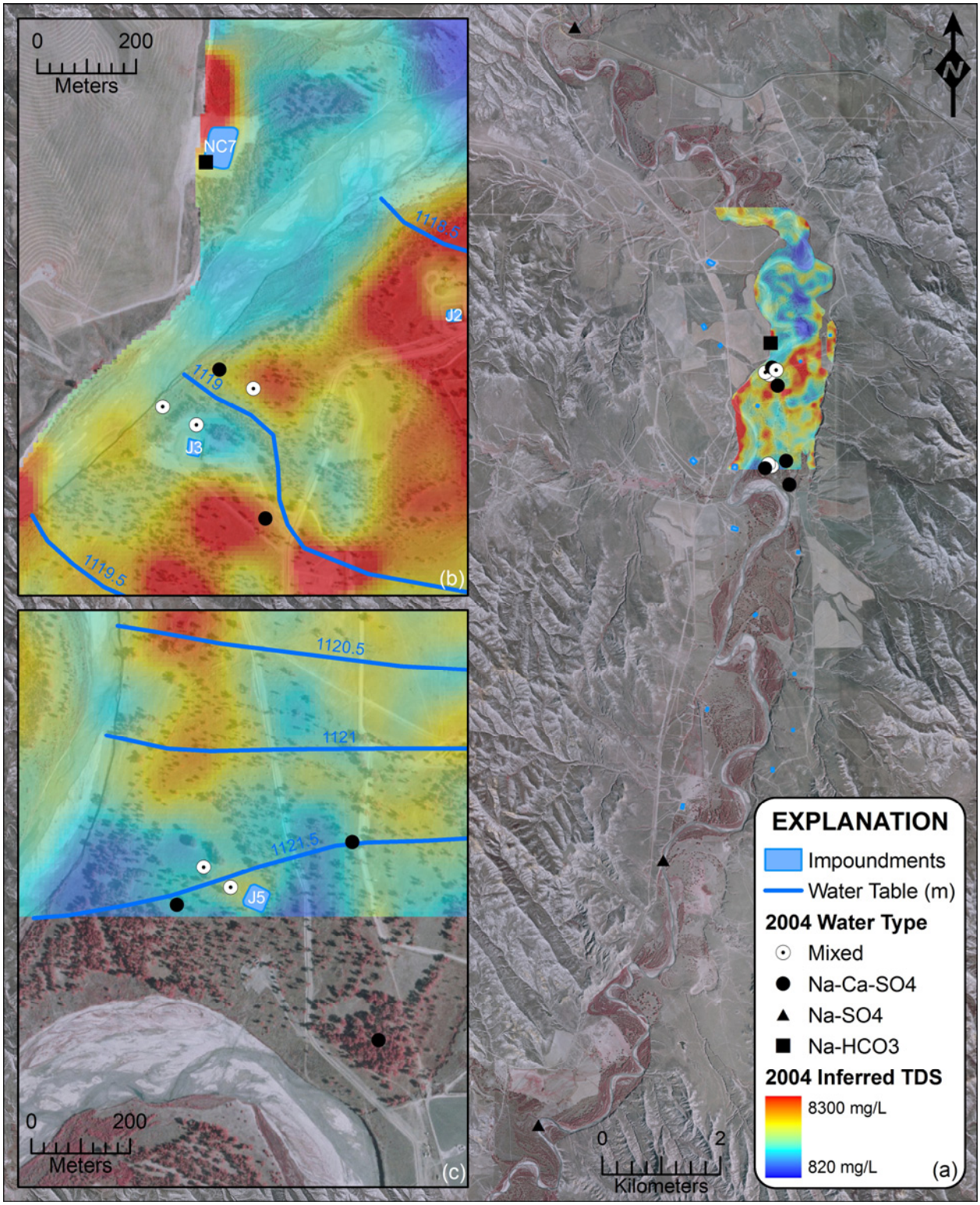

Figure 7.3. Groundwater sample types interpreted from major ion data plotted over the geophysically inferred porewater TDS map for (a) the entire study site, (b) near impoundment J3, and (c) near impoundment J5. Groundwater data are from May 2004 and AEM data are from July 2004. Mixed samples represent mixed alluvial and CBNG produced water.

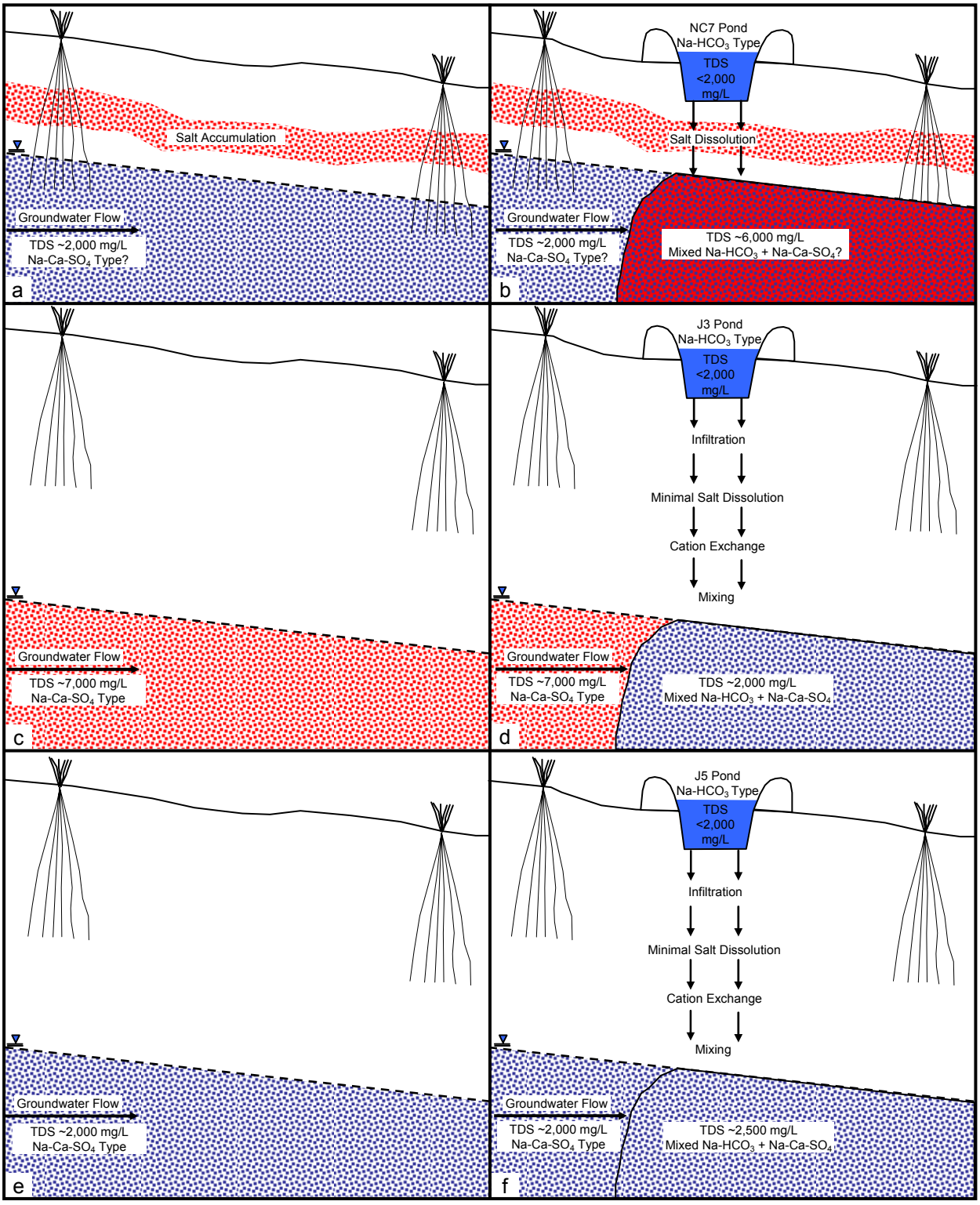

Figure 7.4. Conceptual representation of CBNG impoundment influence on aquifer water quality based on geophysical and geochemical results. (a) Site NC7 prior to pond installation and (b) after disposal. (c) Site J3 prior to pond installation and (d) after disposal. (e) Site J5 prior to pond installation and (f) after disposal. Note the interpreted control of water table depth on vadose zone salt accumulation. Also note the affect of background water salinity levels on the ability AEM to map CBNG water influence.

LITERATURE CITED

Aaltonen, J., and Olofsson, B., 2002, Direct current (DC) resistivity measurements in long-term groundwater monitoring programmes: Environmental Geology, v. 41, p. 662-671.

Aberg, G., 1995, The use of natural strontium isotopes as tracers in environmental studies: Water, Air and Soil Pollution, v. 79, p. 309-322.

Adams, T., 2004, Sampling techniques at the Arvada, Wyoming test site, Personal Communication to Lipinski, B.A. on August 4, 2004.

ARI, 2002, Powder River basin coalbed methane development and produced water management study National Energy Technology Laboratory Department of Energy 2003-1184.

Asprion, U., and Aigner, T., 1999, Towards realistic aquifer models; three-dimensional georadar surveys of Quaternary gravel deltas (Singen Basin, SW Germany), *in* Aigner, T., Teutsch, G., and Huggenberger, P., eds., Sedimentary Geology, Volume 129, p. 281-297.

Ayers, W.B., Jr., 1986, Lacustrine and fluvial-deltaic depositional systems, Fort Union Formation (Paleocene) Powder River basin, Wyoming and Montana: AAPG Bulletin, v. 70, p. 1651-1673.

—, 2002, Coalbed gas systems, resources and production and a review of contrasting cases from the San Juan and Powder River basins: AAPG Bulletin, v. 86, p. 1853-1890.

Bartos, T.T., and Ogle, K.M., 2002, Water quality and environmental isotopic analyses of ground-water samples collected from the Wasatch and Fort Union formations in areas of colbed methane development - implications to recharge and ground-water flow, eastern Powder River Basin, Wyoming: U.S. Geological Survey Open File Report 02-4045.

Beamish, D., 2002, An assessment of inversion methods for AEM data applied to environmental studies: Journal of Applied Geophysics, v. 51, p. 75-96.

BLM, 2003a, Final environmental impact statement and proposed plan amendment for the Powder River Basin oil and gas project: Bureau of Land Management Environmental Impact Statement WY-070-02-065.

—, 2003b, Final statewide oil and gas environmental impact statement and proposed plan amendment for the Powder River Basin and Billings resource management plans: Bureau of Land Management Environmental Impact Statement BLM/MT/PL-03/005.

Burke, W.H., Denison, R.E., Hetherington, E.A., Koepnick, R.B., Nelson, H.F., and Otto, J.B., 1982, Variation of seawater (super 87) Sr/ (super 86) Sr throughout Phanerozoic time: Geology, v. 10, p. 516-519.

Cain, M.J., 2003, Survey Report, Helicopter-borne RESOLVE EM and Magnetic Geophysical Survey, U.S. Department of Energy, Powder River Basin Coal Bed Methane Demonstration Survey: Mississauga, Ontario, Canada, p. 39.

—, 2004, RESOLVE Survey for U.S. Department of Energy, Powder RIver Basin Area, Wyoming: Mississauga, Ontario, Canada, p. 64.

Capo, R.C., Stewart, B.W., and Chadwick, O.A., 1998, Strontium isotopes as tracers of ecosystem processes; theory and methods: Geoderma, v. 82, p. 197-225.

Choate, R., Johnson, C.A., and McCord, J.P., 1984, Geologic overview, coal deposits, and potential for methane recovery from coalbeds; Powder River basin, *in* Rightmire, C.T., Eddy, G.E., and Kirr, J.N., eds., Coalbed Methane Resources of the United States, Volume 17, p. 335-351.

Clark, I., and Fritz, P., 1997, Environmental isotopes in hydrogeology: Boca Raton, Fl, CRC Press, 328 p.

Clark, M.L., and Mason, J.P., 2006, Water-quality characteristics, including sodium-adsorption ratios, for four sites in the Powder River drainage basin, Wyoming and Montana, Water Years 2001-2004: Scientific Investigations Report 2006-5113.

Constable, S.C., Parker, R.L., and Constable, C.G., 1987, Occam's inversion; a practical algorithm for generating smooth models from electromagnetic sounding data: Geophysics, v. 52, p. 289-300.

Corona, W.W., and Mavko, G., 1999, Predicting clay content and porosity from gamma-ray and conductivity logs, *in* Powers, M.H., Cramer, L., and Bell, R.S., eds., Proceedings of the Symposium on the Application of Geophysics to Environmental and Engineering Problems (SAGEEP), vol.1999, p. 425-433.

Curry, W.H.I., 1971, Laramie structural history of the Powder River Basin, Wyoming, Wyoming Geological Association Guidebook, Wyoming Tectonics Symposium, p. 49-60.

Curtis, J., and Grimes, K., 2004, Wyoming Climate Atlas: http://www.wrds.uwyo.edu/wrds/wsc/climateatlas/

Daddow, P.B., 1986, Potentiometric-surface map of the Wyodak-Anderson coal bed, Powder River Structural Basin, 1973-1984: U.S. Geological Survey Water-Resources Investigation 85-4305.

De Bruin, R.H., Lyman, R.M., Jones, R.W., and Cook, L.W., 2004, Coalbed methane in Wyoming: Wyoming Geological Survey Information Pamphlet 7.

DOE, 2003, Coal Bed Methane Primer: New source of natural gas - environmental implications: National Energy Technology Laboratory National Petroleum Technology Office

Doll, W.E., Nyquist, J.E., Beard, L.P., and Gamey, T.J., 2000, Airborne geophysical surveying for hazardous waste site characterization on the Oak Ridge Reservation, Tennessee: Geophysics, v. 65, p. 1372-1387.

Ellis, M.S., Gunther, G.L., Flores, R.M., Ochs, A.M., Stricker, G.D., Roberts, S.B., Taber, T.T., Bader, L.R., and Schuenemeyer, J.H., 1998, Preliminary report on coal resources of the Wyodak-Anderson coal zone, Powder River basin, Wyoming and Montana: U.S. Geological Survey Open-File Report 98-0789-A.

Farquharson, C.G., 2005, Selection of trade-off parameter in EM1DFM, Personal Communication to Lipinski, B.A. on 11/28/2005.

Farquharson, C.G., and Oldenburg, D.W., 2004, A comparison of automatic techniques for estimating the regularization parameter in non-linear inverse problems: Geophysical Journal International, v. 156, p. 411-425.

Farquharson, C.G., Oldenburg, D.W., and Rough, P.S., 2003, Simultaneous 1D inversion of loop-loop electromagnetic data for magnetic susceptibility and electrical conductivity: Geophysics, v. 68, p. 1857-1869.

Faure, G., and Powell, J.L., 1972, Strontium isotope geology: New York, Springer-Verlag, 188 p.

Fitterman, D.V., and Deszcz-Pan, M., 1998, Helicopter EM mapping of saltwater intrusion in Everglades National Park, Florida: Exploration Geophysics, v. 29, p. 240-243.

—, 2002, Helicopter electromagnetic data from Everglades National Park and surrounding areas, Florida; collected 9-14 December 1994: U.S. Geological Survey Open-File Report 02-0101.

Fitterman, D.V., Menges, C.M., Al Kamali, A.M., and Jama, F.E., 1991, Electromagnetic mapping of buried paleochannels in eastern Abu Dhabi Emirate, U.A.E: Geoexploration, v. 27, p. 111-133.

Flores, R.M., 1986, Styles of coal deposition in Tertiary alluvial deposits, Powder River Basin, Montana and Wyoming, *in* Lyons, P.C., and Rice, C.L., eds., Paleoenvironments and tectonic controls in coal-forming basins of the United States: Geological Society of America Special Paper 210, p. 105-122.

Flores, R.M., and Bader, L.R., 1999, Fort Union Coal in the Powder River basin, Wyoming and Montana; a synthesis: U.S. Geological Survey Professional Paper 1625-A.

Flores, R.M., Charpentier, R.R., Cook, T.A., Crovelli, R.A., Klett, T.R., Pollastro, R.M., and Schenk, C.J., 2004, Total petroleum system and assessment of coalbed gas in the Powder River Basin Province, Wyoming and Montana: U.S. Geological Survey Digital Data Series 0069-C.

Flores, R.M., Ochs, A.M., Bader, L.R., Johnson, R.C., and Vogler, D., 1999, Framework geology of the Fort Union Coal in the Powder River basin: U.S. Geological Survey Professional Paper 1625-A.

Fountain, D., 1998, Airborne electromagnetic methods - 50 years of development: Exploration Geophysics, v. 29, p. 1-11.

Fraser, D.C., 1978, Resistivity mapping with an airborne multicoil electromagnetic system: Geophysics, v. 43, p. 144-172.

Frost, C.D., Pearson, B.N., Ogle, K.M., Heffern, E.L., and Lyman, R.M., 2002, Sr isotope tracing of aquifer interactions in an area of accelerating coal-bed methane production, Powder River basin, Wyoming: Geology, v. 30, p. 923-926.

Frost, C.D., and Toner, R.N., 2004, Strontium isotopic identification of water-rock interaction and ground water mixing: Ground Water, v. 42, p. 418-432.

Ganjegunte, G.K., Vance, G.F., and King, L.A., 2005, Soil chemical changes resulting from irrigation with water co-produced with coalbed natural gas: Journal of Environmental Quality, v. 34, p. 2217-2227.

Gosselin, D.C., Harvey, F.E., Frost, C.D., Stotler, R., and Macfarlance, P.A., 2004, Strontium isotope geochemistry of groundwater in the central part of the Dakota (Great Plains) aquifer, USA: Applied Geochemistry, v. 19, p. 0359-0377.

Hammack, R.W., and Mabie, J.S., 2002, Airborne EM and magnetic surveys find fault(s) with Sulphur Bank mercury mine Superfund site: The Leading Edge, v. 21, p. 1092.

Healy, R., 2006, Skewed Reservoir status, Personal Communication to Lipinski, B.A. on 6/12/06.

Hinaman, K., 2005, Hydrogeologic framework and estimates of ground-water volumes in Tertiary and Upper Cretaceous hydrogeologic units in the Powder River basin, Wyoming: U.S. Geological Survey Scientific Investigations Report 2005-5008.

Hotchkiss, W.R., and Levings, J.F., 1986, Hydrogeology and simulation of water flow in strata above the Bearpaw Shale and equivalents of eastern Montana and northeastern Wyoming: U.S. Geological Survey Water-Supply Paper 85-4281.

Huang, H., and Fraser, D.C., 1996, The differential parameter method for multifrequency airborne resistivity mapping: Geophysics, v. 61, p. 100-109.

—, 2001, Mapping of the resistivity, susceptibility, and permittivity of the Earth using a helicopter-borne electromagnetic system: Geophysics, v. 66, p. 148-157.

Hubbard, S.S., Chen, J., Peterson, J., Majer, E.L., Williams, K.H., Swift, D.J., Mailloux, B., and Rubin, Y., 2001, Hydrogeological characterization of the South Oyster bacterial transport site using geophysical data: Water Resources Research, v. 37, p. 2431-2456.

Hubbard, S.S., and Rubin, Y., 2000, Hydrogeological parameter estimation using geophysical data; a review of selected techniques: Journal of Contaminant Hydrology, v. 45, p. 3-34.

Hubbard, S.S., Rubin, Y., and Majer, E., 1999, Spatial correlation structure estimation using geophysical and hydrogeological data: Water Resources Research, v. 35, p. 1809-1825.

Hyndman, D.W., and Gorelick, S.M., 1996, Estimating lithologic and transport properties in three dimensions using seismic and tracer data; the Kesterson Aquifer: Water Resources Research, v. 32, p. 2659-2670.

Hyndman, D.W., and Harris, J.M., 1996, Traveltime inversion for the geometry of aquifer lithologies: Geophysics, v. 61, p. 1728-1737.

Jacobs, J., Tyrrel, P., and Brosz, D., 2003, Wyoming water law: a summary, University of Wyoming, p. 16.

Johnson, T.M., and DePaolo, D.J., 1997a, Rapid exchange effects on isotope ratios in groundwater systems; 1, Development of a transport-dissolution-exchange model: Water Resources Research, v. 33, p. 187-195.

—, 1997b, Rapid exchange effects on isotope ratios in groundwater systems; 2, Flow investigation using Sr isotope ratios: Water Resources Research, v. 33, p. 197-209.

Keller, G.V., and Frischknecht, F.C., 1966, Electrical methods in geophysical prospecting: Oxford, New York, Pergamon Press, 533 p.

Land, L.A., Lautier, J.C., Wilson, N.C., Chianese, G., and Webb, S., 2004, Geophysical monitoring and evaluation of coastal plain aquifers: Ground Water, v. 42, p. 59-67.

Leopold, L.B., and Miller, J.P., 1954, A postglacial chronology for some alluvial valleys in Wyoming: U.S. Geological Survey Water-Supply Paper 1261.

Lesmes, D.P., Decker, S.M., and Roy, D.C., 2002, A multiscale radar-stratigraphic analysis of fluvial aquifer heterogeneity: Geophysics, v. 67, p. 1452-1464.

Limerick, S.H., 2004, Coalbed Methane in the United States, Department of Energy Information Administration.

Lindner-Lunsford, J.B., Parrett, C., Wilson, J.F., Jr., and Eddy-Miller, C.A., 1992, Chemical quality of surface water and mathematical simulation of the surface-water system, Powder River drainage basin, northeastern Wyoming and southeastern Montana: U.S. Geological Survey Water-Resources Investigations 91-4199.

Lipinski, B.A., Capo, R.C., Sams, J., and Harbert, W., 2007a, Geochemical changes in an alluvial aquifer receiving coalbed natural gas produced water discharge, Powder River Basin, Wyoming: In preparation for Ground Water.

Lipinski, B.A., Harbert, W., Hammack, R.W., Sams, J., Veloski, G., and Smith, B.D., 2004, Using airborne and ground electromagnetic surveys and DC resistivity surveys to delineate a plume of conductive water at an in-channel coalbed methane produced water impoundment near the Powder River, Wyoming, 2004 Fall Meeting of the American Geophysical Union: San Francisco.

Lipinski, B.A., Harbert, W., Sams, J., and Smith, B.D., 2007b, Using airborne electromagnetics to monitor coalbed natural gas produced water discharge, Powder River Basin, Wyoming: In preparation for Geophysics.

Lipinski, B.A., Sams, J., Smith, B.D., and Harbert, W., 2006, Airborne geophysical investigation of coalbed natural gas produced water disposal, Powder River Basin, Wyoming: In preparation for Geophysics.

Love, E., Hammack, R., Harbert, W., Sams, J., Veloski, G., and Ackman, T., 2005, Using airborne thermal imagery and helicopter EM imagery to locate mine pools and discharges in the Kettle Creek watershed, norht-central Pennsylvania: Geophysics, v. 70, p. 9.

Malone, G., 2005, "Disturbing trend" comes to light on CBM reservoir permitting, Powder River Breaks, Volume 33: Sheridan, WY, p. 1.

McKinley, M., 2004, Skewed Reservoir groundwater chemistry, Personal Communication to Lipinski, B.A. on 08/01/04.

Montgomery, S.L., 1999, Powder River basin, Wyoming; an expanding coalbed methane (CBM) play: AAPG Bulletin, v. 83, p. 1207-1222.

Negrel, P., and Lachassagne, P., 2000, Geochemistry of the Maroni River (French Guiana) during the low water stage; implications for water-rock interaction and groundwater characteristics: Journal of Hydrology, v. 237, p. 212-233.

Negrel, P., Petelet-Giraud, E., and Widory, D., 2004, Strontium isotope geochemistry of alluvial groundwater; a tracer for groundwater resources characterisation: Hydrology and Earth System Sciences (HESS), v. 8, p. 959-972.

Nimick, D., 2002, Monitoring surface-water quality in the Tongue River Watershed: United States Geological Survey Fact Sheet 02-3011.

Paine, J., 2003, Determining salinization extent, identifying salinity sources, and estimating chloride mass using surface, borehole, and airborne electromagnetic induction methods: Water Resources Research, v. 39, p. 10.

Pashin, J.C., and Hinkle, F., 1997, Coalbed methane in Alabama: Geological Survey of Alabama Circular 192.

Puls, R.W., and Barcelona, M., 1996, Low-flow (minimal drawdown) ground-water sampling procedures: Environmental Protection Agency Ground Water Issue 540/S-95/504.

Reynolds, J.M., 1997, An introduction to applied and environmental geophysics, Wiley, 806 p.

Rhodes, M.K., Carroll, A.R., Pietras, J.T., Beard, B.L., and Johnson, C.M., 2002, Strontium isotope record of paleohydrology and continental weathering, Eocene Green River Formation, Wyoming: Geology, v. 30, p. 167-170.

Rice, C.A., Bartos, T.T., Brooks, M.H., Chong, G.W., Healy, R., Lipinski, B., McBeth, J., McKinley, M., Smith, B.D., and Smith, R.L., 2005, Coalbed natural gas development in the Powder River basin, WY and MT; impacts on land and water in a semiarid environment, Abstracts with Programs - Geological Society of America, Volume 37, p. 25.

Rice, C.A., Ellis, M.S., and Bullock, J.H., Jr., 2000, Water co-produced with coalbed methane in the Powder River basin, Wyoming; preliminary compositional data: U.S. Geological Survey Open-File Report 00-0372.

Rice, D.D., and Claypool, G.E., 1981, Generation, accumulation, and resource potential of biogenic gas: AAPG Bulletin, v. 65, p. 5-25.

Ringen, B.H., and Daddow, P.B., 1990, Hydrology of the Powder River alluvium between Sussex, Wyoming, and Moorhead, Montana: U.S. Geological Survey Water-Resources Investigations 89-4002.

Robineau, B., Ritz, M., Courteaud, M., and Descloitres, M., 1997, Electromagnetic investigations of aquifers in the Grand Brule coastal area of Piton de la Fournaise Volcano, Reunion Island: Ground Water, v. 35, p. 585-592.

Rubin, Y., and Hubbard, S.S., 2005, Introduction to Hydrogeophysics, *in* Rubin, Y., and Hubbard, S.S., eds., Hydrogeophysics, Volume 50: Water Science Technology Library: Dordrecht, Netherlands, Springer, p. 523.

Scanlon, B.R., Paine, J.G., and Goldsmith, R.S., 1999, Evaluation electromagnetic induction as a reconnaissance technique to characterize unsaturated flow in an arid setting: Ground Water, v. 37, p. 296-304.

Sengpiel, K.-P., 1983, Resistivity/depth mapping with airborne electromagnetic survey data: Geophysics, v. 48, p. 181-196.

—, 1986, Groundwater prospecting by multifrequency airborne electromagnetic techniques, *in* Palacky, G.J., ed., Paper - Geological Survey of Canada, vol.86-22, p. 131-138.

Sharp, M., Creaser, R.A., and Skidmore, M., 2002, Strontium isotope composition of runoff from a glaciated carbonate terrain: Geochimica et Cosmochimica Acta, v. 66, p. 595-614.

Smith, B.D., Smith, D.V., Hill, P.L., and Labson, V.F., 2003, Helicopter Electromagnetic and Magnetic Survey Data and Maps, Seco Creek Area, Medina and Uvalde Counties, Texas: U.S. Geological Survey Open-File Report 03-0226.

Smith, R.S., O'Connel, M.D., and Poulsen, L.H., 2004, Using airborne electromagnetic surveys to investigate the hydrogeology of an area near Nyborg, Denmark: Near Surface Geophysics, v. 3, p. 123-130.

Spies, B.R., 1989, Depth of investigation in electromagnetic sounding methods: Geophysics, v. 54, p. 872-888.

Stearns, M., Tindall, J.A., Cronin, G., Friedel, M.J., and Bergquist, E., 2005, Effects of coal-bed methane discharge waters on the vegetation and soil ecosystem in the Powder River Basin, Wyoming: Water, Air, and Soil Pollution, v. 168, p. 33-57.

Tølbøll, R.J., and Christiansen, N.B., 2006, Robust 1D inversion and analysis of helicopter electromagnetic (HEM) data: Geophysics, v. 71, p. G53-G62.

Tronicke, J., Dietrich, P., Wahlig, U., and Appel, E., 2002, Integrating surface georadar and crosshole radar tomography; a validation experiment in braided stream deposits: Geophysics, v. 67, p. 1516-1523.

UBC-GIF, 2000, EM1DFM: A Program Library for Forward Modelling and Inversion of Frequency Domain Electromagnetic Data over 1D Structures.

USDA, 1954, Diagnosis and improvement of saline and alkali soils: Washington, D.C., U.S. Dept. of Agriculture, 160 p.

USGS, 2003, Coal-bed gas resources of the Rocky Mountain Region: U.S. Geological Survey Fact Sheet 158-02.

Van Voast, W.A., 2003, Geochemical signature of formation waters associated with coalbed methane: AAPG Bulletin, v. 87, p. 667-676.

Vanvig, J., 2006, Perserverance wins CBM water loss claim, landowners claim, Powder River Breaks, Volume 34: Sheridan, WY, p. 1.

Wadleigh, M.A., Veizer, J., and Brooks, C., 1985, Strontium and its isotopes in Canadian rivers; fluxes and global implications: Geochimica et Cosmochimica Acta, v. 49, p. 1727-1736.

Whitehead, R.L., 1996, Ground water atlas on the United States, Segment 8, Montana, North Dakota, South Dakota, Wyoming:

WOGCC, 2006, Wyoming Oil and Gas Conservation Commission Online Searchable Database: http://wogcc.state.wy.us/

WRCC, 2006, Western Regional Climate Center - Historical Climate Information: http://www.wrcc.dri.edu/

Wynn, J., and Liner, C., 2002, Evaluating groundwater in arid lands using airborne magnetic/EM methods; an example in the southwestern U.S. and northern Mexico, The Leading Edge (Tulsa, OK), Volume 21, p. 62-64.

Zelt, R.B., Boughton, G.K., Miller, K.A., Mason, J.P., and Gianakos, L.M., 1999, Environmental setting of the Yellowstone River basin, Montana, North Dakota, and Wyoming: U.S. Geological Survey Water-Resources Investigations 98-4269.